CHARLES UNIVERSITY
Faculty of Pharmacy in Hradec Králové
Department of Organic and Bioorganic Chemistry

UNIVERSITY OF HELSINKI
Faculty of Pharmacy
Division of Pharmaceutical Chemistry and Technology

SYNTHESIS OF NATURAL PRODUCT ANALOGUES AS POTENTIAL ANTITUMOUR AGENTS

Diploma thesis

Supervisors: Prof. RNDr. Milan Pour, PhD
Adj. Prof. Paula Kiuru, PhD

2018 **Manuela Voráčová**

UNIVERZITA KARLOVA
Farmaceutická fakulta v Hradci Králové
Katedra organické a bioorganické chemie

HELSINGIN YLIOPISTO
Farmasian tiedekunta
Farmaseuttisen kemian ja teknologian osasto

SYNTÉZA ANALOG PŘÍRODNÍCH LÁTEK JAKO POTENCIÁLNÍCH KANCEROSTATIK

Diplomová práce

Vedoucí diplomové práce: prof. RNDr. Milan Pour, Ph.D.
doc. Paula Kiuru, Ph.D.

2018 **Manuela Voráčová**

Declaration

"I declare that this diploma thesis is entirely my original copyrighted work. All literature and other resources have been properly acknowledged using explicit references. I have not previously used this work, or any version of it, to obtain any other degree."

"Prohlašuji, že tato práce je mým původním autorským dílem. Veškerá literatura a další zdroje, z nichž jsem při zpracování čerpala, jsou uvedeny v seznamu použité literatury a v práci řádně citovány. Práce nebyla využita k získání jiného nebo stejného titulu."

Prague May 2018 .....

Manuela Voráčová

Abstract

Charles University
Faculty of Pharmacy in Hradec Králové
Department of Organic and Bioorganic Chemistry

Candidate: Manuela Voráčová
Supervisors: Prof. RNDr. Milan Pour, PhD
Adj. Prof. Paula Kiuru, PhD
Title: Synthesis of natural product analogues as potential antitumour agents
Keywords: combretastatin, combretafuranone, purpurealidin, cytotoxic, $K_V10.1$ inhibitors, analogue synthesis

Despite numerous efforts and advances in prevention, diagnostics and treatment of human malignancies, cancer is still one of the leading causes of mortality worldwide. In the search for novel drug candidates, the rich biodiversity in the nature remains a valuable source of lead structures. Combretastatin A-4 (CA4) isolated from *Combretum caffrum* tree and purpurealidin I isolated from marine sponge *Pseudoceratina purpurea* are examples of such structures that served as an inspiration in the synthesis of potential anti-cancer agents within my thesis work.

Combretastatin A-4 is a well-known suppressor of tubulin polymerization via interaction with the colchicine binding site. It causes inhibition of cell growth and concurrently acts as a vascular disrupting agent and angiogenesis inhibitor. Being a *cis* stilbene derivative, it can readily isomerize into a thermodynamically more stable, but less active *trans* form. Furthermore, its low aqueous solubility is an issue. The first aim of this project was therefore to synthesize analogues that would overcome the above disadvantages, and to subject them to biological activity testing.

Following the group's previous work on antifungal lactones, the olefinic linker in CA4 was replaced with a furanone moiety and the effects of both oxygenated and halogen-bearing analogues on the biological activity were evaluated. 13 variously functionalized furanones were successfully synthesized in three to five steps starting from commercially available acetophenones or phenacylbromides.

Cytotoxic effects on a panel of cancer and normal cell lines as well as anti-infective activity were evaluated in due course for 12 compounds. Seven derivatives showed cytotoxicity against cancerous cells (the lowest IC_{50} = 0.12 μM) but they retained relatively high toxicity against non-malignant control cell lines. One hydroxymethylated derivative showed activity towards *Staphylococcus aureus* (MIC_{95} = 7.81–15.62 μM) without being cytotoxic up to 40 μM. All tested compounds were antifungally inactive.

The second natural product that inspired the syntheses of potential drug leads was the recently identified purpurealidin I that belongs to the class of marine bromotyrosine alkaloids. Many marine compounds possess a broad spectrum of biological activities, including cytotoxic activity or ion channel inhibition activity. The second aim of this thesis was the synthesis of simplified analogues of purpurealidin I via purpurealidin E to be tested for their cytotoxicity and activity towards the voltage-gated potassium channel K_V10.1. K_V10.1 represents an attractive cancer target since it is expressed ectopically in over 70% of human cancers. Such specificity in treatment could potentially decrease negative side effects connected to cancer treatments and K_V10.1 inhibitors are thus considered to be interesting lead compounds in the development of novel anticancer drugs.

Within the project, purpurealidin E was successfully synthesized in four steps from tyramine in an overall yield of 80%, improving the literature yields. A well-established synthetic route allowed for the synthesis of two novel analogues and the intermediates were coupled with miscellaneous aromatic carboxylic acids to yield the final amides. 12 compounds were then studied for their activity towards the K_V10.1 channel. Apparent inhibition was observed in some derivatives in the micromolar range. Two compounds showed activity against malignant melanoma cell line (IC_{50} < 15.00 μM) but they were comparably toxic to non-malignant cell control.

In conclusion, 27 novel natural product analogues were prepared within this thesis, some of which possessed interesting biological activities. Both projects provided valuable structure-activity data that served as a basis for further research and discovery of more selective analogues.

Abstrakt

Univerzita Karlova
Farmaceutická fakulta v Hradci Králové
Katedra organické a bioorganické chemie

Kandidát: Manuela Voráčová
Školitelé: prof. RNDr. Milan Pour, Ph.D.
doc. Paula Kiuru, Ph.D.

Název: Syntéza analog přírodních látek jako potenciálních kancerostatik

Klíčová slova: kombretastatin, kombretafuranon, purpurealidin, cytotoxický, inhibitory $K_V10.1$, syntéza analog

Nádorová onemocnění jsou jednou z nejčastějších příčin úmrtí i přes značný pokrok v prevenci, diagnostice a léčbě. Ve snaze najít nová potenciální léčiva se i nadále obracíme k přírodě jakožto zdroji vůdčích molekul. Příkladem takovýchto vůdčích molekul, které se staly předlohou pro syntézu potenciálních protinádorových látek v této diplomové práci, jsou kombretastatin A- 4 izolovaný z kůry kmene stromu *Combretum caffrum* a purpurealidin I izolovaný z mořské houby *Pseudoceratina purpurea*.

Kombretastatin A4 je známým supresorem polymerizace tubulinu skrze jeho interakci s kolchicinovým vazebným místem. Způsobuje silnou inhibici buněčného růstu, dále inhibici angiogeneze a rovněž narušuje cévy nádoru. Jedná se o derivát *cis* stilbenu, který snadno podléhá izomerizaci na termodynamicky stálejší, avšak méně aktivní *trans* formu. Jeho nevýhodou je rovněž špatná rozpustnost ve vodě. Prvním z cílů této práce proto byla příprava analog, která tyto nevýhody odstraní a která budou podrobena testům biologické aktivity.

Tato práce volně navázala na předchozí práci naší výzkumné skupiny týkající se antifungálních laktonů. Spojovací můstek v původním kombretastatinu A4 byl proto nahrazen furanonovým seskupením a byly zkoumány vlivy jak oxygenovaných, tak halogenovaných substituentů na biologickou aktivitu. V rámci této práce se v 3 – 5 krokových syntézách podařilo připravit 13 finálních sloučenin z komerčně dostupných substituovaných acetofenonů nebo fenacylbromidů. Následně byly u 12 látek

hodnoceny jejich cytotoxické účinky vůči rakovinným a normálním buněčným liniím a rovněž byly stanoveny protiinfekční účinky těchto látek. Sedm derivátů vykazovalo cytotoxicitu vůči rakovinným buňkám (nejnižší IC_{50} = 0,12 μM), avšak zachovaly si také poměrně vysokou toxicitu i vůči buňkám nenádorovým. U jednoho hydroxymetylovaného derivátu byla zjištěna aktivita vůči bakterii *Staphylococcus aureus* (MIC_{95} = 7,81–5,62 μM), přičemž tento analogon nebyl pro zdravé buňky toxický až do nejvyšší měřené koncentrace – 40 μM. U žádné ze sloučenin nebyla zjištěna aktivita vůči infekčním patogenním houbám.

Druhým přírodním produktem, který inspiroval syntézu potenciálních vůdčích molekul, byl nedávno objevený purpurealidin I patřící mezi bromotyrosinové alkaloidy mořského původu. Mnohé z mořských alkaloidů vykazují širokou škálu biologické aktivity, včetně např. cytotoxicity, či aktivity vůči iontovým kanálům. Druhým cílem této práce tak byla syntéza zjednodušených analog purpurealidinu I přes purpurealidin E k otestování jejich cytotoxicity a inhibice napěťově řízeného draselného kanálu K_V10.1. K_V10.1 se jeví jako atraktivní cíl protinádorového zásahu, jelikož se ektopicky vyskytuje ve více než 70 % lidských nádorů. Protože by takováto specifita mohla potenciálně snížit nežádoucí vedlejší účinky léčby, jsou inhibitory K_V10.1 považovány za vůdčí molekuly při vývoji nových kancerostatik.

V této práci byl purpurealidin E úspěšně syntetizován ve čtyřech krocích z tyraminu s celkovým výtěžkem 80 %, čímž byl vylepšen výtěžek popisovaný v literatuře. Osvědčený postup syntézy umožnil připravit dvě nová analoga a tyto meziprodukty byly podrobeny kaplingu s různými aromatickými karboxylovými kyselinami. U 12 sloučenin byla poté testována inhibiční aktivita vůči K_V10.1 a několik derivátů inhibovalo zmíněný kanál v mikromolárních koncentracích. Dvě z připravených sloučenin vykazovaly aktivitu vůči zhoubné buněčné linii melanomu (IC_{50} < 15 μM), avšak byly ekvimolárně toxické i pro nezhoubné buňky.

Celkově tedy bylo připraveno 27 nových analog přírodních produktů, z nichž některé vykazovaly zajímavou biologickou aktivitu. Výsledky obou projektů poskytly cenná data týkající se vztahů mezi strukturou a aktivitou a tato data posloužila jako základ pro další výzkum a syntézu analog s lepší selektivitou.

To the loving memory of my dear brother Jonáš (1988–2008) and dear friend Lukáš (1993–2017) whose lives were suddenly cut short by deadly diseases.

Acknowledgements

I express my deep sense of gratitude to my supervisors: Prof. RNDr. Milan Pour, PhD and Adj. Prof. Paula Kiuru, PhD for their guidance, valuable advices and criticism during my thesis work.

I am grateful to all my department colleagues for pleasant working environment. My fine appreciation especially belongs to Ingo Aumuller, PhD, Mgr. Zbyněk Brůža, Mukund Ghavre, PhD, Mgr. Lukáš Górecki, Mgr. Pavel Horký, Mgr. Zuzana Rania Hrušková, Mgr. Marek Kolenič, Mgr. Jiří Kratochvíl, PhD, Mgr. Petr Matouš and Mgr. Jiří Mikušek, PhD for their support, advices and insightful academic discussions.

Had it not been for several people, this thesis would have lacked some of the most important data. Thus, I would like to express my sincere appreciation to my collaborators for biological activity evaluations, namely to: RNDr. Klára Konečná, PhD of the Charles University; Mgr. David Sedlák, PhD and RNDr. Petr Bartůněk, CSc. of the Czech Academy of Sciences; Assoc. Prof. Ing. Jan Vacek, PhD of Palacký University; Prof. Jan Tytgat, PhD, Lien Moreels, PhD, Steve Peigneur, PhD and Hannah Goovaerts of the Catholic University of Leuven; Farrah Zahed, PhD and Prof. Luis Pardo, PhD of the Max-Planck-Institute of Experimental Medicine and Katja-Emilia Lillsunde, MSc (Pharm) and Adj. Prof. Päivi Tammela, PhD of the University of Helsinki. Furthermore, I am grateful for HRMS measurements to Assoc. Prof. PharmDr. Lucie Nováková, PhD and Nina Sipari, PhD and I am thankful to Assoc. Prof. PharmDr. Jiří Kuneš, PhD for NMR measurements within the combretafuranone project.

The financial support from the Charles University (SVV-260-062 and GA UK 1906214), Czech Science Foundation (P207/10/2048) and University of Helsinki is gratefully acknowledged. Furthermore, I am thankful to the European Pharmacy Student's Association and Prof. Jari Yli-Kauhaluoma, PhD who provided me with the wonderful opportunity to carry out a part of my thesis research at the University of Helsinki.

My warmest thanks belong to Petr and my family for support and understanding.

Table of Contents

LIST OF FIGURES

LIST OF SCHEMES

LIST OF TABLES

LIST OF APPENDIX TABLES

LIST OF ABBREVIATIONS

A-375	Human malignant melanoma (cell line)
A549	Human lung carcinoma (cell line)
Ac	Acetyl
APCI	Atmospheric pressure chemical ionization
ATCC	American Type Culture Collection
ATP	Adenosine triphosphate
ATR	Attenuated total reflection
bFGF	Basic fibroblast growth factor
BJ	Human primary fibroblasts (cell line)
Boc	*Tert*-butyloxycarbonyl
CA1	Combretastatin A1
CA4	Combretastatin A4
CA4P	Combretastatin A phosphate
Calcd	Calculated
Camp	Campthotecin
CB1	Combretastatin B1
CC1	Combretastatin C1
CD1	Combretastatin D1
cfu	Colony forming unit
Cipr	Ciprofloxacin
CLSI	Clinical and Laboratory Standards Institute
COX-2	Cyclooxygenase-2
cRNA	Complementary ribonucleic acid
CV	Column volume
DCM	Dichloromethane
DIC	*N*,*N*′-diisopropylcarbodiimide
DIPEA	*N*,*N*-diisopropylethylamine
DMAP	4-dimethylaminopyridine
DMEM	Dulbecco's Modified Eagle's Medium
DMF	*N,N*-dimethylformamide
DMSO	Dimethylsulfoxide
EAG	Ether à-go-go
EC	*Escherichia coli* (bacterial strain)
ED50	Median effective dose
EDC	1-ethyl-3-(3-dimethylaminopropyl)carbodiimide
EF	*Enterococcus faecalis* (bacterial strain)
EGFR	Epidermal growth factor receptor
Eq, Equiv	Equivalents
ESI	Electrospray ionization
Et	Ethyl
EtOAc	Ethyl acetate
EU	European Union
F-12K	Kaighn's Medium

Fig	Figure
FBS	Fetal bovine serum
G2/M	Growth/mitosis phase of cell cycle
H116	Human colon cancer (cell line)
H_1	Type of histamine receptor
HBTU	(2-(1*H*-benzotriazol-1-yl)-1,1,3,3-tetramethyluronium hexafluorophosphate
HDMS	High definition mass spectrometry
hEag1	Human ether à go-go potassium channel
HeLa	Human cervix adenocarcinoma (cell line)
Hep G2	Human hepatocyte carcinoma (cell line)
HEPES	4-(2-hydroxyethyl)-1-piperazineethanesulfonic acid
hERG	Human ether-à go-go-related gene
HL-60	Human acute myeloid leukaemia (cell line)
HOBt	Hydroxybenzotriazole
HRMS	High resolution mass spectrometry
Hs27	Human foreskin fibroblast line
HTS	High throughput screening
IC_{50}	Half maximal inhibitory concentration
IC_{80}	80% maximal inhibitory concentration
IMDM	Iscove's modified Dulbecco's medium
IR	Infrared
K562	Human chronic myelogenous leukaemia (cell line)
KP	*Klebsiella pneumoniae* (bacterial strain)
KP-E	*Klebsiella pneumoniae* (bacterial strain)
$K_V10.1$	Type of potassium channel
LC-MS	Liquid chromatography–mass spectrometry
LIMS	Laboratory information management system
LogP	Partition coefficient
LRMS	Low resolution mass spectrometry
MCF7	Breast adenocarcinoma (cell line)
Me	Methyl
MH	Mueller-Hinton (agar)
MIC	Minimum inhibitory concentration
MIC_{95}	Minimum inhibitory concentration, at least 95% inhibition
MRSA	Methicillin-resistant *Staphylococcus aureus* (bacterial strain)
MS	Mass spectrometry
MW	Microwave
NEAA	Non-essential amino acids
NMR	Nuclear magnetic resonance
P388	*Mus musculus* lymphoma (cell line)
PA	*Pseudomonas aeruginosa* (bacterial strain)
PC-3	Human prostate adenocarcinoma (cell line)
Pen-Strep	Penicillin-streptomycin
pH	Potential of hydrogen
PHT	Pyrrolidone hydrotribromide

ppm	Parts per million
Pr	Propyl
QT	Waves in electrocardiography
QTOF	Quadrupole time-of-flight (mass spectrometer)
Rf	Retention factor
RPE-1	Human retina epithelium (cell line)
RPMI	Roswell park memorial institute medium
rt	Room temperature
S.E.M	Standard error of the mean
SA	*Staphylococcus aureus* (bacterial strain)
SAR	Structure-activity relationship
SE	*Staphylococcus epidermidis* (bacterial strain)
SfiI	Type of restriction enzyme
SH-SY5Y	Homo sapiens bone marrow neuroblast (cell line)
siRNA	Small interfering ribonucleic acid
SMe	Methylsulfanyl
S_N	Nucleophilic substitution
SNAP KP-Sil	Type of cartridge for flash chromatography
TEA	Triethylamine
TFA	Trifluoroacetic acid
THF	Tetrahydrofuran
TLC	Thin layer chromatography
TOF-ESI	Time-of-flight electrospray ionisation
UV	Ultraviolet
$X^{(-)}$	Halogen ion

1 INTRODUCTION

Despite numerous efforts and advances in prevention, diagnostics and treatment of human malignancies, cancer is still one of the leading causes of mortality worldwide, with 8.8 million cancer victims in 2015.[1] The low efficacy and safety of current anticancer therapies remain to be a persisting issue. The identification of novel anticancer strategies endued with a better pharmacological profile and toxicological safety is therefore essential.[2] In the search for novel drug candidates, the rich biodiversity in the nature and especially sea remains a valuable source of lead structures. Combretastatin A-4 **1** (CA4, Fig. 1) isolated from *Combretum caffrum* tree[3] and purpurealidin I **2** (Fig. 1) isolated from marine sponge *Pseudoceratina purpurea*[4] are examples of such structures that served as an inspiration in the synthesis of potential anti-cancer agents within my thesis work.

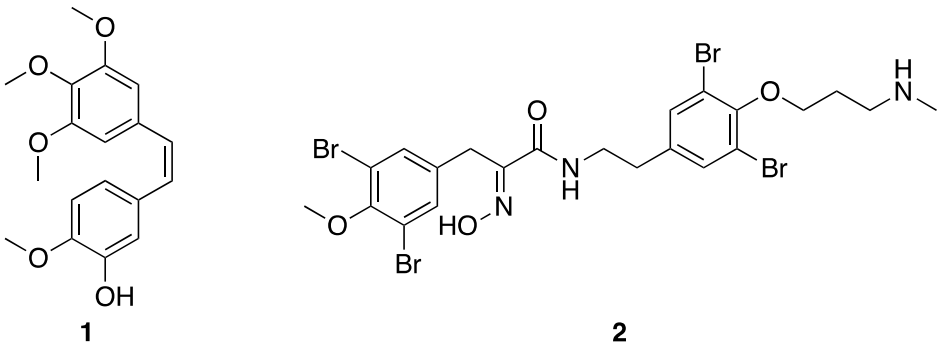

Figure 1 The structures of combretastatin A-4 **1** and purpurealidin I **2**.

The thesis consists of two projects that deal with analogue synthesis of **1** and **2** and are discussed separately. The principle, however, remains the same. The original compounds are variously modified in order to obtain structure-activity data that can lead to identification of compounds with improved physico-chemical properties, more potent biological activity and lowered toxicity.

The first project is focused on the synthesis of furanone analogues of **1**, referred to as combretafuranone analogues, to be tested for their biological activity, especially cytotoxicity towards various cancer cell lines. The second project is focused on the synthesis of simplified analogues of **2**, referred to as purpurealidin analogues, to target the cancer-relevant K^+ channel $K_V10.1$.

2 THEORETICAL BACKGROUND

2.1 Combretafuranone analogues project

2.1.1 Combretastatins

Combretastatins are natural products isolated from the bark of African willow tree *Combretum caffrum* with remarkable cytotoxic activity against a panel of cell lines, including multi-drug resistant cancer cell lines.[5] They are currently divided into four major groups based on their structure. These include *cis*-stilbenes (A-series; **3**, CA1), diarylethylenes (B-series; **4**, CB1), quinones (C-series; **5**, CC1) and macrocyclic lactones (D-series; **6**, CD1).[6] Representative members of each of these groups are depicted in Fig. 2. Among the most potent compounds are those based on the *cis*-stilbene core, with combretastatin **1** being of intense therapeutic interest.[7]

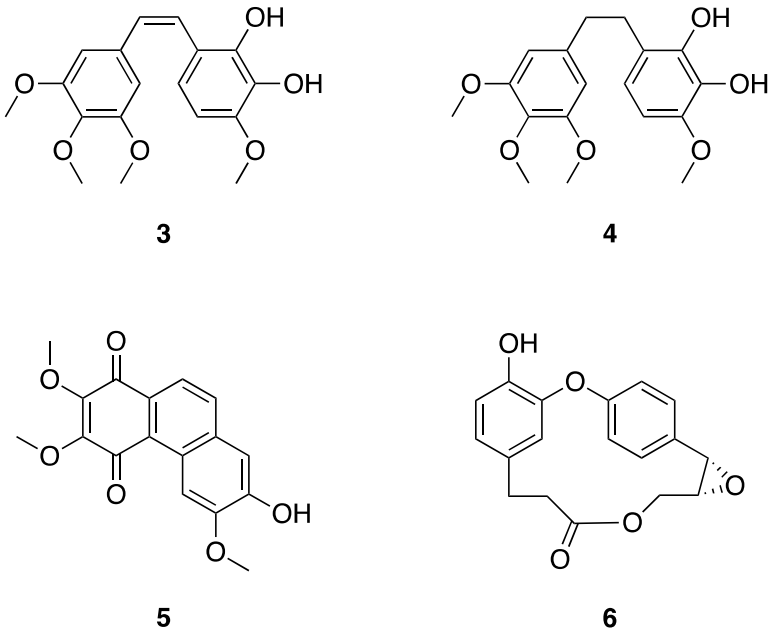

Figure 2 Combretastatin groups - representative structures **3**–**6.**

2.1.2 Combretastatin A4

2.1.2.1 Bioactivity and mechanism of action

In vitro antitumour evaluation of CA4 was performed against more than 60 human tumour cell lines with the mean growth inhibition (GI_{50}) of 3.2 nM.[8] CA4 acts as a strong tubulin inhibitor (IC_{50} 2.5 μM)[7] via interacting with the colchicine binding site and thus prevents heterodimers from assembling into microtubules.[6] Concomitantly, it promotes depolymerisation of microtubules.[9] This greatly affects essential cellular functions such as cell motility, cell proliferation signalling and intracellular transport, eventually leading to a cell-cycle arrest (G2/M phase) and apoptosis.[10] Even though healthy cells are also affected, tumour cells are targeted predominantly since they rapidly proliferate while relying on microtubule dynamics.[6]

Furthermore, CA4 has vascular disrupting properties[11] and prevents angiogenesis.[9] The former is characterized by destruction of the existing vasculature due to CA4's ability to induce morphological changes within endothelial cells, while the latter means the inhibition of the formation of new vessels.[6,12,13] Both mechanisms disrupt tumour's vasculature and the cessation of blood delivery eventually causes hypoxia and necrosis of the tumour.[14,15] Interestingly, selective activity of CA4 towards the micro vessels of tumours can be observed, and may be the result of cytoskeletal variability in rapidly proliferating endothelial cells.[6,15]

2.1.2.2 Structure of CA4 and its advantages and disadvantages

It is not only the robust mechanism of action that makes combretastatin A-4 be of high therapeutic interest, but also its simplicity in terms of chemical structure. It contains two phenyl rings which are tilted at 50–60° to each other due to the steric hindrance of oxygen-containing substituents.[6] These rings (referred to as cores **A** and **B**, Fig. 3) are connected by an unsaturated two-carbon bridge that is responsible for its *cis* configuration.[16] Such configuration is necessary for an efficient binding to tubulin and hence the natural tendency of *cis*-stilbene to isomerize to the more stable but less active *trans* isomer is an issue of concern.[17]

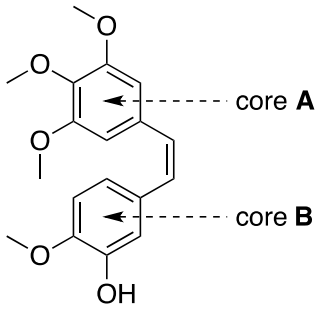

1

Figure 3 Cores **A** and **B** in CA4 **1**.

Another disadvantage is the poor solubility of CA4 in water.[10] The aqueous solubility of a drug is crucial for its absorption after oral administration and together with drug permeability, dissolution rate, first-pass metabolism and susceptibility to efflux mechanism, it is fundamental for the overall oral bioavailability. Furthermore, it governs the possibility of parenteral administration.[18,19] The resolution of this issue had thus been ineluctable and lead to the development of water-soluble prodrugs and analogues in the mid-1990s to allow for *in vivo* testing. The most commonly used prodrug has been fosbretabulin **7** (Fig. 4, CA4P), the disodium phosphate salt of **1**.[20] It is metabolized *in vivo* to the active form **1** by phosphatase, which is highly expressed in tumour environment.[21] Another derivative with improved aqueous solubility is ombrabulin **8** (Fig. 4) that was shortly granted an orphan drug status by the European Medicines Agency for the treatment of soft tissue sarcoma in the years 2011–2014.[22]

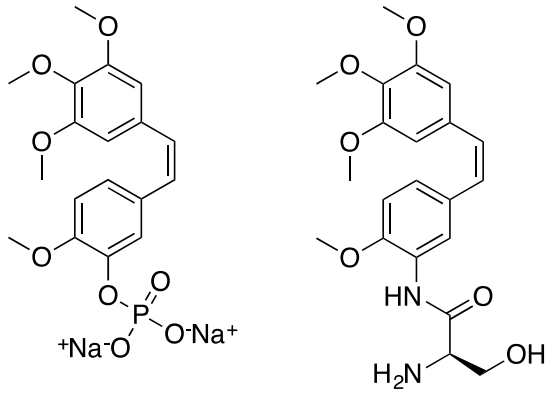

7 **8**

Figure 4 Prodrugs and analogues of CA4 **7** and **8** with increased aqueous solubility.

2.1.2.3 Current status in clinical trials

To date, CA4P **7** has been employed in numerous clinical trials both in monotherapy and in combination with other chemotherapeutic agents (e.g. bevacizumab, paclitaxel, carboplatin) or with radiation therapy.[10,23,24] The dose-limiting toxicities were assessed in several studies and the maximum tolerated dose was about 65 mg/m^2.[6,25] CA4P was well tolerated by patients, causing mild to moderate side effects (nausea, headache, tumour pain, vomiting, tachycardia or bradycardia, hypertension) that usually disappeared within a few hours after CA4P administration. However, when higher doses were administered, more severe side effects occurred. These included dyspnea, hypoxia and QT prolongation.[26]

During clinical trials, inhibition of blood flow in the tumour tissue was observed in solid tumours. CA4P exerted such effects on the inner part of the tumour tissue, leaving a rim of viable tumour cells at the periphery when used in monotherapy. Therefore, combination therapy with agents that are more effective in treating the outer tumour region was defined to be more effective.[6,10] CA4P appears to be effective especially when treating anaplastic thyroid cancer and ovarian cancer resistant to platinum.[23]

In conclusion, the antitumour activity of CA4P has been demonstrated in numerous clinical trials, and the compound is proposed to be used in association with other classical anticancer agents. However, its structural instability and dosing limitations continue to exist, and could be resolved by the synthesis of analogues.[6,23]

2.1.3 Cis-restricted analogues of combretastatin A4

As previously mentioned, *cis*-stilbenes are prone to isomerization to the more stable *trans* isomers. Such isomerization occurs during storage upon photo activation or in response to exposure to acidic media.[27] The isomeric instability and lower activity of the *trans* isomer are the reasons why significant efforts have been directed into the development of analogues with *cis*-restricted geometry.[5] To maintain the positions of the two vicinal substituted phenyl rings, a large number of analogues in which the olefinic linker is replaced by a rigid motive was synthesized. Various heterocycles such as azetidinone,[28,29] pyrrole,[30] pyrazole,[31,32] imidazole,[33,34] tetrazole,[35] thiazole,[36]

oxazole,[37] furan,[38,39] thiophene,[40, 41] etc. were used and besides rigidity, they also provided alteration of pharmacokinetic and pharmacodynamic properties. Even nanomolar cytotoxic activities superior to CA4 were recorded in some derivatives, such as in a novel series of 3,4-diaryl-1,2,5-selenadiazoles.[42] Five-membered heterocycles seemed to be more potent than six-membered ones.[33] Carbocyclic, aromatic, fused and open aliphatic analogues have been prepared as well.[5]

2.1.3.1 Structure-activity relationship

The substitution of most analogues follows the highly oxygenated substitution pattern of CA4. The heterocyclic derivatives were, in the majority of cases, designed in accordance with the SARs developed around the substitution on the phenyl cores **A** and **B** in **1**. As regards core **A**, the presence of the 3,4,5-trimethoxy substitution seems to be crucial for the activity even though no definitive answer to this issue has yet been given.[5] In core **B**, the 3-OH group may be replaced with bromine, fluorine, azide, boronic acid moieties etc. and the anti-proliferative effects still remain high if the 4-OCH_3 group is concurrently present, as in compound **9** (Fig. 5).[32,43] Conveniently, 3-OH may be exchanged to amino group to allow for a further derivatization, as seen in compound **10** (Fig. 5) or ombrabulin **8** (Fig 4).[39]

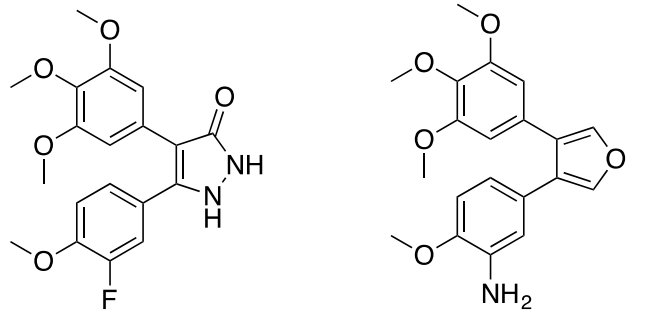

HeLa IC_{50} = 158.0 nM — **9**

SH-SY5Y IC_{50} = 5.1 nM — **10**

Figure 5 Heterocyclic analogues **9** and **10** with an alteration of 3-substituent in core **B**.

The intact 4-methoxy group in core **B**, present in majority of *cis*-restricted analogues, appears to be of high importance. Other modifications of position 4 were not employed so frequently, even though an early screening of CA4's lipophilic isosters and homologues demonstrated excellent low nanomolar levels of biological activity of

analogues containing -SMe, -Me, -Et (Fig. 6, **11**) and -Pr groups. The branched *tert*-butyl group raised the values higher to a micromolar range (Fig. 6, **12**).[44]

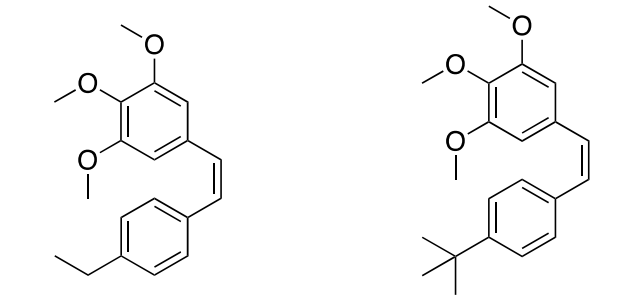

11 **12**

Figure 6 Homologues of CA4, compounds **11** and **12**.

Additionally, **B** core itself can be replaced by e.g. naphthyl, *N*-methyl-indol-5-yl or indol-5-yl resulting in cytotoxic analogues when combined with the 3,4,5-trimethoxyphenyl system.[5] Even though such modification sometimes did lower the cytotoxic activity to micromolar levels, some compounds (Fig. 7, e.g. **13**) showed nanomolar activities as well. However, both aqueous solubility and toxicity to normal cells might be an issue for **13**, although such parameters were not considered.[45]

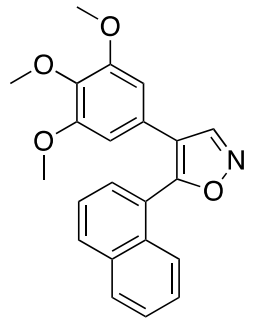

13

Figure 7 C*is*-locked analogue **13** with core **B** replaced by naphthyl.

Altogether, despite a vast number of *cis*-restricted analogues having been prepared, with some of them possessing truly amazing low nanomolar biological activities, no such analogue advanced to clinical trials as of this date.[46]

2.1.4 Aryl-2,5-dihydrofuranones

The *cis*-restricted analogues prepared within this thesis are based on the dihydrofuranone scaffold, and are thus called combretafuranones. The furan moiety is highly valued in medicinal chemistry since the ether oxygen adds potential for hydrogen bonding and can increase the polarity of a compound. Furan itself is present in a number of marketed drugs (e.g. nitrofuran and some cephalosporin antibiotics, amiodarone, ranitidine, furosemide etc.) while the presence of aryldihydrofuranones has been less frequent.[47] Most notably, aryldihydrofuranones can be found in a class of COX-2 selective inhibitors. A member of this nonsteroidal anti-inflammatory group of drugs – rofecoxib **14** (Fig. 8) was previously used to treat osteoarthritis, rheumatoid arthritis, acute pain and dysmenorrhoea. It was, however, withdrawn from the market due to safety concerns about an increased risk of heart attack.[48]

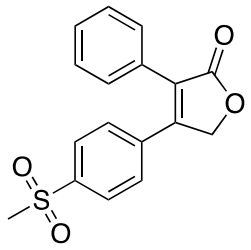

14

Figure 8 Rofecoxib **14** - COX-2 inhibitor based on the 2,5-dihydrofuranone scaffold.

The use of the 2,5-dihydrofuranone core in combretastatin-like derivatives has been reported only once by Kim *et al*. in 2002.[38] Their small library of compounds comprised of highly oxygenated analogues with intact 3,4,5-trimethoxy substitution pattern in core **A** (phenyl in C3 position) and a variation of substituents in core **B** (phenyl in C4 position). Although the carbonyl group changes the electronic effects of the molecule, only analogues with the trimethoxyphenyl ring attached to the electron-rich position to carbonyl (C3) were prepared. The inclusion of the highly polarizing carbonyl group did not seem to influence the cytotoxic activities negatively and four compounds with excellent IC_{50} values of less than 20 nM were discovered. Compound **15** in Fig. 9 bears identical substituents as CA4 **1**, and compound **16** confirms that 3-substitution of core **B** is likely to be superfluous, at least regarding cytotoxicity exclusively. Unfortunately, no data were provided on the general cellular toxicity of these compounds.

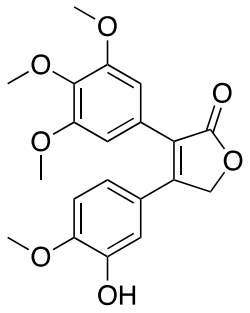

A549 IC_{50} = 16.3 nM

15

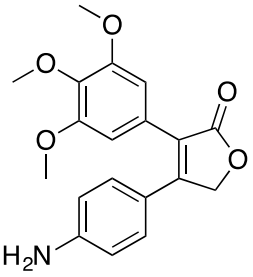

A549 IC_{50} = 54.7 nM

16

Figure 9 Furanone analogues **15** and **16**.

The idea that prompted the research described in this thesis also partially stems from the group's previous work[49] on the derivatives of (-)incrustoporin **17** (Fig. 10).

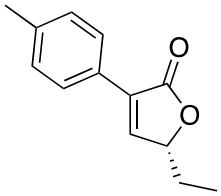

17

Figure 10 The structure of (-)incrustoporin **17**.

High antifungal activities comparable to those of amphotericin B were found in some halophenyl derivatives, e.g. **18** that was evaluated against 12 fungal strains (Fig. 11). The early work of Šenel *et al.*[50] on the expansion of the initial analogues to diarylfuranones showed some cytotoxic potential as well – e.g. compound **19**.

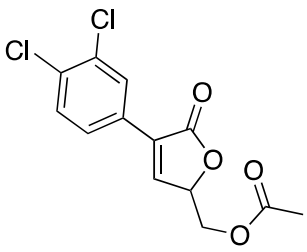

Antifungal IC_{50} = 0.5 - 15.6 μM

18

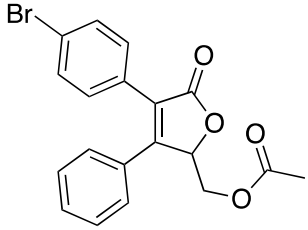

HeLa S3 IC_{50} = 2.8 μM

19

Figure 11 Biologically active dihydrofuranones **18** and **19**.

Another goal consequently addressed has therefore been the investigation of the impact of several structural modifications, including: 1. Combination of oxygenation and halogenation within the same molecule. 2. Attachment of the trimethoxyphenyl moiety to the electron-deficient position (C4) on the furanone ring. 3. Various structural modifications in the core **A** while maintaining the lipophilic substitution in core **B**. 4. Hydroxymethylation of furanone C5 position, and other measures to increase aqueous solubility. Some of these investigations were the subjects of my interest and are discussed within this thesis.

2.2 Purpurealidin analogues project

2.2.1 Bromotyrosine and bromotyramine alkaloids

Bromotyrosine and bromotyramine alkaloids are a large group of compounds that provide a unique diversity of both chemical structures and biological activities. They are marine sponge metabolites that have been isolated mainly from the order Verongida whose members use them to capture prey or as a defence against predators.[51,52] A large number of these derivatives were found to possess antibacterial, antifungal, antiviral, cytotoxic, antifouling or enzyme-modulatory properties. With the current critical need for novel anti-infectives and more effective anticancer drugs, bromotyrosines and bromotyramines are attractive candidates to be used as scaffolds for the syntheses of analogues.[51,53,54]

2.2.2 Cytotoxic purpurealidin alkaloids as the project inspiration

The alkaloids that acted as an inspiration for the syntheses of analogues within this thesis originate from *Pseudoceratina (Psammaplysilla) purpurea.* Since its identification in the late 19th century,[55] several compounds were isolated from this sponge and many of them showed cytotoxic properties. Among them were compounds with very simple structures based on bromotyramine, such as ceratinamine **20** and moloka'iamine **21** (Fig. 12).

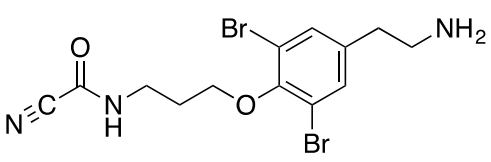

P388 IC_{50} = 3.4 μg/mL

20

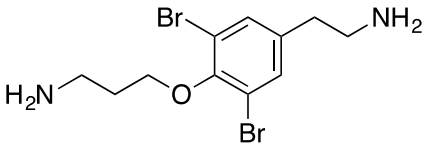

P388 IC_{50} = 5.0 μg/mL

21

Figure 12 Simple bromotyramines ceratinamine **20** and moloka'iamine **21**.

Ceratinamine **20** was the first reported metabolite among natural products containing the cyanoformamide moiety.[56] It exhibits antifouling activity and cytotoxicity against murine leukaemia cells P388, similarly to moloka'iamine **21**, that additionally targets four human cancerous cell lines at similar concentrations.[51]

More structurally complex cytotoxic compounds that employ the bromotyrosine unit can be seen in Fig. 13. Purealidin Q **22**, apart from cytotoxic activity,[57] also showed activity against *Salmonella typhi*.[58] Aplysamine 3 **23** was found to be cytotoxic to mouse lymphoid neoplasm and three carcinomas (lung, colon and oral epidermoid carcinoma).[59] It also showed mild antibacterial activity against *Staphylococcus aureus*.[51] Bastadin 14 **24**, besides its moderate cytotoxic activity, inhibited topoisomerase II with IC_{50} of 2.0 μg/mL.[60] The last cytotoxic compound in Fig. 13 is psammaplysin E **25** with an interesting 1,6-dioxa-2-azaspiro[4.6]undeca-2,7,9-triene skeleton.[51]

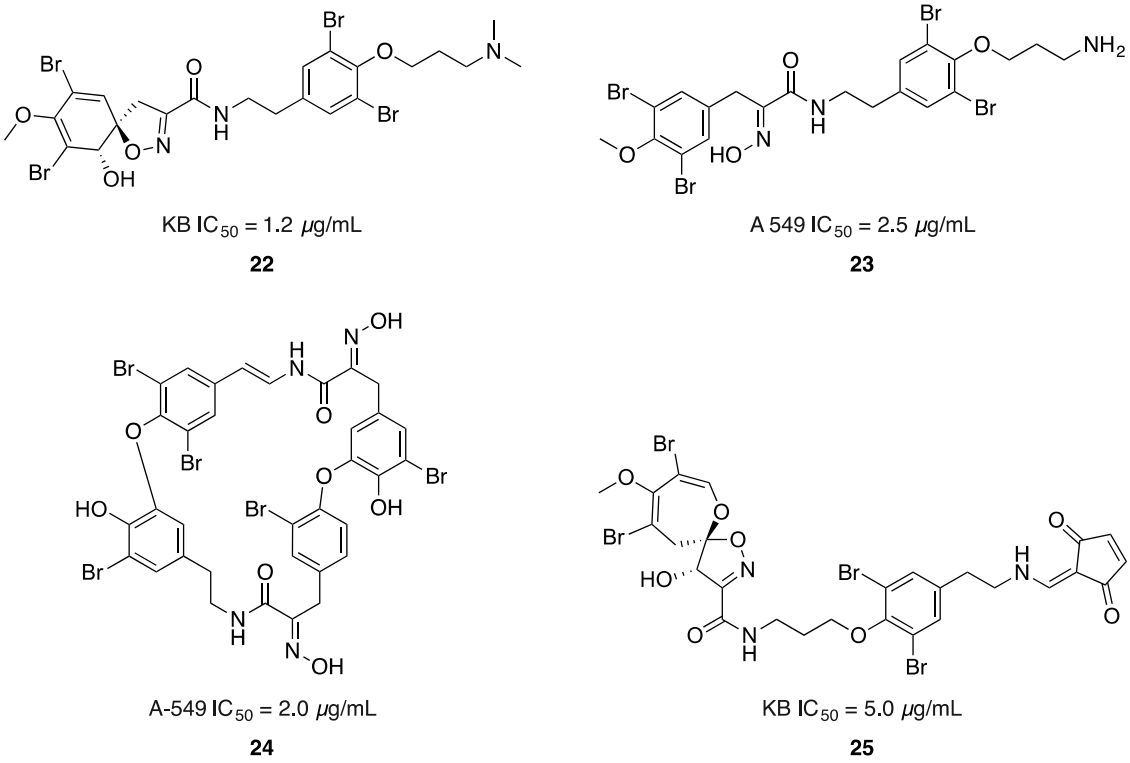

Figure 13 Bromotyrosines **22–25** with cytotoxic properties.

It can be noted that majority of these alkaloids are at least partially based on the structure of purpurealidin E **26** (Fig. 14). Even though no interesting biological activity of this metabolite has been reported to date,[54] it can serve as the starting molecule in total syntheses of bromotyrosine alkaloids and novel purpurealidin analogues.

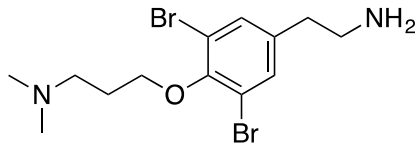

26

Figure 14 Purpurealidin E **26**.

When the novel bromotyrosine alkaloid purpurealidin I **2** (Fig. 1) was identified among other alkaloids by Tilvi and D'Souza[4] within the framework of the MAREX[61] project, efforts had begun in order to confirm the isolated structure by synthetic means and test it for biological activity. During the synthetic attempts towards the total synthesis of purpurealidin I within our research group, simplified amide analogues were prepared first. Preliminary testing showed the analogue **27** inhibited oncogenic $K_V10.1$ channel with IC_{50} values of 25.0 μM (Fig 15). This unpublished observation directed research towards finding a potential inhibitor of $K_V10.1$ channel based on simplified analogues of **2**.

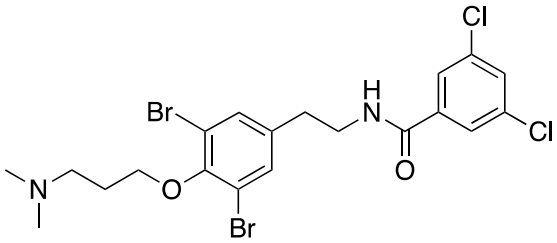

$K_V10.1$ inhibition: IC_{50} = 25.0 μM

27

Figure 15 First simplified analogue **27** with activity towards $K_V10.1$ channel.

2.2.3 Potassium channel $K_V10.1$ as a cancer target

$K_V10.1$ (hEag1, ether à go-go) is a membrane protein that belongs to the EAG family of voltage-gated potassium channels. While it is physiologically only expressed in the central nervous system and restricted cell populations in the body, it is aberrantly expressed in over 70% of human tumours.[62] This makes $K_V10.1$ an interesting subject for cancer biology research, indicating $K_V10.1$ may be used as a tumour marker, a possible prognostic factor or a therapeutic target.[63]

The ectopic expression of K_V10.1 was first reported in 1998 by Pardo *et al*. who observed it in diverse tumour cell lines.[64] Ever since, many clinical samples of tumours have been studied and showed a great abundance of K_V10.1 channel.[65,66,67] The high expression of K_V10.1 in tumours is correlated with a bad prognosis of several oncological diseases, such as acute myeloid leukemia,[68] glioblastoma multiforme, brain metastases,[69] colonic carcinoma,[70] sarcoma[71] etc. As regards the uses of K_V10.1 as a potential marker of cancer development, there has been tangible evidence for the use in the detection of e.g. cervical dysplasia[72] or head and neck squamous cell carcinoma.[73]

The role of K_V10.1 within a cancer cell is highly complex and the underlying molecular mechanism has not yet been properly elucidated.[63] In general, the development of cancer is known to be a multistep process requiring a functional disruption of numerous proteins that play a key role in cell proliferation, apoptosis and differentiation. K_V10.1 is involved in cell proliferation, angiogenesis, migration and invasion and this has been supported by both *in vitro* and *in vivo* experiments.[62] Cells transfected with K_V10.1 had the ability to grow under total serum starvation and they lost contact inhibition. Similarly, when xenografts were implanted *in vivo* into immunodeficient mice, growth of aggressive tumours was observed.[64]

On the molecular level, the expression of K_V10.1 impacts and is influenced by miscellaneous cellular pathways, likely through a broad protein-protein interaction network. According to Wu *et al*.,[74] the activity seems to be regulated by epidermal growth factor receptor kinase (EGFR kinase), which is known to facilitate tumour progression. A recent study by Lin *et al*. [75] showed the expression of K_V10.1 might be also indirectly controlled by p53, a protein that has been well known for its tumour suppressing properties in healthy functioning cells. As proposed by Zhu *et al*., [76] the inactivation of p53 that is present in many cancers could therefore lead to the overexpression of K_V10.1.[62]

2.2.3.1 Inhibitors of K_V10.1

It can be concluded that silencing of K_V10.1 expression or direct inhibition of the K_V10.1 channel shows an enormous potential for the treatment of oncological diseases. Silencing of K_V10.1 expression was already successfully performed *in vitro*, using e.g. antisense oligonucleotides, monoclonal antibody or siRNA.[77,78] Two venom-derived

micromolar peptide inhibitors κ-hefutoxin 1 and APETx4 were discovered only the last year.[79,80] Furthermore, pharmacological inhibitors of K_V10.1 were found among already marketed drugs (Fig. 16). Recently, there has been burst in publications that indicate the use of imipramine **28** and astemizole **29** is associated with reduced cell proliferation in cancer cell lines.[81,82,83,84]

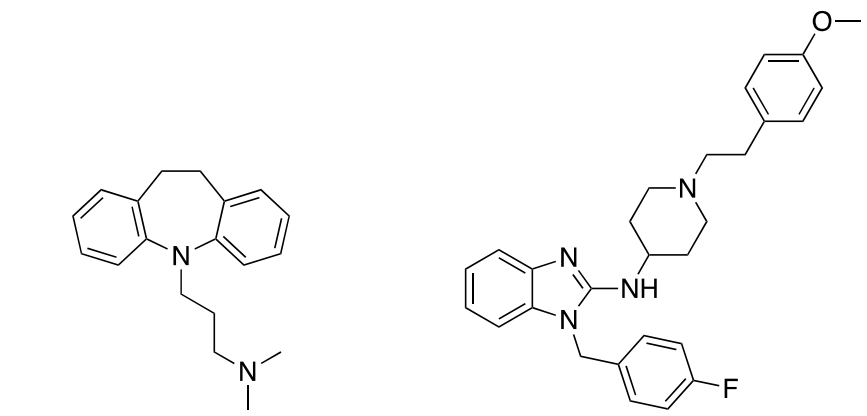

K_V10.1 inhibition: IC_{50} ~ 2 μM
28

K_V10.1 inhibition: IC_{50} ~ 200 nM
29

Figure 16 Inhibitors of Kv10.1 imipramine **28** and astemizole **29**.

The most potent drug astemizole **29** was shown to reduce progression of tumours as well as the frequency of metastasis in lung carcinoma.[81] It has been suggested as a potential treatment for hepatocellular carcinoma,[85] lung,[86] cervical,[87] or breast cancer,[88,89] especially in combination with current therapies. Although astemizole is a potent nanomolar blocker of K_V10.1, it is also known to be a non-selective drug that targets many receptors. Previously used as H_1 receptor antagonist for the treatment of allergies, it has been withdrawn from the market due to rare, but potentially fatal side effects. These were related to hERG channel blockade and manifested as arrhythmias and QT interval prolongations.[90,91] Even though this fact somehow underscores astemizole's potential, due to the fact that oncologic treatments are carefully monitored, it might be that astemizole will have its comeback in the form of drug repositioning.

Despite the above findings, the need to identify new inhibitors of K_V10.1 still remains critical since the therapeutic potential of the K_V10.1 channel is still vastly underexploited. Especially structural channel data, and information on the exact binding site of inhibitors, would be helpful. Furthermore, there are only a few leads and their

drawbacks are either low selectivity or unfavorable physicochemical or pharmacological properties.[53,62,63]

In conclusion, $K_V10.1$ inhibitors are considered to be important lead compounds in the development of novel anticancer drugs. If a highly selective inhibitor was found, only minor side effects could be expected since normal cells expressing $K_V10.1$ are protected by the blood-brain barrier or represent the terminal stage of normal differentiation.[67] The synthesis of potential inhibitors based on the simplification of marine product **2** is therefore the second important subject of this thesis.

3 AIMS OF THE THESIS

The aims of this thesis were the syntheses of novel analogues of two natural products (combretastatin A4 **1**, purpurealidin I **2**) and evaluation of their biological, especially antitumor activity. The principal objective was to be achieved by:

1. Syntheses of *cis*-restricted furanone analogues of **1** bearing various substituents, mainly oxygenated and halogenated, in order to gain SAR data (Scheme 1).

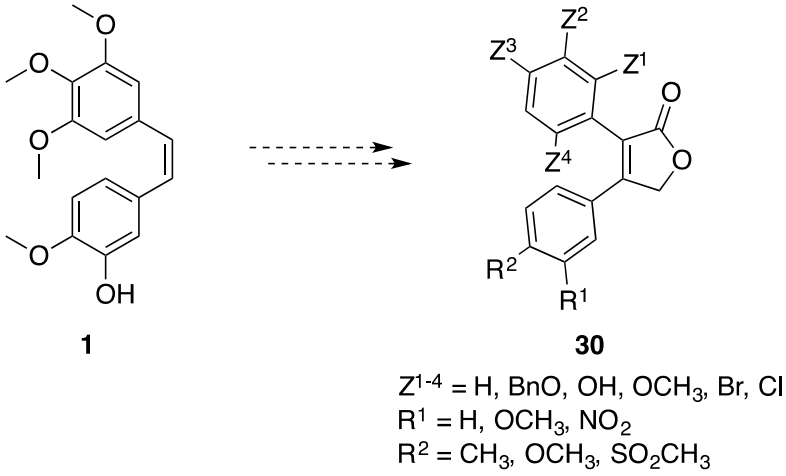

Scheme 1 Design of target combretafuranones – general structure **30**.

2. Further derivatizations of selected combretafuranones by dealkylation (Scheme 2) or γ-substitution (Scheme 3) to obtain more hydrophilic derivatives.

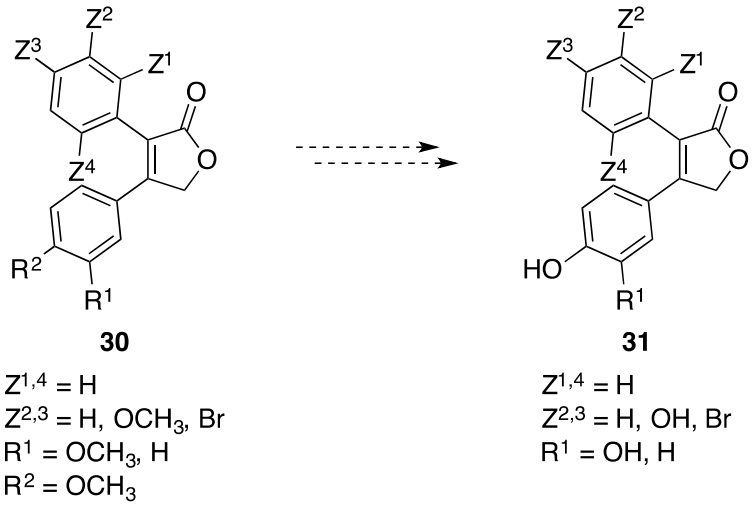

Scheme 2 Design of dealkylated derivatives - general structure **31**.

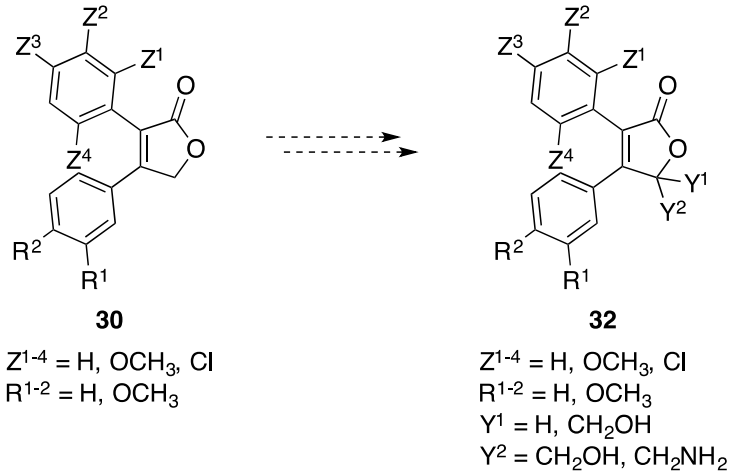

Scheme 3 Design of γ-substituted derivatives - general structure **32**.

3. Syntheses of purpurealidin E **26** and its analogues **33a** and **33b** as the starting materials for subsequent syntheses of purpurealidin analogues (Scheme 4).

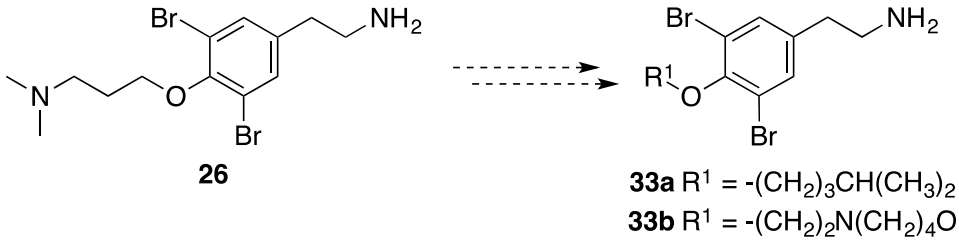

Scheme 4 Design of purpurealidin E **26** and its analogues **33a** and **33b**.

4. The syntheses of simplified analogues of purpurealidin I **2** from purpurealidin E **26** or its analogue **33a** or tyramine with special attention paid to developing a suitable purification method (Scheme 5). Ar = various aromatic acids.

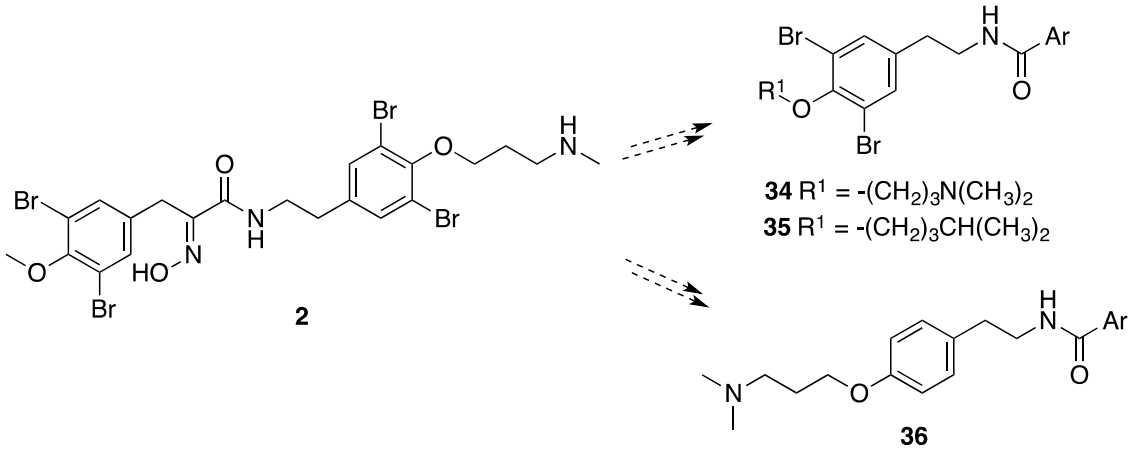

Scheme 5 Design of the target amides **34–36**.

4 RESULTS AND DISCUSSION

4.1 Synthesis of combretafuranone analogues

The general synthetic design of novel combretafuranones is depicted in Scheme 6. A substituted acetophenone **37** is brominated to yield bromoketone **38**. The bromoketone is then esterified with a substituted phenylacetic acid **39**. The resultant ester **40** is subjected to intramolecular aldolization under basic conditions. Subsequent dehydration of the intermediate **41** using acidic work-up yields the target combretafuranone **30.** The target molecule can be further derivatized in γ-position or in aromatic cores to yield analogues **31** or **32**. Synthetic procedures were performed similarly as published[50] unless otherwise stated.

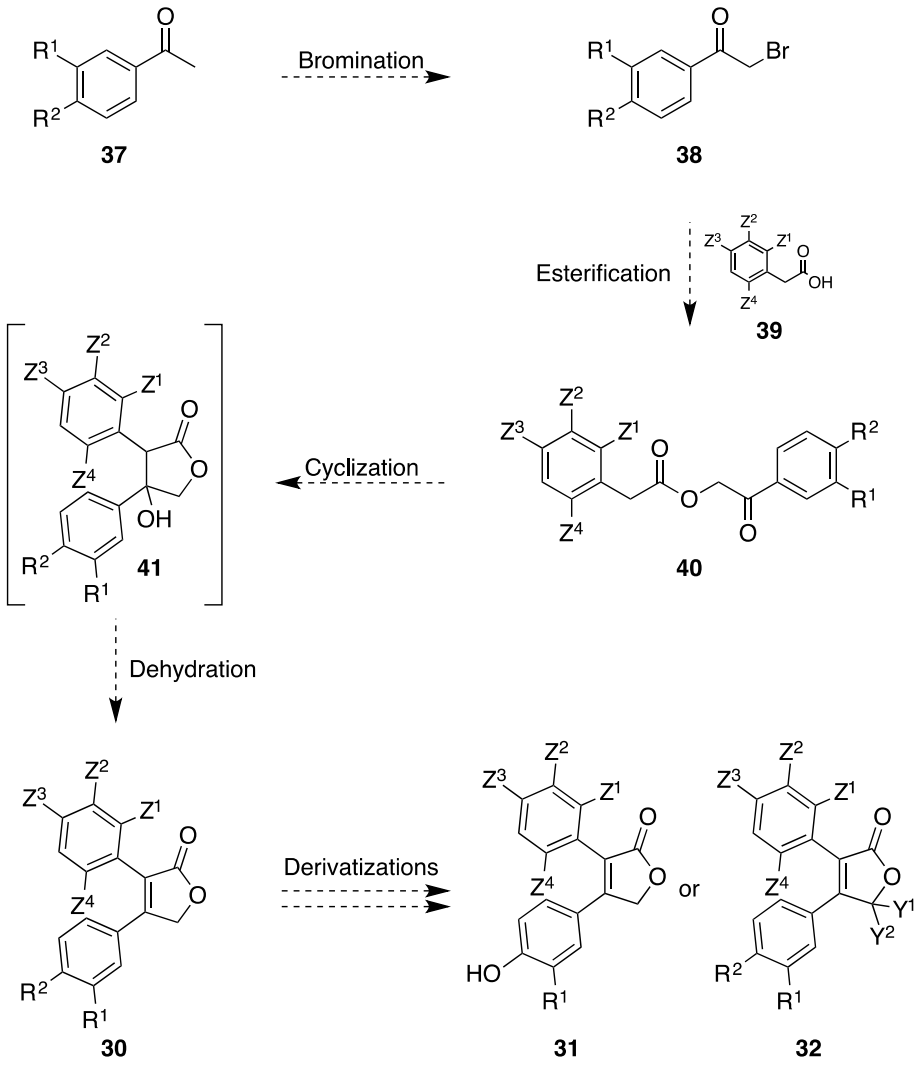

Scheme 6 Synthetic route towards final combretafuranones of general structures **30, 31** and **32**.

4.1.1 Syntheses of bromides of general structure 38

The synthetic route started with the bromination of the commercially available acetophenones **37a**–**d**. α-Halogenation was performed using pyridinium tribromide or pyrrolidone hydrobromide in neutral (THF) or acidic (CH_3COOH) conditions at room temperature (Scheme 7).

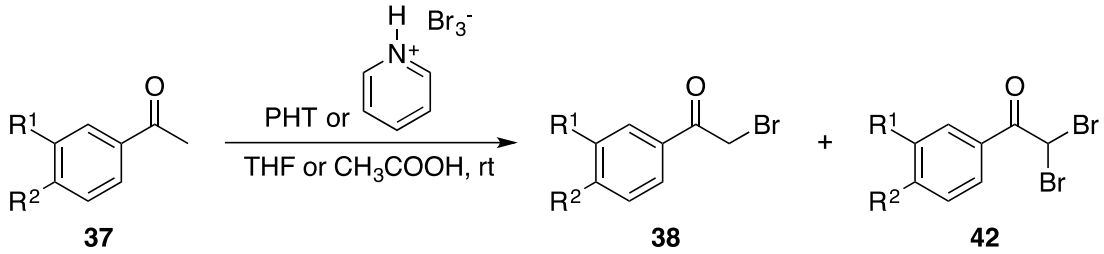

Starting material:	Substituents:		Major product:	Minor product:	Yield:
	R^1	R^2			
37a	H	OCH_3	**38a**	**42a**	Not specified. Used as a crude mixture.
37b	H	SO_2CH_3	**38b**	**42b**	**48% major**
37c	OCH_3	OCH_3	**38c**	**42c**	Not specified. Used as a crude mixture.
37d	NO_2	OCH_3	**38d**	**42d**	Not specified. Used as a crude mixture.

Scheme 7 Bromination of acetophenones **37a-d**.

In acidic conditions, the carbonyl oxygen is protonated first and an enol intermediate is formed. It is then attacked by bromine, and addition-elimination sequence occurs. The monobrominated product is favored in acidic environment over dibrominated since each successive halogenation is slower due to the decreased basicity of the carbonyl oxygen after first halogen substitution.[92] However, both monobrominated **38a**–**d** and dibrominated products **42a**–**d** were detected in the reaction mixtures by TLC and/or ^{1}H NMR analysis. For example, the singlet (-CO-C$\underline{H}_2$-Br) for the monobrominated product **38a** was found at 4.39 ppm in the ^{1}H NMR spectrum. In the case of the dibrominated side-product **42a**, the singlet (-CO-C$\underline{H}$-Br_2) was located more downfield, at 6.67 ppm. Since the separation of the dibrominated side-product was easier after the subsequent esterification, the products were used in the subsequent reaction as crude mixtures. The product **38b** was purified by washing the solidified crude with cold hexane (54% yield).

4.1.2 Synthesis of protected acid 39b

The majority of acids used in the syntheses of combretafuranones were obtained commercially and used as such in the second step – esterification. However, the substituted phenylacetic acid **39b** needed to be protected first in order to prevent the formation of side products in subsequent reactions (Scheme 8).

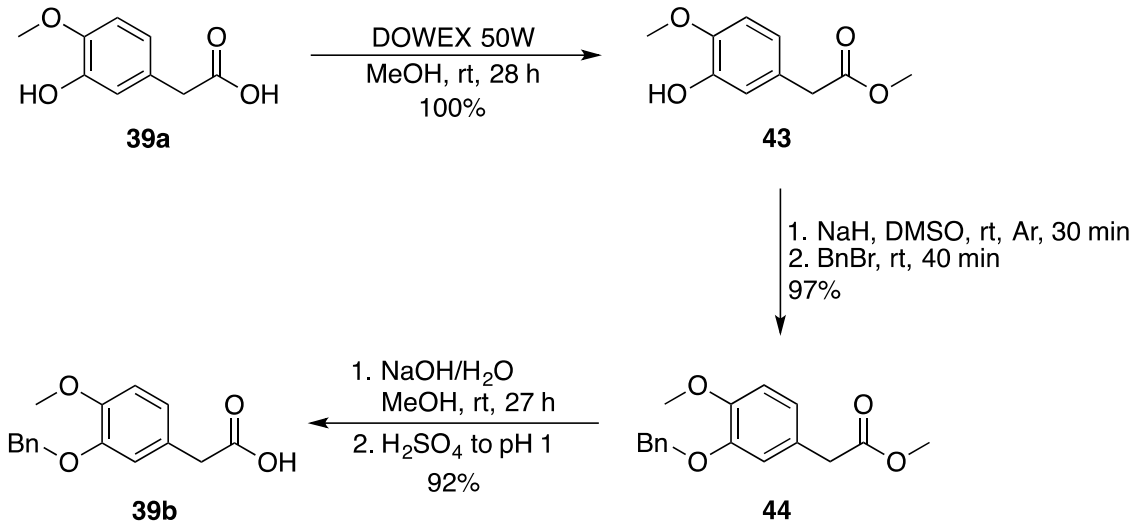

Scheme 8 Synthesis of protected acid **39b**.

Methylester **43** was synthesized from acid **39a** using methanol in the presence of the strongly acidic resin DOWEX 50W (approx. 1:1 weight equiv.). The mixture was stirred at room temperature and then filtered to obtain **43** in quantitative yield. An additional singlet at 3.68 ppm (-OC<u>H</u>$_3$) seen in the ^{1}H NMR spectrum confirmed the presence of the desired product. The methylester **43** was then dissolved in dry DMSO under argon atmosphere. NaH (60%, 1.1 equiv.) was used to deprotonate the phenolic hydroxyl that was subsequently alkylated with benzyl bromide (1.05 equiv.). The reaction proceeded well and the product **44** was obtained in an excellent yield and used in the next reaction without characterization. Subsequent hydrolysis using excess of NaOH (10 equiv.) in aqueous methanol gave the free carboxylic acid **39b** in excellent yield after acidic workup. The spectral data were in accordance with the literature.[93]

4.1.3 Formation of esters 40a–i

The next step towards the target combretafuranones was ester formation. Various phenylacetic acids **39b**–**h** were *in situ* deprotonated by triethylamine (1.0 equiv.), and the liberated carboxylates participated in nucleophilic substitution with bromides **38a**–**e** to yield the corresponding esters **40a**–**i** (Scheme 9).

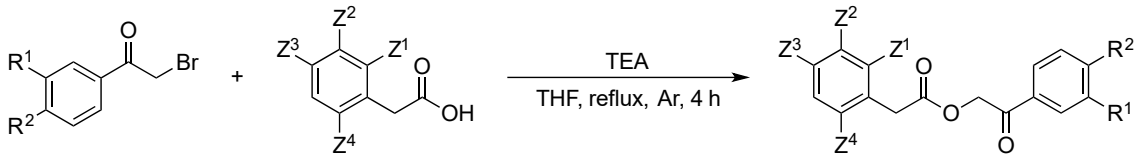

38 **39** **40**

Starting materials:		Substituents:						Product:	Yield:
Bromide	**Acid**	**Z^1**	**Z^2**	**Z^3**	**Z^4**	**R^1**	**R^2**		
38a	**39c***	H	H	Br	H	H	OCH_3	**40a**	48%
38a*									84%
38a	**39d***	Cl	H	H	Cl	H	OCH_3	**40b**	48%
38a	**39e***	H	Cl	Cl	H	H	OCH_3	**40c**	64%
38b	**39f***	H	H	OCH_3	H	H	SO_2CH_3	**40d**	81%
38c	**39f***	H	H	OCH_3	H	OCH_3	OCH_3	**40e**	46%
38c	**39g***	H	-OCH_2O-		H	OCH_3	OCH_3	**40f**	34%
38d	**39b**	H	BnO	OCH_3	H	NO_2	OCH_3	**40g**	66%
38e*	**39h***	Cl	H	Cl	H	H	CH_3	**40h**	95%
38e*	**39e***	H	Cl	Cl	H	H	CH_3	**40i**	86%

Scheme 9 Formation of esters **40a-i** by nucleophilic substitution.

The asterisk indicates the use of a commercially available reagent.*

Reflux in dry THF was shown to be optimal, although the reactions also occurred at room temperature (as with **40c**), albeit longer reaction times were needed. Otherwise typically 4–5 hours were sufficient for the reaction to be complete, as detected by TLC analysis.

Moderate yields were obtained when the synthesized bromides were used since all of them (except **38b**) were used as crude mixtures that also contained some amount of the dibrominated derivatives. Very good to excellent yields were obtained when commercially available bromides were used (e.g. compare the two different yields obtained for **40a**). It was therefore the purity of a starting material that played a role in the yield obtained. The substituents themselves did not seem to have a significant

influence on the yield although they may have influenced the reaction time. The lowest yield for **40f** may have been due to a one-time use of 2.0 equivalents of base.

Ester formation was confirmed by the presence of two characteristic singlets in the ^{1}H NMR spectrum. The chemical shifts naturally slightly varied depending on substitution, although in the majority of cases the singlets were found at around 5.3 ppm for Ar-CO-C$\underline{H}_2$-O- and 3.7 ppm for Ar-C$\underline{H}_2$-CO-. A more significant difference was observed in the case of compound **40b** in which the benzylic hydrogen atoms were deshielded by the adjacent electron-withdrawing 2,6-dichloro substituents. The singlet was thus located more downfield, at 4.22 ppm.

4.1.4 Cyclization to target combretafuranones 30a–30i

The last two steps towards the final combretafuranones consisted of an intramolecular aldol condensation followed by dehydration, performed in one pot (Scheme 10). In the first step, NaH is used to deprotonate the slightly acidic benzylic hydrogen in ester **40** to form an enolate. The enolate then attacks carbonyl to form a 5-membered saturated ring - intermediate **41**. In the second step, dehydration occurs upon acidifying the mixture with HCl to give the target combretafuranone **30**.

Both steps were accompanied by visual changes in the reaction mixture. An evolution of hydrogen gas and darkening of the reaction mixture could be observed in the first step. A color change to yellow/orange was observed in the second step because a conjugated system was formed.

The reaction was performed at room temperature on a small scale. Scales above 7 mmol were usually cooled using an ice bath and hydride was added in two batches. The addition of hydride (60% oil dispersion, 1.0 or 1.1 equiv.) was done quickly into an open flask under positive pressure of argon.

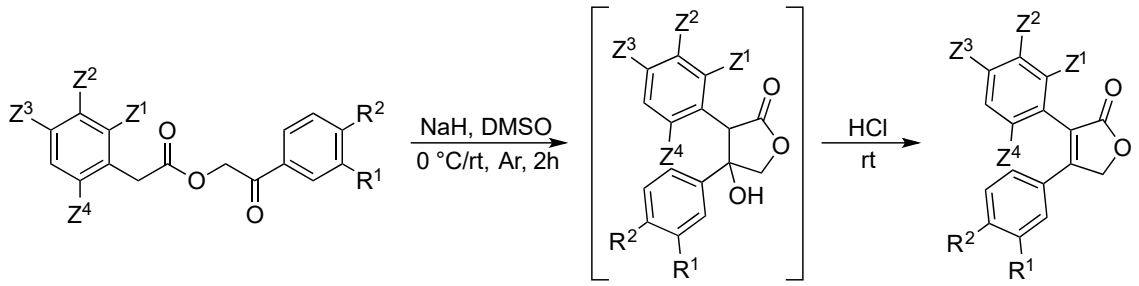

Starting material:	Substituents:						Product:	Yield:
	Z^1	Z^2	Z^3	Z^4	R^1	R^2		
40a	H	H	Br	H	H	OCH_3	**30a**	91–95%
40b	Cl	H	H	Cl	H	OCH_3	**30b**	92%
40c	H	Cl	Cl	H	H	OCH_3	**30c**	62%
40d	H	H	OCH_3	H	H	SO_2CH_3	**30d**	11%
40e	H	H	OCH_3	H	OCH_3	OCH_3	**30e**	54%
40f	H	-OCH_2O-		H	OCH_3	OCH_3	**30f**	55%
40g	H	BnO	OCH_3	H	NO_2	OCH_3	**30g**	0%
40h	Cl	H	Cl	H	H	CH_3	**30h**	96%
40i	H	Cl	Cl	H	H	CH_3	**30i**	95%

Scheme 10 Synthesis of combretafuranones **30a–i**.

Results in Scheme 10 show that strongly electron-withdrawing groups (such as -SO_2CH_3 in **30d** and -NO_2 in **30g**) influenced the reaction negatively. Especially in the case of **30g**, numerous tailing and overlapping products were observed by TLC analysis. Since only traces of possible product were detected in ^{1}H NMR, purification was not attempted.

All other compounds (except **30c** that was not used in biological testing) were obtained in high purity and were fully characterized by ^{1}H, ^{13}C, IR, LRMS or HRMS and elemental analysis. Two singlets characteristic of an ester disappeared from the ^{1}H NMR spectrum and a new singlet characteristic of methylene hydrogen atoms was formed at around 5.1–5.4 ppm. In the IR spectra, the carbonyl in a 5-membered saturated lactone is generally found at frequencies around 1770 cm^{-1}, and its absorbance is typically lowered by conjugation.[94] Thus, the carbonyl stretch in IR spectra of combretafuranones was found to be as low as at 1711 cm^{-1} (**30b**) but also as high as 1792 cm^{-1} (**30e**), depending on substitution.

4.1.5 Dealkylation of aromatic methoxy groups in compound 30

In order to increase the hydrophilicity of our combretafuranones and bearing in mind that such transformation might bring valuable information with regard to biological activity, dealkylation of aromatic methoxy groups was performed with compounds **30a**, **30e** and **30f** using BBr_3 in hexane/DCM at -50 °C. The reaction was completed within an hour and upon quenching with water gave compounds **31a**–**b** (Scheme 11).

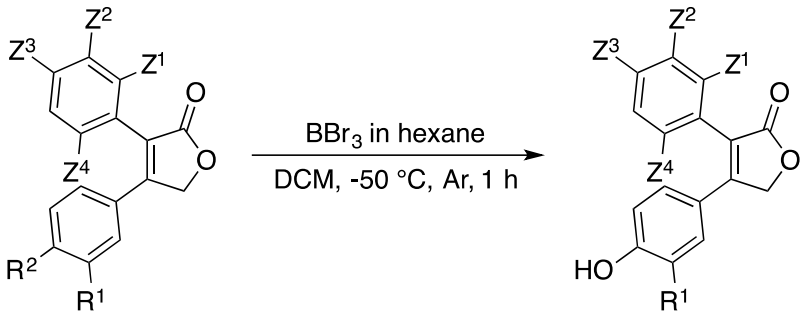

30 **31**

Starting material:	Substituents:					Product:	Substituents:				Yield:
	Z^1/Z^4	Z^2	Z^3	R^1	R^2		Z^1/Z^4	Z^2	Z^3	R^1	
30a	H	H	Br	H	OCH_3	**31a**	H	H	Br	H	79% 92%
30e	H	H	OCH_3	OCH_3	OCH_3	**31b**	H	H	OH	OH	87%
30f	H	-O-CH_2-O-		OCH_3	OCH_3	**31c**	H	OH	OH	OH	N/A

Scheme 11 Dealkylation of methoxy groups.

The work-up and purification methods varied. Since some lipophilic impurities were always present in reaction mixtures according to TLC analysis, it was logical to try an acid-base extraction first. The reaction mixture of **31a** was therefore washed with saturated Na_2CO_3 and extracted to EtOAc. TLC indicated that the assumed product was present in both aqueous and organic layer. Due to concerns about using stronger base together with EtOAc for extraction, no attempts to further basify the mixture were made. Instead, the procedure was repeated in order to transfer as much compound as possible to the aqueous layer. Subsequently, the water layer was acidified to pH 2–3 and re-extracted three times with EtOAc. Upon solvent removal *in vacuo*, the crude product was purified by silica gel column chromatography with addition of 1% of CH_3COOH and gave the target compound **31a** in 79% yield.

When the reaction was performed for the second time using the same reaction procedure with the same compound **31a** (2nd try), only saturated sodium chloride was used in the extraction procedure with a favourable outcome. Column chromatography was performed similarly as before and the yield improved to 92%. It can therefore be assumed that the lower yield obtained in the first try was due to unsuitable extraction procedure. The compound was fully characterized by ^{1}H, ^{13}C, IR, HRMS and elemental analysis. Disappearance of the singlet at 3.83 ppm (-OC$\underline{H}_3$) in the ^{1}H NMR spectrum as well as the peak characteristic of the stretching vibration of an aromatic hydroxyl (3237 cm^{-1}) in the IR spectrum confirmed the presence of the desired product.

Surprisingly, with compound **31b** that bears three phenolic moieties, the extraction procedure only with the neutral saturated NaCl did not pose any challenges, either. The silica gel column chromatography was performed with the addition of 1% CH_3COOH as in the previous case, but the elution was extremely lengthy. Furthermore, since the product was diluted, TLC detection was difficult. Therefore, the amount of CH_3COOH was increased to 5% in midst of the elution. The product was finally obtained in a very good yield (87%). The full characterization of **31b** is provided as well. Stretching vibrations at 3314, 3566 and 3629 cm^{-1} could be observed in the IR spectrum, and confirmed the presence of three free aromatic hydroxyl moieties.

However, when the established extraction procedure was applied to the last compound **31c** with four phenolic hydroxyls, a large amount of product remained in the aqueous phase, even though the extraction with EtOAc was done repeatedly. Subsequent acidification with diluted HCl was helpful. Both solvents were then separately removed *in vacuo* and the crude from aqueous layer was suspended in acetone. That, together with subsequent filtration on Celite was carried out in order to minimize the presence of NaCl. Unfortunately, due to lack of time, the compound could not be purified by column chromatography. A suitable phase for separation, detection and chromatography was, however, found: $CHCl_3$/MeOH 6:4 + 3% CH_3COOH since the compound did not move on TLC when EtOAc was used as the mobile phase.

Summary of the results is provided in Table 1.

Table 1 Summary of purification methods and results of dealkylation.

Compound:	Extraction:	Chromatography:	Yield:
31a_1	Acid-base Troublesome	Hexane/EtOAc 6:4 + 1% CH_3COOH	79%
31a_2	Sat. NaCl Successful	Hexane/EtOAc 8:2 → 7:3 +1% CH_3COOH	92%
31b	Sat. NaCl Successful	Hexane/EtOAc 1:1 → 2:8 + 1→ 5% CH_3COOH	87%
31c	Sat. NaCl Unsuccessful	N/A	N/A

4.1.6 Syntheses of γ-substituted derivatives

4.1.6.1 Hydroxymethylation of selected derivatives

Another method performed in order to increase the hydrophilicity of our combretafuranones was the hydroxymethylation of γ-position.[95] Combretafuranones were enolized under basic conditions (Na_2CO_3, 1–2 equiv.) in methanol and subsequently reacted with paraformaldehyde (Scheme 12).

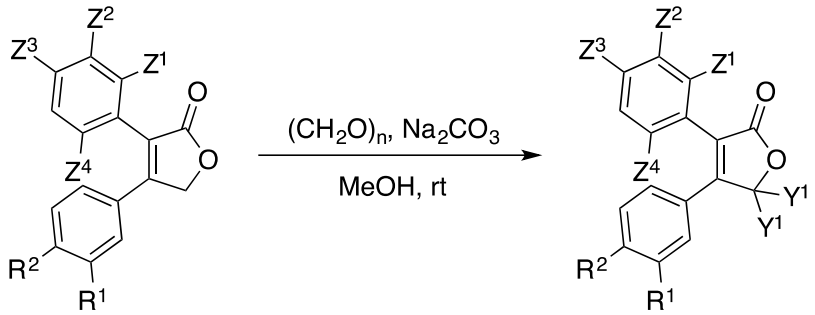

30 **32**

Starting material:	Substituents:							Product:	Yield:
	Z^1=Z^4	Z^2	Z^3	R^1	R^2	Y^1	Y^2		
30c	H	Cl	Cl	H	OCH_3	CH_2OH	CH_2OH	**32a**	25%
30e	H	H	OCH_3	OCH_3	OCH_3	CH_2OH	H	**32b**	26%
	H	H	OCH_3	OCH_3	OCH_3	CH_2OH	CH_2OH	**32c**	15%

Scheme 12 Hydroxymethylation of compounds **30c** and **30e**.

The reaction was in both cases very low-yielding and never proceeded to completion. Several side products were detected using TLC and their separation was rather difficult. Regardless of the amount of base used, the bishydroxymethylated derivative was obtained in either case. The reaction of **30e** continued for 4 days and included mild heating. Nevertheless, a high amount of the starting material (54%) was recovered. This suggests the other side products detected by TLC were present in low amounts. The separation of mono and bishydroxymethylated derivatives was easy when a careful gradient was chosen during chromatography. In the reaction of **30c**, only the bishydroxymethylated derivative **32a** was isolated.

All compounds were fully characterized by ^{1}H, ^{13}C, HRMS or IR and elemental analyses. The disappearance of the singlet at 5.15 ppm in ^{1}H NMR of **32c** and the appearance of a doublet of doublets at 5.49 ppm with lower intensity (**32b**) confirmed that the starting combretafuranone **30e** was substituted in γ-position. The methylene (-C$\underline{H}_2$OH) hydrogen atoms in **32b** gave separate signals – multiplets at 3.73–3.66 and 4.07–4.00 ppm. A new peak in the IR spectrum (3401 cm^{-1}) was characteristic of the vibration of the hydroxyl group in **32a**.

4.1.6.2 Conversion of hydroxyl to amino moiety in 32b

In order to explore the effects of various substitutions on biological activity, the preparation of amine derivative was attempted with **32b**. Since this reaction was not previously performed on this type of compounds, a suitable method for the conversion of hydroxyl to amine group was searched for in literature. Most commonly, alcohols are first converted to the corresponding halides or sulfonates. Subsequently, they are substituted by azide anion and resultant azides are reduced to amines. Alternatively, Mitsunobu conditions using hydrazoic acid, triphenylphosphine and diethylazodicarboxylate have been frequently used.[96]

I followed the one-pot protocol published by Reddy *et al.*[97] Alcohol **32b** was treated with sodium azide (1.2 equiv.) and two equivalents of triphenylphosphine in CCl_4/DMF (1:4). The mixture was then heated to 90 °C and stirred for several hours (Scheme 13) with TLC monitoring.

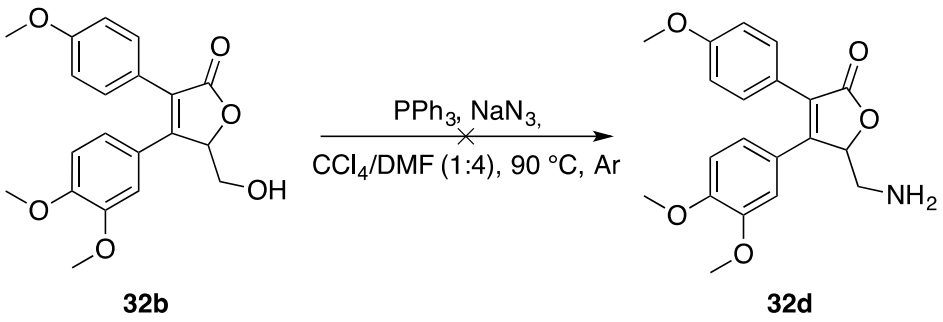

Scheme 13 Unsuccessful conversion of alcohol **32b** to amine **32d**.

The reaction mechanism is interesting and involves the activation of PPh_3 by the reaction with CCl_4, followed by the nucleophilic attack of the alcohol oxygen at phosphorus to generate an oxyphosphonium intermediate. Subsequently, a series of S_N2 displacements occurs, beginning with halide attack of the oxyphosphonium intermediate, followed by azide attack of the newly formed halide. The resultant azide reacts with the second equivalent of PPh_3 to form an amine upon hydrolysis with water.

However, two doublets at 5.28 and 4.90 ppm with same intensities and coupling constant $J = 2.5$ Hz observed in ^{1}H NMR spectrum indicated the formation of the 5-methylene compound.

4.2 Biological activity of combretafuranone analogues

Twelve of the final combretafuranones prepared within this thesis were tested for their cytostatic, antibacterial and antifungal activity. Additionally, LogP, solubility and bioavailability were calculated in order to predict the druglikeness of the molecules, and the data are included in Appendix A. Structures of all tested compounds are summarized in Appendix B.

4.2.1 Cytotoxicity

Cytotoxicity was assessed on a panel of five cancer cell lines including two leukaemia models K562 and HL-60, prostate adenocarcinoma cells PC-3, breast adenocarcinoma cells MCF7 and hepatocellular carcinoma Hep G2. Two non-malignant cell lines were used for comparison – retina epithelium cells RPE-1, and human primary fibroblasts BJ. The compounds were incubated with the cells for 48 hours, and tested in the dose-response fashion in the concentration range from 40 μM to 1 nM. Cell viability was assessed by determining the level of intracellular ATP in a luminescent assay. Caspase 3/7 activity data were obtained in order to determine the type of cell death. The results are summarized in the Table 2. Results of Hep G2 cell line testing are not shown since all compounds (except for standard: (*S*)-(+)-camptothecin) were inactive.

Table 2 Cytotoxic and apoptotic profiling.

Cell lines used: RPE-1: human normal immortalized cells from pigmented epithelium in retina; BJ: human primary fibroblasts; Hep G2: human hepatocellular carcinoma; K562: human chronic myelogenous leukaemia; HL-60: human acute myeloid leukaemia; PC-3: human prostate adenocarcinoma; MCF7: human breast adenocarcinoma. Camp: (S)-(+)-Camptothecin.

Compound:	Cytotoxicity: [IC_{50}, µM]						Caspase 3/7 Activity: [IC_{50}, µM]			
	RPE-1	BJ	K562	HL-60	PC-3	MCF7	RPE-1	K562	HL-60	PC-3
30a	3.35	>40	**0.53**	**0.83**	>40	**14.28**	56.42	>40	**2.18**	>40
30b	>40	>40	**14.43**	**15.08**	>40	>40	>40	**16.25**	**12.50**	>40
30d	>40	>40	>40	>40	>40	>40	>40	>40	>40	>40
30e	>40	>40	>40	42.72	**15.87**	>40	>40	>40	>40	>40
30f	35.53	>40	**16.01**	**17.39**	>40	>40	>40	>40	>40	>40
30h	0.91	>40	**0.19**	**0.27**	>40	**23.92**	>40	**10.09**	>40	**0.44**
30i	0.54	>40	**0.12**	**0.23**	>40	**15.40**	>40	**3.50**	>40	**0.54**
31a	>40	>40	>40	>40	>40	>40	>40	>40	>40	>40
31b	>40	>40	**16.19**	>40	>40	>40	>40	>40	>40	>40
32a	>40	>40	>40	>40	>40	>40	>40	>40	>40	>40
32b	>40	>40	>40	>40	>40	>40	>40	>40	>40	>40
32c	>40	>40	>40	>40	>40	>40	>40	>40	>40	>40
Camp	>40	>40	0.09	0.02	0.40	0.34	27.20	0.71	0.07	>40

The testing provided valuable data especially on the new type of analogues with halogen substituents. Nanomolar cytotoxic effects against both leukemic cell lines were found in the chlorinated derivatives and isomers **30h** and **30i**. Unfortunately, relatively low selectivity index was determined (4.8 and 4.5, respectively) and both compounds were toxic to the non-malignant RPE-1 line. In the analogues that combine 4-methoxy substitution in core **B** as in CA4 **1** and halogen substitution in core **A**, high submicromolar cytotoxicity was detected for **30a** (selectivity index 6.3 for K562). Since the demethylated analogue **31a** was not cytotoxic to all cell types up to 40 µM,

lipophilic substitution in core **B** was deemed to be important for these types of compounds. As regards compound **30b**, micromolar activity and selectivity against both leukemic cell lines K562 and HL60 with IC_{50} 14.43 and 15.08 μM, respectively was observed. The induction of apoptosis is likely to be the possible cause of death, since **30b** activates the caspase 3/7 pathway at nearly the same concentrations as needed for cytotoxic effects.

In the case of derivatives **30e**, **30f** and **31b** that followed the highly oxygenated substitution patter of CA4 **1**, only minor activities were found confirming a high degree of oxygenation is needed for these types of molecules to be active.

Lastly, no cytotoxic activity was observed in the coxib-like molecule **30d**, as expected. Likewise, γ-substituted derivatives **32a, 32b and 32c** were nontoxic up to 40 μM. This was a valuable finding since γ-hydroxymethylation was shown to boost antimicrobial activity *(vide infra)*.

In conclusion, this research brought very interesting data that were supported by closer investigations done within the research group.[98,99] Additional SAR studies that included syntheses of bioisosters and homologues lead to the discovery of analogues with more selective cytotoxic activity. Furthermore, it was discovered that the activity in novel halogenated diarylfuranones was also connected to the furanone ring. Active compounds with identical substituents based on furan lacked the cytotoxic activity. Since such difference was not observed in CA4 **1** and its direct analogues, we might be dealing with a novel class of compounds that might even possess a different mechanism of action. Further studies are certainly needed to confirm this hypothesis.

4.2.2 Antibacterial activity

In vitro screening for antibacterial activity was performed against a panel of both standard references and clinical isolates, including antibiotic-resistant strain MRSA. The broad-spectrum antibiotic ciprofloxacin (a fluoroquinolone derivative) was used as a standard. The results are summarized in Table 3.

The majority of combretafuranones involved in this study showed no or very low activity against the tested bacterial strains. However, halogenated γ-substituted lactone **32a** was able to inhibit *Staphylococcus aureus* strain ATCC 6538 at low MIC_{95} levels (7.81–15.62 μM). Its activity against methicillin-resistant clinical isolate in comparison with almost inactive ciprofloxacin was also interesting. This finding corresponded with the data obtained for other molecules prepared within the research group. It was mainly compounds bearing halogens (Br, Cl) in core **A** together with lipophilic para-substitution in core **B** and hydroxymethylation in γ-position that showed selective activities against *Staphylococcus aureus* comparable to ciprofloxacin.[98]

As previously mentioned, practically all γ-substituted derivatives, including **32a** were non-toxic up to 40 μM to human normal cells RPE-1 and BJ. Since they also possess improved solubility parameters, they can be considered for additional SAR and biological studies. Their further development as potential therapeutic agents is therefore well justified.

Table 3 Antimicrobial activities.

*Antimicrobial activities expressed as MIC (minimal inhibition concentration) of compounds **30a–b**, **30d–f**, **30h–i**, **31a–b** and **32a–c** against following strains: **SA**: Staphylococcus aureus ATCC 6538, **MRSA**: Staphylococcus aureus HK5996/08, **SE**: Staphylococcus epidermidis HK6966/08, **EF**: Enterococcus sp. HK14365/08, **EC**: Escherichia coli ATCC 8739, **KP**: Klebsiella pneumoniae HK11750/08, **KP-E**: Klebsiella pneumoniae HK14368/08; and **PA**: Pseudomonas aeruginosa ATCC 9027. Cipr = ciprofloxacin.*

Bacterial strain & Incubation time:		**Compound [MIC_{95}, µM]:**								
		30a	**30b**	**30d**	**30e, 30f, 30h, 30i, 31a**	**31b**	**32a**	**32b**	**32c**	**Cipr**
SA	24h	>1000	**62.5**	>500	>125	250	**7.81**	125	>500	0.98
	48h	>1000	125	>500	>125	500	**15.62**	125	>500	0.98
MRSA	24h	>1000	>500	>500	>125	250	**62.5**	125	500	500
	48h	>1000	>500	>500	>125	500	125	125	500	500
SE	24h	1000	125	>500	>125	250	250	**62.5**	250	250
	48h	>1000	250	>500	>125	500	250	**62.5**	250	250
EF	24h	>1000	>500	>500	>125	500	500	>125	>500	0.98
	48h	>1000	>500	>500	>125	500	>500	>125	>500	0.98
EC	24h	>1000	>500	>500	>125	>500	>500	>125	>500	0.06
	48h	>1000	>500	>500	>125	>500	>500	>125	>500	0.06
KP	24h	>1000	>500	>500	>125	>500	>500	>125	>500	0.12
	48h	>1000	>500	>500	>125	>500	>500	>125	>500	0.12
KP-E	24h	>1000	>500	>500	>125	>500	>500	>125	>500	>500
	48h	>1000	>500	>500	>125	>500	>500	>125	>500	>500
PA	24h	>1000	>500	>500	>125	>500	>500	>125	>500	3.90
	48h	>1000	>500	>500	>125	>500	>500	>125	>500	7.81

4.2.3 Antifungal activity

The antifungal activity testing was performed on a panel of fungal strains including both *Candida* species and filamentous fungi. No antifungal effects were detected up to 1 mM concentration.

4.3 Synthesis of purpurealidin analogues

The general synthetic design towards simplified amides is depicted in Scheme 14. The synthetic sequence starts with a four-step synthesis of purpurealidin E **26** or respective analogues **33a** and **33b** from tyramine **45** and these primary amines are coupled with miscellaneous aromatic carboxylic acids **50** to yield the final amides (purpurealidin analogues) of general structures **34** and **35**.

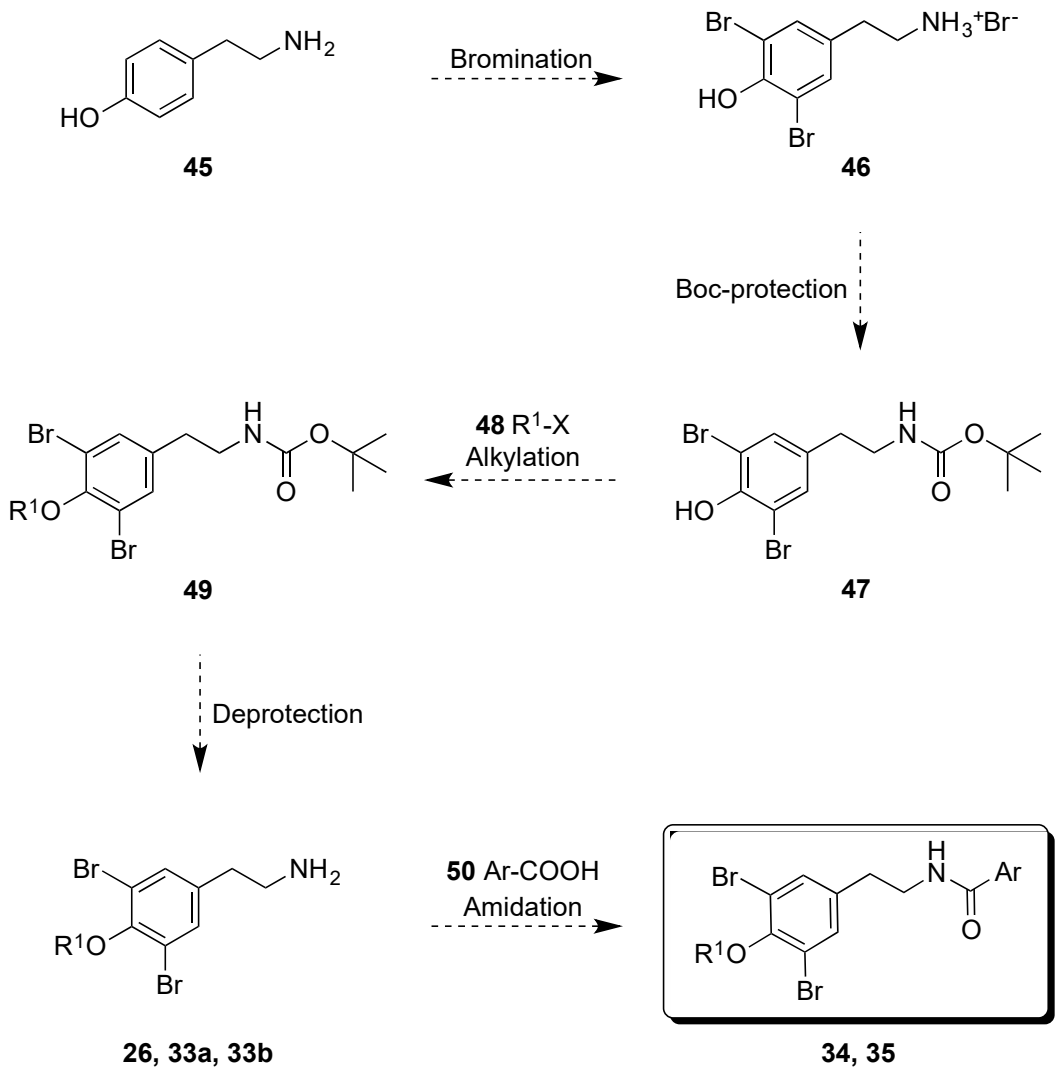

Scheme 14 The general route towards simplified purpurealidin analogues **34** and **35**.

4.3.1 Synthesis of purpurealidin E and its analogues

4.3.1.1 First step: Bromination of tyramine

The synthetic route started with the bromination of tyramine **45** under acidic conditions. The procedure previously described in the literature by Wada *et al.*[100] was used. As expected, the electrophilic aromatic substitution of tyramine **45** proceeded smoothly at room temperature due to the presence of activating substituents that stabilize the cationic intermediate. The desired product **46** crystallized out of the reaction mixture and was obtained in an excellent yield (97%; Scheme 15).

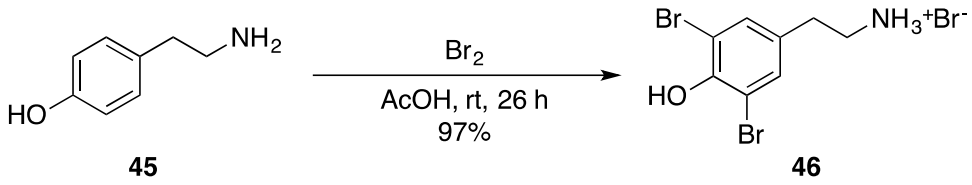

Scheme 15 Bromination of tyramine **45**.

The spectral data were in accordance with the previous publication,[101] although the signals of the phenolic group and ammonium moiety were also observed in the ^{1}H NMR spectrum. The former as a singlet located at 9.79 ppm, the latter as a broad singlet at 7.78 ppm.

4.3.1.2 Second step: Boc protection

The next step was Boc protection of the amino moiety to prevent nucleophilic substitution in the third step to occur on both phenolic hydroxyl and amine. Standard reaction conditions using 1.2 equivalents of di-*tert*-butyl dicarbonate in the presence of 3.0 equivalents of triethylamine in anhydrous methanol were used. The reaction was completed in 4 hours, and compound **47** was obtained in an excellent yield (98%) after an acidic work-up (Scheme 16).

The characteristic singlet for Boc group was detected at 1.44 ppm in the ^{1}H NMR spectrum. ^{13}C NMR signals corresponding to Boc group were located at 28.5, 77.0 and 155.9 ppm.

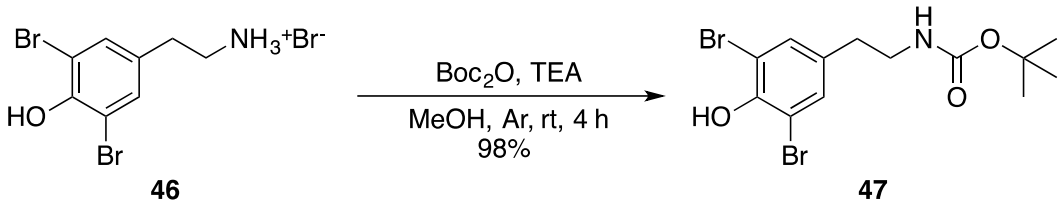

46 **47**

Scheme 16 Boc protection of bromotyramine **46**.

4.3.1.3 Third step: Alkylation

The third step allowed for a convenient variation of substituents by the means of Williamson ether synthesis. The procedure previously described for **49a** by Kottakota *et al.*[54] was used to alkylate the free phenolic hydroxyl in **47** (Scheme 17). Carbamate **47** was reacted with different halides **48a**–**c** (1.25 equiv.) under basic conditions (K_2CO_3, 2.5 equiv.) in refluxing acetone. The corresponding products **49a**–**c** were isolated in very good yields (85–89%). The suitable work-up method and crystallization improved the literature yield (75%) for the carbamate of purpurealidin E **49a**.

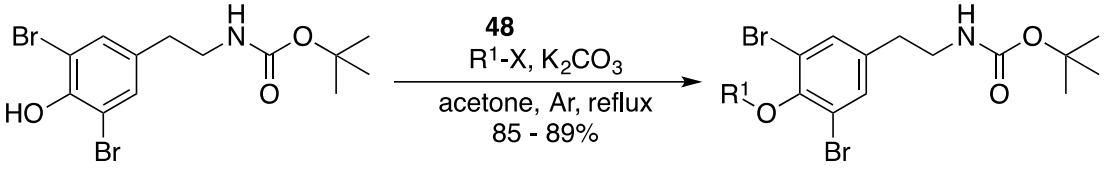

47 **49**

Halide:	Substituents:		Product:	Yield:
	R^1	X		
48a**	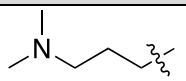	Cl	**49a**	85%
48b	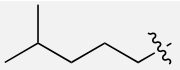	Br	**49b**	89%
48c**	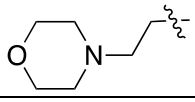	Cl	**49c**	88%

Scheme 17 Alkylation of phenolic hydroxyl in **47**.
***Halide reagent was used as hydrochloride.*

The reaction times varied significantly. While the alkylation with alkyl bromide **48b** was complete after 6 hours according to TLC analysis, in the case of alkyl chloride **48c** the starting material was still present in the reaction mixture after 29 hours of reflux. This can be explained by the different reactivity of primary halides with regard to the strength of C-X bond and stability of $X^{(-)}$ as a leaving group.[92,102] Furthermore, steric

reasons may have played a role in this reaction and the fact that half the amount of solvent was used in the case of the previous reaction with **48b**.

The work-up procedure was performed using 0.1 M NaOH/$CHCl_3$ in the case of **49a**. During the attempts to recrystallize the product from hexane, a brown side product appeared in the flask. Therefore the remaining solution without the brown side product was transferred by pipette into another flask and **49a** was obtained after subsequent recrystallization from hexane. NMR and HRMS analyses confirmed the presence of the desired product. The protons of dimethylamino group were observed as a singlet at 2.26 ppm in the ^{1}H NMR spectrum.

Later in the case of **49b**, only water was used in the extraction procedure and no brown side-product was observed during recrystallization. Furthermore, in order to avoid the use of $CHCl_3$ for extraction, EtOAc was used instead. Problems with solubility, however, occurred and DCM was thus chosen as a suitable solvent. The recrystallization was then effortlessly done from boiling hexane. The newly introduced alkyl chain gave 5 signals in the aliphatic region of the ^{1}H NMR spectrum, including a doublet at 0.93 ppm distinctive of terminal -C$\underline{H}_3$ groups.

The morpholine analogue **49c** was pre-purified by flash chromatography due to the oily nature of the crude material (probably due to the 4-day long reflux and possible side-products) and was subsequently recrystallized from hexane/DCM. Two multiplets in the ^{1}H NMR spectrum at 2.65–2.56 and 3.79–3.65 ppm were characteristic of the morpholine ring in the ^{1}H NMR spectrum.

4.3.1.4 Fourth step: Boc deprotection

The last step was quantitative removal of the Boc protecting groups in the compounds of general structure **49** using TFA in DCM (1:2) followed by a basic work-up procedure to obtain the corresponding free amines **26**, **33a** and **33b** (Scheme 18).

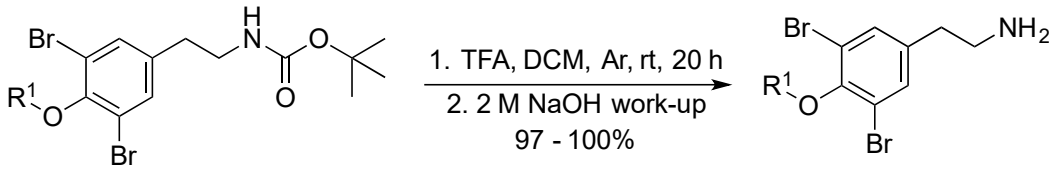

49 **26, 33a, 33b**

Starting material:	Substituent: R[1]	Product:	Yield:
49a	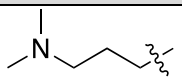	**Purpurealidin E 26**	99%
49b	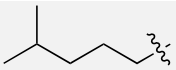	**33a**	97%
49c	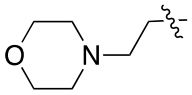	**33b**	100%

Scheme 18 Boc deprotection of compounds **49a–c**.

In the case of **49c**, the reaction was initially attempted with only 2.25 equivalents of TFA. However, no product was detected on TLC after 4 hours of stirring, although Kottakota *et al*. reported using as little as 1.2 equivalents for successful deprotection.[54] Therefore, the previously proven conditions were used again and yielded the desired product **33b**. The singlet typical of the Boc group disappeared from the ^{1}H NMR spectrum and a broad singlet characteristic of the -N$\underline{H}_2$ group was observed at 1.3 ppm for compounds **26** and **33a**.

In conclusion, purpurealidin E **26** was synthesized in four reaction steps in the overall yield of 80%, improving the literature yields 35–66%.[54,103,104] Two novel analogues **33a** and **33b** were obtained in very good overall yields 82% and 84%, respectively.

4.3.2 Syntheses of amides

The last step in the synthesis of simplified amides was the amidation reaction. A total of 13 amide analogues were synthesized and characterized by ^{1}H and ^{13}C NMR. Twelve of them were successfully purified, their structure and purity was confirmed by NMR and HRMS analysis and they were subjected to biological activity testing.

4.3.2.1 Reaction conditions

In the process of finding suitable reaction conditions, different coupling reagents (EDC•HCl, DIC) and different bases (DMAP, TEA, DIPEA) were tried at the beginning in order to obtain final purpurealidin analogues of general structure **34** (Scheme 19). However, a significant improvement in the reaction yields was not observed, mainly because of difficult purification.

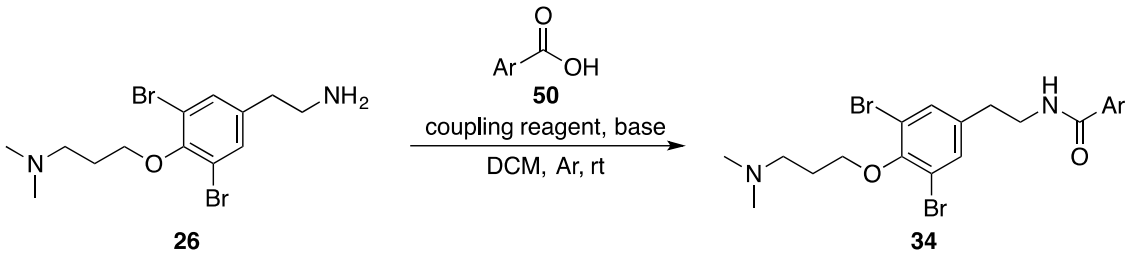

Starting material:	Substituent:	Reagents:			Product:	Yield:
Acid	Ar	Coupling reagent (equiv.)	Base (equiv.)	Additive		
50a	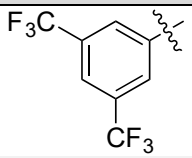	EDC•HCl (1.25 + 0.5)	TEA (2.0) then DMAP (1.0)	N/A	**34a**	0 %
50b	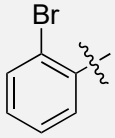	EDC•HCl (1.20)	DIPEA (2.4)	HOBt	**34b**	46%
50c	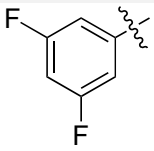	DIC (1.20)	DIPEA (2.4)	HOBt	**34c**	21%
50d	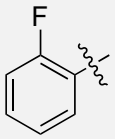	EDC•HCl (1.20)	DIPEA (2.4)	HOBt	**34d**	62%

Scheme 19 Amidation reaction.

Once the first compound was isolated in a satisfactory yield (above 50%), a general procedure began to be employed using EDC•HCl with the addition of HOBt to enhance the reactivity (Scheme 20).

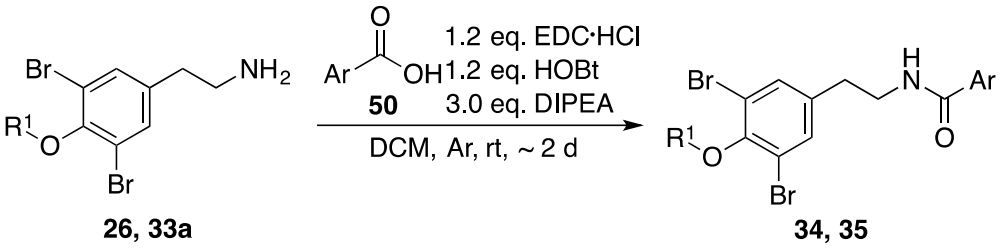

26, 33a **34, 35**

Starting material:		Substituents:		Product:	Yield:
Amine	Acid	R^1	Ar		
26	**50a**	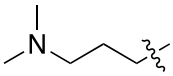	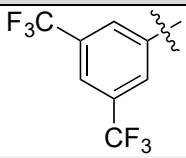	**34a**	30%
26	**50e**	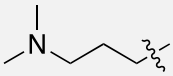	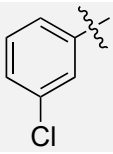	**34e**	N/A
26	**50f**	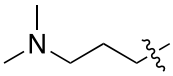	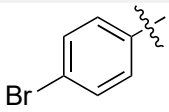	**34f**	59%
26	**50g**	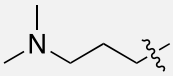	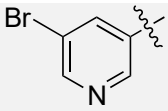	**34g**	57%
26	**50h**	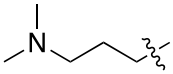	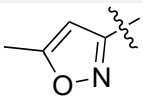	**34h**	13%
33a	**50i**	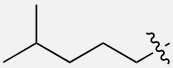	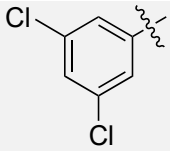	**35a**	63%
33a	**50j**	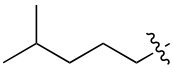	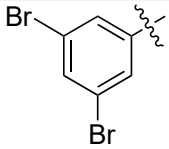	**35b**	59%

Scheme 20 Amidation using the general procedure.

N/A: Purification was unsuccessful - 58% yield containing 9% impurities.

Finally, the reaction was carried out using microwave irradiation under similar conditions. It was completed in 2 hours starting from purpurealidin E **26** and gave compound **34i** in a good yield (74%, Scheme 21).

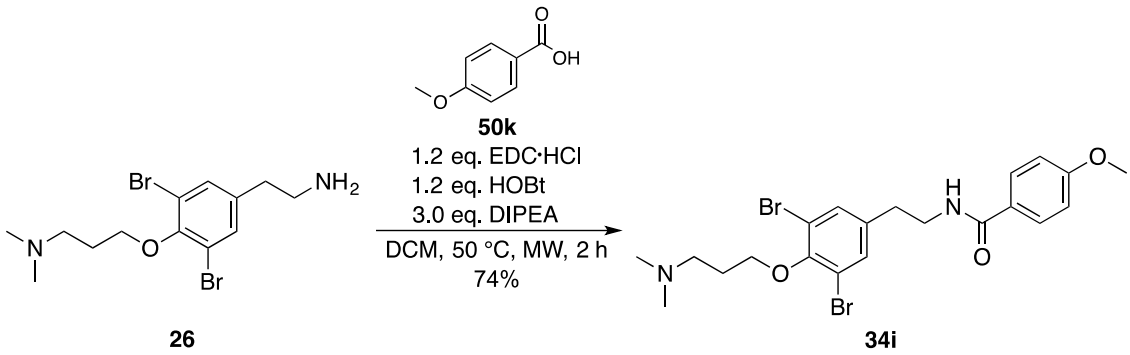

Scheme 21 Amidation using microwave irradiation.

4.3.2.2 Purification of amides and discussion

The purification of purpurealidin analogues was challenging from the beginning. Combination of acid-base extraction and Biotage chromatography were used in the group previously without success. Only a few derivatives were obtained after crystallization in poor yields < 30%.[104]

Upon analysing the reaction mixtures obtained, several compounds were detected together with a starting acid and DMAP that was used as a base. Therefore both the synthetic procedure and the purification method were subjected to modification. In order to remove the starting acid, only basic extraction was performed. Furthermore, based on a similar experience with the first reaction (**50a**) using DMAP, using DMAP was terminated even though it is known to accelerate peptide coupling reactions.[105] In principle, DMAP is soluble in water and should be removed during extraction. However, that did not happen, likely due to the basic nature of the reaction mixture and extraction procedure. During the flash chromatography, the product **50a** was eluted together with DMAP. Because the tertiary amine moiety is present in the final compounds, they tend to get retained on silica gel and the elution is difficult. That, together with the presence of a basic reagent and the basic starting material, contributed to the unsuccessful isolation. In order to minimize the problems mentioned, a volatile base – DIPEA was later employed.

Regarding the chromatography procedure, after the first unsuccessful flash chromatography of compound **50a**, a traditional column chromatography was performed in the case of compound **50b**. The solvent system hexane/acetone + 3% TEA used in a gradient elution provided a perfect and quick separation. However, a new

aliphatic impurity was detected by ^{1}H NMR compared to the analysis of the crude product. Since the same phenomenon was observed when purifying compounds **50c** and **50d**, it was concluded the impurity originated from the TEA reagent.

Subsequently, the Biotage flash chromatography was attempted again, finally with success. Due to the previous negative experience using TEA as a chromatography additive, another solvent system (DCM/MeOH) was chosen, in which the amine products were not tailing extensively. The procedure was optimized and started with elution using the weaker solvent (DCM). Once the first impurity was eluted, a gradient was set up to 20% MeOH. More hydrophilic impurities were eluted next, followed by the desired product (Fig. 17).

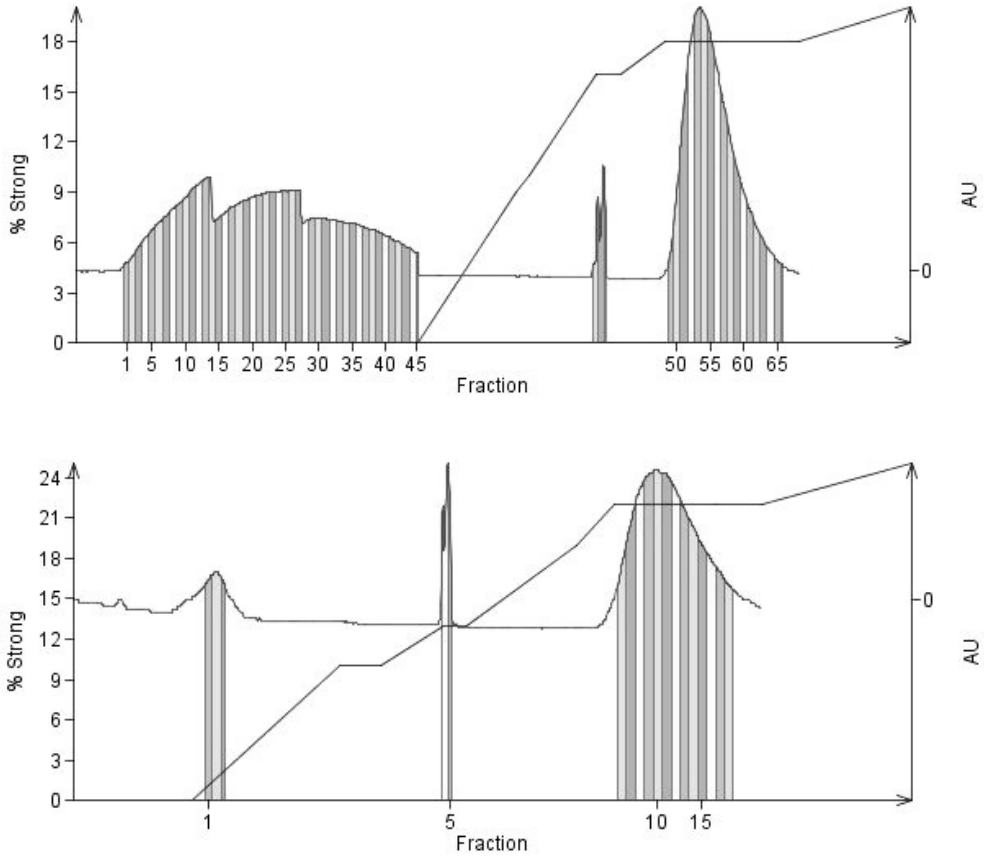

Figure 17 Examples of Biotage purification (compounds **34f** and **34g**) using a gradient elution. *Products **34f** and **34g**, respectively, can be seen as the tailing peaks at the right part of the chromatograms. The diagonal lines are marking the increasing gradient.*

Unfortunately, at some point during the syntheses, many compounds got contaminated with grease during transfer to smaller vials. Even though the amount of grease was

usually around 2% or less (according to ^{1}H NMR), since the compounds were to be used for biological testing, they had to be re-purified. In some cases, repeated purifications were done and only with a part of the product. This can explain the low yields obtained for many compounds.

Apart from compound **34e**, all other compounds were obtained in excellent purity and were characterized by ^{1}H, ^{13}C NMR and HRMS analyses. The signal of the newly formed amide bond was a broad singlet or triplet in the range 6.2–6.4 ppm in the ^{1}H NMR spectrum. In the ^{13}C NMR spectrum of compounds **34a**, **34c** and **34d**, the coupling of fluorine to carbon was clearly observed. 1-bond carbon–fluorine coupling ranged from 247.5–273.1 Hz, 2-bond from 11.6–34.0 Hz, 3-bond from 3.3–12.1 Hz and 4-bond from 2.2–2.9 Hz. Signals were seen as quartets or multiplets (**34a**), triplets, doublet of doublets or multiplets (**34c**) and doublets (**34d**).

4.3.3 Synthesis of non-brominated analogue

In order to obtain more diverse compounds for biological testing, a simple reaction route was performed once to obtain a non-brominated analogue of **27** – the first active purpurealidin analogue that inspired the project. Tyramine **45** was coupled with acid **50i** using HBTU to give amide **51** in a poor yield (30%). The amide **51** was then alkylated under the same conditions as above and gave the non-brominated analogue **36a** in a fair yield (68%). The compound was used in biological testing and therefore fully characterized by NMR and HRMS. In comparison with compounds based on the bromotyramine scaffold, a set of two multiplets typical of *p*-substitution of the aromatic core was observed in ^{1}H NMR at 7.15–7.08 and 6.90–6.83 ppm.

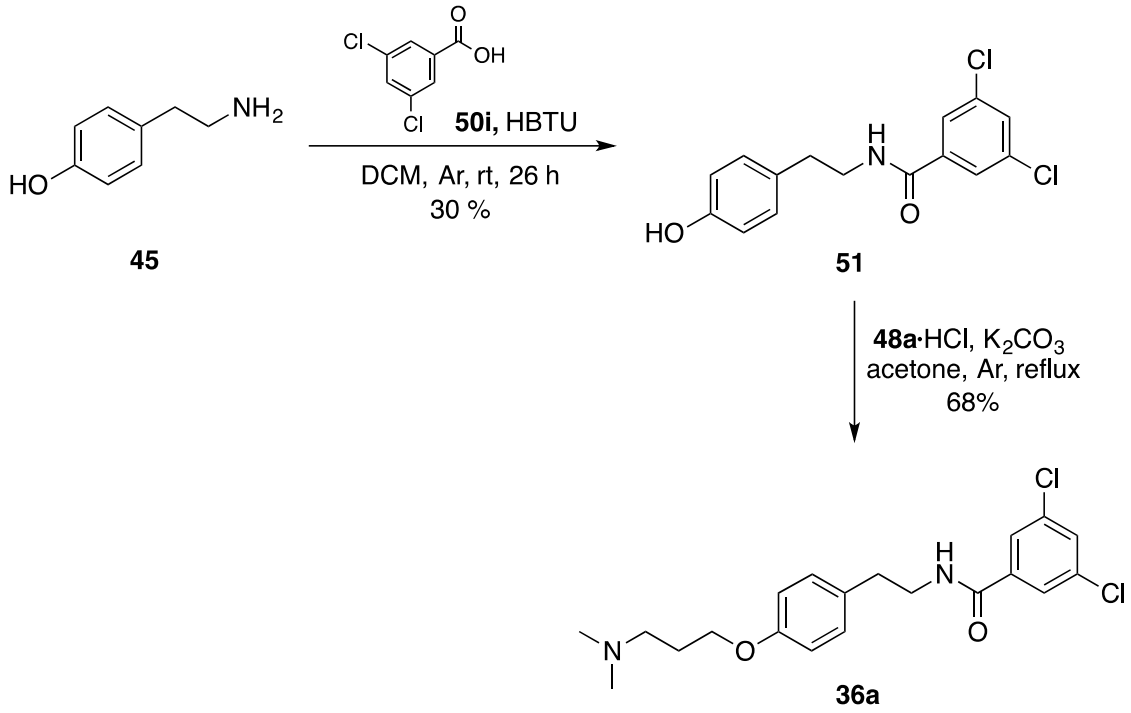

Scheme 22 The short route to the non-brominated analogue **36a**.

4.4 Biological activity of purpurealidin analogues

Secondary metabolites of marine sponges are known to possess various interesting bioactivities. 12 analogues prepared within this thesis project were tested for their ability to inhibit the cancer-related potassium channel $K_V10.1$ and were subsequently evaluated for their cytotoxicity. Structures of all tested compounds are summarized in Appendix C.

4.4.1 $K_V10.1$ channel inhibition

Since a preliminary screening in 2014 showed bromotyramine alkaloids were able to inhibit $K_V10.1$ channels, analogues were requested by the Catholic University of Leuven in order to study the structure-activity relationship. First, oocytes expressing $K_V10.1$ were prepared by microinjecting cRNA into *Xenopus laevis* oocytes. Afterwards, the inhibitory effect on $K_V10.1$ was evaluated electrophysiologically during perfusion of 40 µM of each compound as an extracellular solution. The average current inhibitions (%) are shown in Fig. 18.

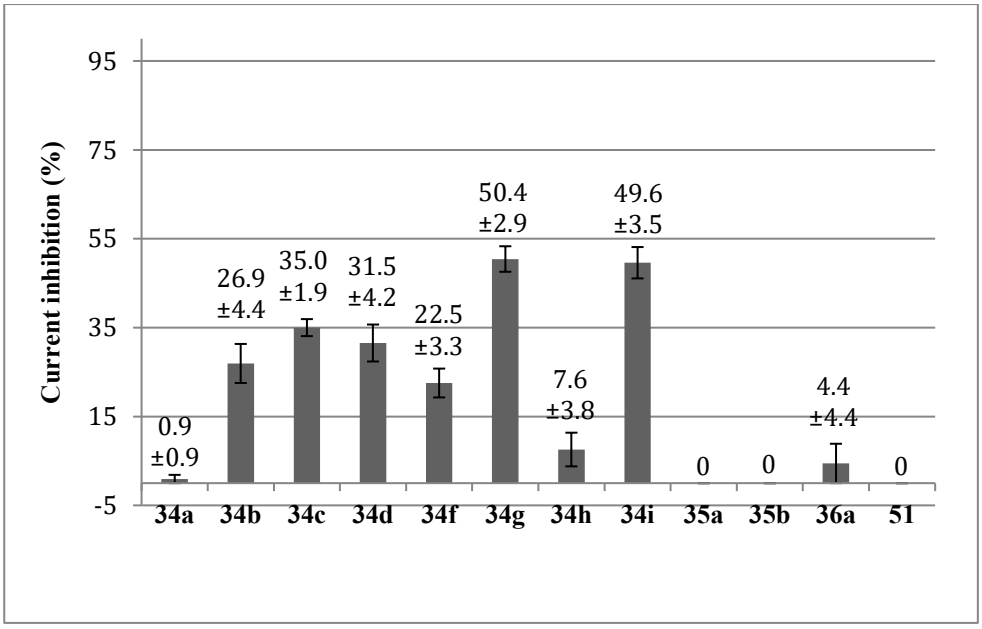

Figure 18 $K_V10.1$ current inhibition for each compound (40 µM).

Compounds **35a**, **35b** and **51** that lacked the tertiary amine moiety on the bromotyramine part showed no inhibition of the channel. Similarly, almost no activity

was observed for **36a** that lacked bromine substituents in the tyramine part. The tertiary amine moiety connected to bromotyramine was therefore found to be pivotal for the K_V10.1 channel inhibition.

The most potent modulators of K_V10.1 within this series were the amides of purpurealidin E **34g** and **34i** with inhibition of 50.4% and 49.6%, respectively. The 3-halogen substitution in **34g** and 4-methoxy substitution in **34i** and were later shown to be of high importance. The combination of all the features mentioned led to the discovery of a low micromolar inhibitor **52** (Fig. 19) that has served as a valuable tool for studying the properties and gating of the cancer-related potassium channel K_V10.1.[106]

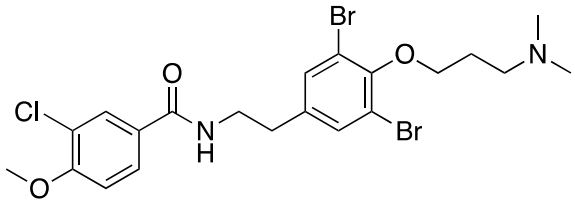

$IC_{50} = 7.7 \pm 1.0\ \mu M$

52

Figure 19 The most potent inhibitor discovered during direct continuation of the project.

4.4.2 Cytotoxicity

Since K_V10.1 inhibitors can be interesting anticancer drug lead compounds, all compounds tested for their K^+ channel inhibitory effects were also screened for their cytotoxicity. Initially, preliminary screening was performed against malignant melanoma A375 cells. The compounds were incubated with cells for 48 hours and tested in a dose-response fashion at 50 μM concentration. Overview of the results is provided in Fig. 20.

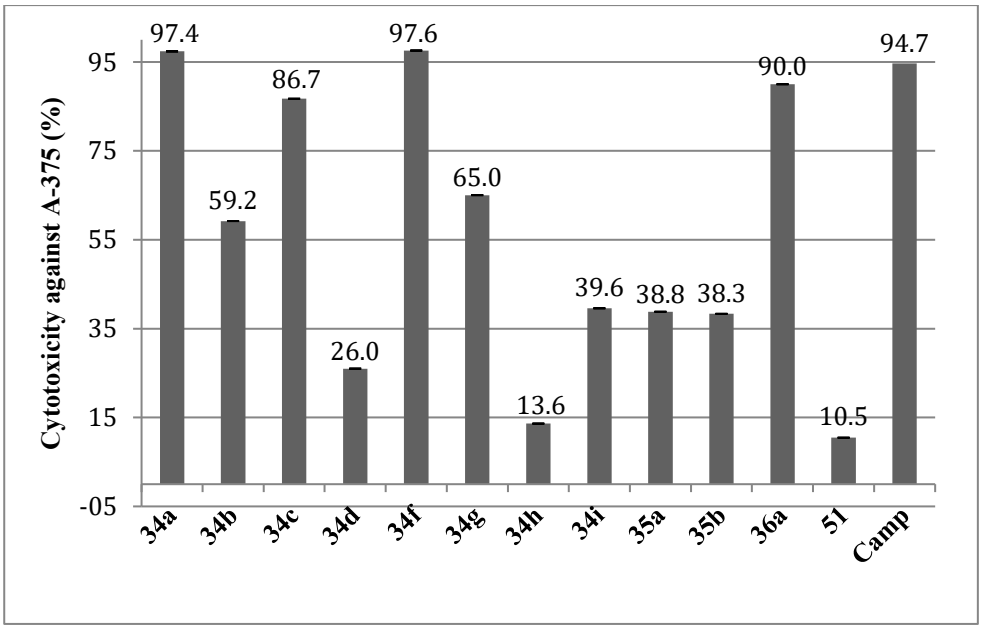

Figure 20 Preliminary cytotoxicity test results (50 μM).

Cell viability was assessed by determining the level of intracellular ATP in a luminescent assay. Whenever the cytotoxicity observed in preliminary testing was at least 80%, IC_{50} values were determined. Compounds with IC_{50} of less than 20 μM were then tested against normal foreskin fibroblast cells Hs27 to evaluate selectivity (Table 4).

Table 4 Cytotoxicity results against cancerous and non-cancerous cell line.
*A-375: Homo sapiens skin malignant melanoma; Hs27: Homo sapiens skin, foreskin normal; Camp: Camptothecin; n.d: Not determined; * Unable to fit the dose-response curve.*

Cell line	Cytotoxicity [IC_{50}, μM]												
	34a	**34b**	**34c**	**34d**	**34f**	**34g**	**34h**	**34i**	**35a**	**35b**	**36a**	**51**	**Camp**
A-375	**13.2**	n.d	33.5	n.d	**13.1**	n.d	n.d	n.d	n.d	n.d	27.7	n.d	0.1
Hs27	6.8	n.d	n.d	n.d	11.3	n.d	n.d	n.d	n.d	n.d	*	n.d	5.5

Unfortunately, compounds **34a** and **34f** that showed low-micromolar activities against melanoma cell line A-375 were also toxic to healthy cells Hs27. Further development of simplified purpurealidin analogues as anti-cancer agents was therefore terminated.

5 CONCLUSIONS

The main aim of this thesis was the synthesis of natural product analogues inspired by combretastatin A-4 **1** and purpurealidin I **2**.

Within the combretafuranone project, eight lactones **30a–f** and **30h–i** were prepared in poor to excellent overall yields. Synthesis of nitro derivative **30g** was unsuccessful due to problems occurring in the cyclization step. Derivatizations towards more hydrophilic derivatives resulted in five more analogues **31a–b** and **32a–c**. One product of dealkylation, compound **31c**, was not isolated and the synthesis of aminomethylated derivative **30d** was not successful due to the formation of a dehydration product.

Twelve final combretafuranones were screened for their cytotoxic, antibacterial and antifungal activity. Analogues **30a–b**, **30e-i** and **31b** exhibited cytotoxic effects. The highest cytotoxic effects in nanomolar range were found in derivatives **30a**, **30h**, **30i** that combined halogen substitution in core **A** and 4-CH_3 or 4-OCH_3 substituent in core **B**. Unfortunately, the analogues were relatively toxic to the non-malignant cell line RPE-J. Compounds bearing oxygenated substituents with a lower degree of oxygenation compared to CA4 **1** were not as active. γ-Hydroxymethylation was shown to knock out cytotoxic effect completely, and, in the case of compound **32a**, boosted activity towards *Staphylococcus aureus*. All evaluated compounds were antifungally inactive.

Within the purpurealidin project, purpurealidin E **26** and its two novel analogues **33a** and **33b** were obtained first in very good overall yields. Subsequent coupling with acids yielded desired purpurealidin analogues. Modifications in the synthesis and work-up procedure together with the use of flash chromatography lead to successful isolations of the target amides. Only derivative **34e** was not purified. Compounds were obtained in poor to moderate yields mainly due to grease contamination. However, the last procedure developed under microwave irradiation provided satisfactory yield. Furthermore, one non-brominated analogue, compound **36a**, was synthesized through shortened route.

12 purpurealidin analogues were evaluated for their cytotoxicity and inhibitory activity towards $K_V10.1$. Compounds **34f** and **34a** showed low micromolar activities against melanoma cell line A-375, but were also toxic to healthy cells. The most potent modulators of $K_V10.1$ were amides **34g** and **34i** with inhibition of 50.4% and 49.6% at 40 μM, respectively. The 4-methoxy and 3-halogen substitution, bromotyramine unit and aminoalkyl moiety increased the inhibitory activity against $K_V10.1$.

In conclusion, 27 analogues were successfully synthesized and obtained in high purity after three- to five-step syntheses. 24 of these analogues were subjected to testing for their biological activity and some possessed interesting biological properties. In four cases, either purification or synthetic method was unsuccessful. Most importantly, both projects provided valuable structure-activity data that served as a basis for further research and discovery of more selective analogues. It can be concluded that secondary plant and marine metabolites continue to serve as interesting sources of compounds with bioactive properties.

6 EXPERIMENTAL SECTION

6.1 Combretafuranone analogues

6.1.1 Reagents and devices

All reactions were carried out using commercially available starting materials and used without further purification unless otherwise stated. Solvents (THF, DCM) were distilled prior to use from sodium and calcium hydride, respectively. ^{1}H and ^{13}C NMR spectra were recorded with Varian Mercury VxBB 300 or VNMR S500 instruments. Chemical shifts (δ) are given in parts per million (ppm) relative to the NMR reference solvent signals ($CDCl_3$: 7.26 ppm and 77.16 ppm; CD_3OD: 3.31 ppm and 49.0 ppm). Multiplicities are indicated by s (singlet), br s (broad singlet), br t (broad triplet), d (doublet), dd (doublet of doublet), ddd (doublet of doublets of doublets), t (triplet), q (quartet) and m (multiplet). The coupling constants *J* are quoted in Hertz (Hz). IR spectra were recorded on a Nicolet 6700 FT-IR equipped with an ATR device. MS data were measured on an Agilent Tech 500 Iontrap spectrometer. HR-MS data were recorded on a QTOF mass spectrometer using the electrospray ionization mode. Column chromatography was carried out using Merck Silica gel 60 (0.040–0.063 mm). TLC analyses were performed using Merck TLC Silica gel 60-F_{254} TLC plates and visualized by UV in combination with staining [solution of: $Ce(SO_4)_2 \bullet 4H_2O$ (2 g), $H_3[P(Mo_3O_{10})_4]$ (4 g), conc. H_2SO_4 (10 mL), H_2O (200 mL)] and plate heating.

6.1.2 Synthesis of combretafuranone analogues

6.1.2.1 Syntheses of bromides

6.1.2.1.1 2-Bromo-1-(4-methoxyphenyl)ethan-1-one (38a)

Acetanisole **37a** (1.01 g, 6.75 mmol) and PHT (3.35 g, 6.75 mmol, 1.0 equiv.) were dissolved in THF (50 mL). The reaction mixture was stirred at room temperature for 44 hours during which the mixture turned into a white suspension. The mixture was then filtered and the solvent was removed *in vacuo*. The crude product was dissolved in diethylether (50 mL) and washed with sat. NaCl (3 × 60 mL). The organic layer was dried over Na_2SO_4, filtered and the solvent was removed *in vacuo* to give yellow viscous liquid (mixture of **38a** and **42a** according to ^{1}H NMR and TLC) that was used in subsequent reactions without purification or characterization.

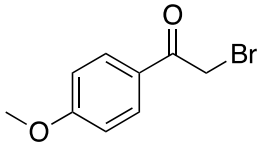

6.1.2.1.2 2-Bromo-1-(4-(methylsulfonyl)phenyl)ethan-1-one (38b)

4'-(Methylsulfonyl)acetophenone **37b** (3.40 g, 17.2 mmol) and pyridinium tribromide (5.49 g, 17.2 mmol, 1.0 equiv.) were dissolved in CH_3COOH (80 mL). The reaction mixture was stirred at room temperature for 53 hours. The reaction mixture was then extracted with EtOAc (180 mL) and washed with Na_2CO_3 (4 × 120 mL). The organic layer was dried over Na_2SO_4, filtered and the solvent was removed *in vacuo.* The oily crude mixture was put into a freezer and it solidified. The resultant yellow solid was washed with cold hexane several times (30 mL) to give **38b** as a beige solid (2.55 g, 54% yield).

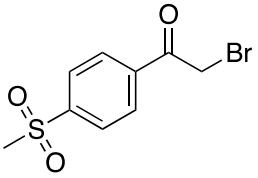

^{1}H NMR (500 MHz, $CDCl_3$) δ 8.19–8.14 (m, 2H), 8.09–8.05 (m, 2H), 4.46 (s, 2H), 3.09 (s, 3H); **^{13}C NMR** (126 MHz, $CDCl_3$) δ 190.3, 145.0, 138.0, 130.0, 128.1, 44.4, 30.4.

6.1.2.1.3 2-Bromo-1-(3,4-dimethoxyphenyl)ethan-1-one (38c)

3',4'-Dimethoxyacetophenone **37c** (3.00 g, 16.7 mmol) and pyridinium tribromide (90%, 5.91 g, 16.7 mmol, 1.0 equiv.) were dissolved in THF (50 mL). The reaction mixture was heated to 40 °C and a white precipitate formed. The mixture was then stirred for 1 hour after

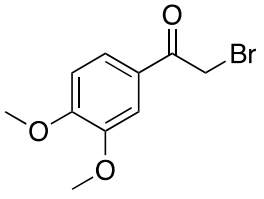

which the starting material could not be detected using TLC (hexane/EtOAc, 1:1). The mixture was then filtered and the solvent was removed *in vacuo*. The crude was adsorbed on a silica plug and the product was eluted using a gradient elution: hexane/EtOAc (85:15 → 70:30). The yellow viscous liquid gained (6.38 g) was a mixture of mono and dibrominated derivative (**38c** and **42c**, respectively) and it was used in subsequent reactions without further purification or characterization.

6.1.2.1.4 2-Bromo-1-(4-methoxy-3-nitrophenyl)ethan-1-one (38d)

4'-Methoxy-3'-nitroacetophenone **37d** (1.80 g, 9.22 mmol) and PHT (4.57 g, 9.22 mmol, 1.0 equiv.) were dissolved in THF (40 mL). The resultant red mixture was stirred at room temperature for 18 hours. TLC analysis (hexane/EtOAc, 1:1) indicated the starting material was still present in the reaction mixture. Thus the reaction mixture was stirred for an additional day. Then it was filtered and the solvent was removed *in vacuo*. The orange crude oil was adsorbed on a silica plug and the product was eluted using hexane/EtOAc, 8:2. The gained yellow solid was a mixture of mono and dibrominated derivative (**38d** and **42d**, respectively) and it was used in subsequent reactions without further purification or characterization.

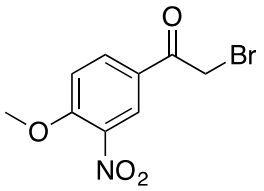

6.1.2.2 Synthesis of protected acid

6.1.2.2.1 Methyl 2-(3-hydroxy-4-methoxyphenyl)acetate (43)

3-Hydroxy-4-methoxyphenylacetic acid **39a** (2.18 g, 11.9 mmol) was dissolved in MeOH (50 mL). DOWEX® 50W (1.10 g, approx. 1:1 weight ratio) was added and the mixture was stirred for 5 hours at room temperature. TLC (hexane/EtOAc, 2:8) indicated there was still a lot of starting material (R_f 0.47) in the reaction mixture. The mixture was therefore stirred for additional 23 hours after which TLC indicated the reaction had completed. The reaction mixture was then filtered twice (using first cotton wool, then paper filter) and the solvent was removed *in vacuo* to give **43** as a white solid (2.33 g, 100%).

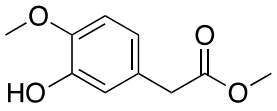

***R*f** 0.75 (hexane/EtOAc, 2:8); **^{1}H NMR** (500 MHz, $CDCl_3$) δ 6.87 – 6.85 (m, 1H), 6.81 – 6.78 (m, 1H), 6.76 – 6.73 (m, 1H), 3.86 (s, 3H), 3.68 (s, 3H), 3.53 (s, 2H); **^{13}C NMR** (126 MHz, $CDCl_3$) δ 172.4, 145.9, 145.7, 127.3, 120.9, 115.7, 110.9, 56.1, 52.1, 40.7.

6.1.2.2.2 Methyl 2-(3-(benzyloxy)-4-methoxyphenyl)acetate (44)

Methylester **43** (2.27 g, 11.6 mmol) was dissolved in dry DMSO (40 mL) under argon atmosphere at 0 °C. Sodium hydride 60% dispersion in mineral oil (510 mg, 12.8 mmol, 1.1 equiv.) was subsequently added in a single batch and the mixture was stirred until gas evolution ceased (30 min). Benzyl bromide (1.45 mL, 12.2 mmol, 1.05 equiv.) was then added dropwise and the mixture was stirred at room temperature as a purple suspension. TLC (hexane/EtOAc, 1:1) indicated the reaction had completed within 40 minutes. The reaction was left stirred for additional 18 hours after which it was quenched with sat. NaCl (30 mL) and extracted with EtOAc (3 × 40 mL). The combined organic layers were dried over Na_2SO_4, filtered and the solvent was removed *in vacuo*. The crude product was purified by silica gel column chromatography using a gradient elution: hexane/EtOAc (1:0 → 8:2) to give **44** as a white solid (3.21 g, 97% yield). R_f 0.71 (hexane/EtOAc, 9:1). The compound was used in the next step without further purification or characterization.

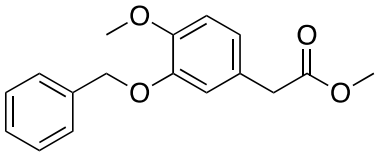

6.1.2.2.3 2-(3-(Benzyloxy)-4-methoxyphenyl)acetic acid (39b)

To the stirred suspension of ester **44** (3.19 g, 11.1 mmol) in MeOH (30 mL) was added a warm solution of NaOH (4.47 g, 0.11 mol, 10.0 equiv.) in water (30 mL). The mixture was then sonicated in order to dissolve the starting material without success. Subsequently, the mixture was vigorously stirred at room temperature for 27 hours. Then it was extracted with EtOAc and the organic layer was disposed of. The aqueous layer was acidified with conc. H_2SO_4 to pH ~ 1 and extracted with EtOAc (3 × 80 mL). The combined organic layers were dried over Na_2SO_4, filtered and the solvent was removed *in vacuo* to give **39b** as a white solid (2.94 g, 92% yield).

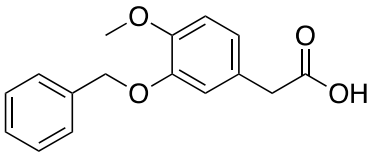

***R*f** 0.33 (hexane/EtOAc, 1:1, tailing); **^{1}H NMR** (500 MHz, $CDCl_3$) δ 7.46–7.42 (m, 2H), 7.39–7.33 (m, 2H), 7.32–7.27 (m, 1H), 6.88–6.82 (m, 3H), 5.14 (s, 2H), 3.87 (s, 3H), 3.54 (s, 2H); **^{13}C NMR** (126 MHz, $CDCl_3$) δ 178.0, 149.2, 148.3, 137.1, 128.6, 128.0, 127.6, 125.8, 122.3, 115.5, 112.1, 71.2, 56.2, 40.6.

6.1.2.3 Syntheses of esters

Esters were synthesized and worked-up using the general method as follows, unless otherwise stated.

General method:

Bromide **38a**–**e** (0.85–16.7 mmol) and substituted phenylacetic acid **39b**–**h** (1.0 equiv.) were dissolved in dry freshly-distilled THF (5 mL per 1 mmol) under argon atmosphere. To the solution was dropwise added dry TEA (1.0 equiv.) and the mixture was refluxed for 4 hours. It was then allowed to cool to room temperature and concentrated *in vacuo*. The crude mixture was extracted with EtOAc (3–10 mL per mmol) and washed with 5% Na_2CO_3 (2 ×; compounds **40a**–**40d**) or brine (2 ×; compounds **40e**–**40i**). The organic layer was dried over Na_2SO_4, filtered and the solvent was removed *in vacuo*.

6.1.2.3.1 2-(4-Methoxyphenyl)-2-oxoethyl 2-(4-bromophenyl)acetate (40a)

The title compound was prepared twice in separate reactions using the same method.

1st try: The compound **40a** was synthesized using the general method, starting from bromide **38a** (the crude mixture, 0.54 g, 2.36 mmol) and 4-bromophenylacetic acid **39c** (0.50 g, 2.36 mmol, 1.0 equiv.). The worked-up mixture was purified by silica gel column chromatography using a gradient elution: hexane/EtOAc (95:5 → 75:25) to give **40a** as a white solid (410 mg, 48% yield).

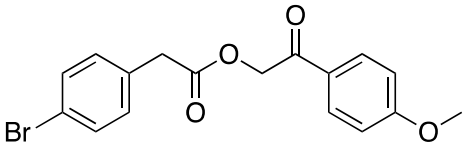

2nd try: Starting from commercially available 4-methoxyphenacyl bromide **38a** (3.75 g, 16.35 mmol) and 4-bromophenylacetic acid **39c** (3.46 g, 16.35 mmol, 1.0 equiv.) The worked-up mixture was purified by silica gel column chromatography using a gradient elution: hexane/EtOAc (9:1 → 8:2) to give **40a** as a white solid (4.98 g, 84% yield).

***R*f** 0.22 (hexane/EtOAc, 9:1); **^{1}H NMR** (500 MHz, $CDCl_3$) δ 7.90–7.82 (m, 2H), 7.49–7.43 (m, 2H), 7.25–7.20 (m, 2H), 6.98–6.89 (m, 2H), 5.31 (s, 2H), 3.87 (s, 3H), 3.77 (s, 2H); **^{13}C NMR** (126 MHz, $CDCl_3$) δ 190.4, 170.7, 164.2, 132.7, 131.8, 131.3, 130.2, 127.3, 121.4, 114.2, 66.3, 55.7, 40.4.

6.1.2.3.2 2-(4-Methoxyphenyl)-2-oxoethyl 2-(2,6-dichlorophenyl)acetate (40b)

The title compound was synthesized using the general method, starting from bromide **38a** (the crude mixture, 195 mg, 0.851 mmol) and 2,6-dichlorophenylacetic acid **39d** (175 mg, 0.851 mmol, 1.0 equiv.). The worked-up mixture was purified by silica gel column chromatography using a gradient elution hexane/EtOAc (9:1 → 75:25) to give **40b** as a white solid (146 mg, 48% yield).

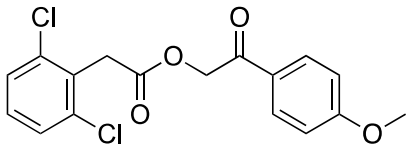

***R*f** 0.27 (hexane/EtOAc, 8:2); **^{1}H NMR** (500 MHz, $CDCl_3$) δ 7.90–7.84 (m, 2H), 7.33 (d, J = 8.1 Hz, 2H), 7.19–7.15 (m, 1H), 6.96–6.90 (m, 2H), 5.33 (s, 2H), 4.22 (s, 2H), 3.87 (s, 3H); **^{13}C NMR** (126 MHz, $CDCl_3$) δ 190.4, 169.2, 164.2, 136.4, 131.0, 130.3, 129.2, 128.2, 127.4, 114.2, 66.5, 55.7, 36.5.

6.1.2.3.3 2-(4-Methoxyphenyl)-2-oxoethyl 2-(3,4-dichlorophenyl)acetate (40c)

The title compound was synthesized using the general method, starting from bromide **38a** (the crude mixture, 1.90 g, 8.29 mmol) and 3,4-dichlorophenylacetic acid **39e** (1.70 g, 8.29 mmol, 1.0 equiv.). Unlike in the general procedure, the reaction mixture was stirred for 40 hours at room temperature. The worked-up mixture was purified by silica gel column chromatography using a gradient elution: hexane/EtOAc (1:0 → 1:1) to give **40c** as a white solid (1.77 g, 64% yield).

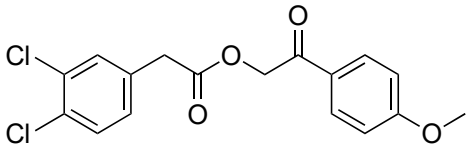

***R*f** 0.29 (hexane/EtOAc, 8:2); **^{1}H NMR** (500 MHz, $CDCl_3$) δ 7.89–7.82 (m, 2H), 7.45 (d, J = 2.1 Hz, 1H), 7.42–7.37 (m, 1H), 7.20 (ddd, J = 8.3, 2.1, 0.5 Hz, 1H), 6.96–6.91 (m, 2H), 5.32 (s, 2H), 3.87 (s, 3H), 3.77 (s, 2H); **^{13}C NMR** (126 MHz, $CDCl_3$) δ 190.3, 170.3, 164.3, 133.8, 132.7, 131.6, 131.5, 130.6, 130.2, 129.1, 127.2, 114.2, 66.5, 55.7, 40.0.

6.1.2.3.4 2-(4-(Methylsulfonyl)phenyl)-2-oxoethyl 2-(4-methoxyphenyl)acetate (40d)

The title compound was synthesized using the general method, starting from bromide **38b** (1.51 g, 5.46 mmol) and 4-methoxyphenylacetic acid **39f** (0.91 g, 5.46 mmol, 1.0 equiv.). Unlike in the general procedure, the mixture was refluxed for 4 hours and then stirred at room temperature for additional 20 hours. The brown solid crude was purified by silica gel column chromatography using a gradient elution: hexane/EtOAc (8:2 → 6:4) to give **40d** as a white solid (1.60 g, 81% yield). The compound was used in the next step without characterization.

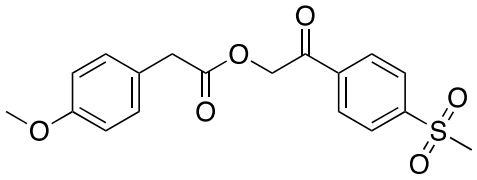

6.1.2.3.5 2-(3,4-Dimethoxyphenyl)-2-oxoethyl 2-(4-methoxyphenyl)acetate (40e)

The title compound was synthesized using the general method, starting from bromide **38c** (the crude mixture, 4.31 g, 16.7 mmol) and 4-methoxyphenylacetic acid **39f** (2.77 g, 16.7 mmol, 1.0 equiv.). The worked-up mixture was purified by silica gel column chromatography eluting with hexane/EtOAc (7:3) to give **40e** as orange oil (2.64 g, 46% yield).

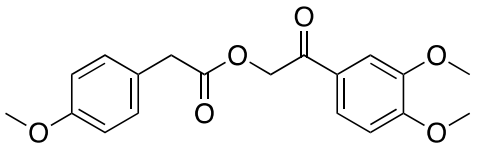

***R*f** 0.18 (hexane/EtOAc, 7:3); **^{1}H NMR** (500 MHz, $CDCl_3$) δ 7.49–7.44 (m, 2H), 7.28–7.24 (m, 2H), 6.90–6.84 (m, 3H), 5.31 (s, 2H), 3.94 (s, 3H), 3.91 (s, 3H), 3.79 (s, 3H), 3.76 (s, 2H); **^{13}C NMR** (126 MHz, $CDCl_3$) δ 190.8, 171.5, 158.9, 154.0, 149.4, 130.5, 127.5, 125.8, 122.3, 114.1, 110.3, 110.1, 66.1, 56.2, 56.1, 55.4, 40.1.

6.1.2.3.6 2-(3,4-Dimethoxyphenyl)-2-oxoethyl 2-(3,4-methylenedioxophenyl)acetate (40f)

The title compound was synthesized using the general method, starting from bromide **38c** (the crude mixture, 3.91 g, 15.1 mmol) and 2-(3,4-methylendioxophenyl)acetic acid **39g** (2.99 g, 16.6 mmol, 1.1 equiv.). Unlike in the general procedure, the mixture was refluxed for 2 hours and 30 minutes. The worked-up product was purified by silica gel column chromatography eluting with hexane/EtOAc (7:3) to give **40f** as yellow oil (1.84 g, 34% yield). The compound was used in the next step without characterization.

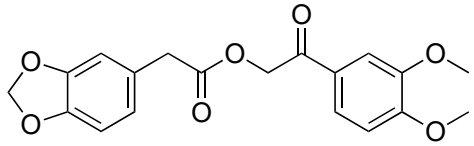

6.1.2.3.7 2-(4-Methoxy-3-nitrophenyl)-2-oxoethyl 2-(3-(benzyloxy)-4-methoxyphenyl)acetate (40g)

The title compound was synthesized using the general method, except 1.15 equivalents of bromide **38d** (the crude mixture, 0.84 g, 3.05 mmol, 1.15 equiv.) were used with respect to the acid **39b** (0.72 g, 2.66 mmol). The crude product was purified by silica gel column chromatography eluting with hexane/EtOAc (6:4) to give **40g** as a yellow solid (0.82 g, 66% yield).

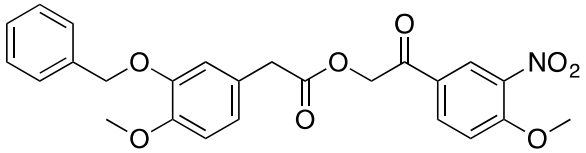

^{1}H NMR (500 MHz, $CDCl_3$) δ 8.35 (d, J = 2.2 Hz, 1H), 8.04 (dd, J = 8.8, 2.2 Hz, 1H), 7.47–7.42 (m, 2H), 7.38–7.33 (m, 2H), 7.31–7.26 (m, 1H), 7.12 (d, J = 8.9 Hz, 1H), 6.92 (d, J = 1.9 Hz, 1H), 6.88–6.81 (m, 2H), 5.22 (s, 2H), 5.14 (s, 2H), 4.02 (s, 3H), 3.87 (s, 3H), 3.69 (s, 2H); **^{13}C NMR** (126 MHz, $CDCl_3$) δ 189.6, 171.2, 156.8, 149.1, 148.3, 139.4, 137.2, 133.8, 128.6, 127.9, 127.6, 126.6, 125.8, 122.3, 115.2, 113.7, 112.0, 71.1, 66.2, 57.1, 56.1, 40.4.

Note: Overlapping peaks in the aromatic region in ^{13}C NMR spectrum.

6.1.2.3.8 2-Oxo-2-(*p*-tolyl)ethyl 2-(2,4-dichlorophenyl)acetate (40h)

2-(2,4-Dichlorophenyl)acetic acid **39h** (2.43 g, 11.9 mmol) was dissolved in dry THF (35 mL) under argon atmosphere. To the solution was dropwise added TEA (1.30 mL, 9.35 mmol, 0.79 equiv.) and the mixture was stirred for 15 minutes. Then, 2-bromo-1-(*p*-tolyl)ethan-1-one **38d** (90%, 3.02 g, 11.9 mmol) was

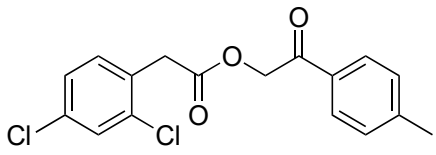

added and the mixture was brought to reflux. After 4 hours of reflux, the starting material was still detected by TLC (R_f 0.60, hexane/EtOAc, 8:2) and the mixture was thus stirred overnight. Then, additional TEA (0.470 mL, 3.37 mmol, 0.28 equiv.) was added due to previous miscalculation. The reaction mixture was refluxed for additional 18 hours after which TLC showed a complete consumption of the starting material. The mixture was then extracted with EtOAc (1 × 40 mL), washed with sat. NaCl (2 × 40 mL) and the water phase was re-extracted again with EtOAc (1 × 60 mL). The combined organic layers were dried over Na_2SO_4, filtered and the solvent was removed *in vacuo*. The crude product was purified by silica gel column chromatography using a gradient elution: hexane/EtOAc (9:1 → 6:4) to give **40h** as a white solid (3.81 g, 95% yield).

***R*f** 0.42 (hexane/EtOAc, 8:2); **^{1}H NMR** (500 MHz, $CDCl_3$) δ 7.82–7.75 (m, 2H), 7.41 (d, J = 2.2 Hz, 1H), 7.35 (d, J = 8.2 Hz, 1H), 7.28–7.22 (m, 3H), 5.35 (s, 2H), 3.94 (s, 2H), 2.42 (s, 3H); **^{13}C NMR** (126 MHz, $CDCl_3$) δ 191.5, 169.8, 145.1, 135.4, 134.1, 132.5, 131.8, 130.8, 129.7, 129.4, 128.0, 127.4, 66.6, 38.2, 21.9.

6.1.2.3.9 2-Oxo-2-(p-tolyl)ethyl 2-(3,4-dichlorophenyl)acetate (40i)

The title compound was synthesized using the general method, starting from commercially available 2-bromo-1-(*p*-tolyl)ethan-1-one **38d** (90%, 3.41 g, 14.4 mmol) and 3,4-dichlorophenylacetic acid **39e** (2.95 g, 14.4 mmol). Unlike in the general procedure, the mixture was refluxed for 19 hours. The crude product was purified by silica gel column chromatography eluting with hexane/EtOAc (9:1) to give **40i** as a white solid (4.15 g, 86% yield).

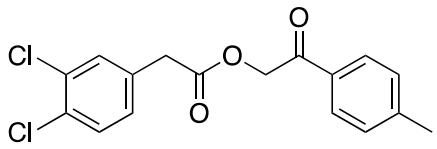

***R*f** 0.47 (hexane/EtOAc, 8:2); **^{1}H NMR** (500 MHz, $CDCl_3$) δ 7.80–7.76 (m, 2H), 7.45 (d, J = 2.1 Hz, 1H), 7.41 (d, J = 8.3 Hz, 1H), 7.29–7.25 (m, 2H), 7.23–7.19 (m, 1H), 5.34 (s, 2H), 3.77 (s, 2H), 2.42 (s, 3H); **^{13}C NMR** (126 MHz, $CDCl_3$) δ 191.4, 170.2, 145.1, 133.8, 132.6, 131.7, 131.6, 130.6, 129.7, 129.0, 128.0, 66.6, 39.9, 21.9.

Note: one peak in ^{13}C NMR cannot be detected in the aromatic region.

6.1.2.4 Target combretafuranones

Target combretafuranones were synthesized and worked-up using the following general method, unless otherwise stated:

Ketoester **40a**–**40i** (0.41–13.5 mmol) was dissolved in dry DMSO (5 mL per mmol) under argon atmosphere. Sodium hydride 60% dispersion in mineral oil (1.0 equiv.) was then added and the mixture was stirred for 90 minutes during which gas evolution was observed and the initially yellow solution darkened to wine red or black. Then, 1M HCl was added to the mixture (to pH~1) during which the solution warmed and usually changed its color (to bright yellow; orange). The reaction mixture was then extracted with EtOAc (5–10 mL per mmol) and washed with 5% Na_2CO_3 (3 × 5–10 mL per mmol). The organic layer was dried over Na_2SO_4, filtered and the solvent was removed *in vacuo*.

6.1.2.4.1 3-(4-Bromophenyl)-4-(4-methoxyphenyl)-2,5-dihydrofuran-2-one (30a)

The title compound was prepared twice in separate reactions using the same method.

1st try: The title compound was synthesized using the general method starting from ketoester **40a** (410 mg, 1.13 mmol) and using sodium hydride 60% dispersion in mineral oil (48 mg, 1.20 mmol, 1.06 equiv.). The yellow solid crude mixture was purified by silica gel column chromatography using a gradient elution: hexane/EtOAc (9:1 → 6:4) to give **30a** as a light yellow solid (356 mg, 91% yield).

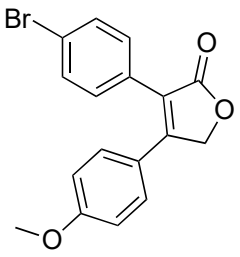

2nd try: Similarly starting from ketoester **40a** (4.93 g, 13.6 mmol). The yellow solid crude mixture was purified by silica gel column chromatography using a gradient elution: hexane/EtOAc (8:2 → 6:4) to give **30a** as a light yellow solid (4.43 g, 95% yield).

Analytical data are on the next page.

***R*f** 0.48 (hexane/EtOAc, 6:4); **^{1}H NMR** (500 MHz, $CDCl_3$) δ 7.55–7.49 (m, 2H), 7.35–7.30 (m, 2H), 7.29–7.25 (m, 2H), 6.89–6.83 (m, 2H), 5.15 (s, 2H), 3.83 (s, 3H); **^{13}C NMR** (126 MHz, $CDCl_3$) δ 173.5, 161.8, 156.4, 132.1, 131.1, 129.7, 129.2, 123.2, 123.0, 122.8, 114.7, 70.6, 55.5; **IR** (ATR) ν_{max} 1165, 1100, 1165, 1181, 1261, 1306, 1369, 1426, 1454, 1488, 1518, 1571, 1605, 1641, 1727, 1915, 2852, 2925 cm^{-1}; **LRMS** (APCI$^+$): *m/z* (relative intensity) 345 $[M+H]^+$, 266 (4), 221 (4); **HRMS** (TOF-ESI+) *m/z* calcd for: $C_{17}H_{14}BrO_3$ $[M+H]^+$: 345.0131, found: 345.0130; **Anal**. Calcd for $C_{17}H_{13}BrO_3$: C, 59.15; H, 3.80; found: C, 59.37; H, 3.78.

6.1.2.4.2 3-(2,6-Dichlorophenyl)-4-(4-methoxyphenyl)-2,5-dihydrofuran-2-one (30b)

The title compound was synthesized using the general method starting from ketoester **40b** (146 mg, 0.41 mmol) and using sodium hydride 60% dispersion in mineral oil (16.8 mg, 0.42 mmol, 1.02 equiv.). The yellow solid crude mixture was purified by silica gel column chromatography eluting with hexane/EtOAc (8:2) to give **30b** as a light yellow solid (127 mg, 92% yield).

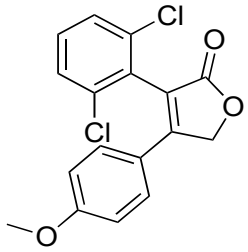

***R*f** 0.56 (hexane/EtOAc, 1:1); **^{1}H NMR** (500 MHz, $CDCl_3$) δ 7.45–7.41 (m, 2H), 7.36–7.32 (m, 1H), 7.19–7.14 (m, 2H), 6.86–6.82 (m, 2H), 5.36 (s, 2H), 3.81 (s, 3H); **^{13}C NMR** (126 MHz, $CDCl_3$) δ 172.2, 162.2, 158.3, 135.8, 130.8, 130.1, 128.7, 128.6, 122.8, 120.4, 114.8, 70.8, 55.5; **IR** (ATR) ν_{max} 1028, 1063, 1098, 1181, 1261, 1335, 1431, 1518, 1606, 1650, 1711, 1748, 2850, 2928, 3075 cm^{-1}; **LRMS** (APCI$^+$): *m/z* (relative intensity) 335 $[M+H]^+$, 309 (1), 291 (1), 135 (2); **Anal**. Calcd for $C_{17}H_{12}Cl_2O_3$: C, 60.92; H, 3.61; found: C, 60.99; H, 3.66.

6.1.2.4.3 3-(3,4-Dichlorophenyl)-4-(4-methoxyphenyl)-2,5-dihydrofuran-2-one (30c)

The title compound was synthesized using the general method starting from ketoester **40c** (1.77 g, 5.28 mmol) and using sodium hydride 60% dispersion in mineral oil (212 mg, 5.30 mmol, 1.0 equiv.). The yellow solid crude mixture was purified by silica gel column chromatography using a gradient elution: hexane/EtOAc (1:0 → 7:3) to give **30c** as a light yellow solid (1.09 g, 62% yield).

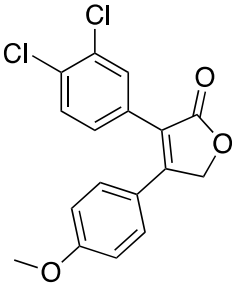

Analytical data are on the next page.

^{1}H NMR (500 MHz, $CDCl_3$) δ 7.58 (dd, J = 2.1, 0.7 Hz, 1H), 7.45 (dd, J = 8.3, 0.7 Hz, 1H), 7.30–7.24 (m, 3H), 6.90–6.85 (m, 2H), 5.16 (d, J = 0.7 Hz, 2H), 3.84 (d, J = 0.8 Hz, 3H); **^{13}C NMR** (126 MHz, $CDCl_3$) δ 173.0, 161.9, 157.1, 133.0, 132.9, 131.2, 130.7, 130.7, 129.1, 128.7, 122.3, 121.9, 114.7, 70.4, 55.4.

6.1.2.4.4 3-(4-Methoxyphenyl)-4-[4-(methylsulfonyl)phenyl]-2,5-dihydrofuran-2-one (30d)

The title compound was synthesized using the general method starting from ketoester **40d** (1.56 g, 4.32 mmol) using sodium hydride 60% dispersion in mineral oil (173 mg, 4.32 mmol, 1.0 equiv.). Unlike when using the general method, once the reaction mixture was extracted with EtOAc (45 mL) and washed with Na_2CO_3 (3 × 40 mL), a rapid color change from bright red to dark green occurred. The orange solid crude product was purified by silica gel column chromatography using a gradient elution: hexane/EtOAc (6:4 → 4:6) to give **30d** as a yellow solid (161 mg, 11% yield).

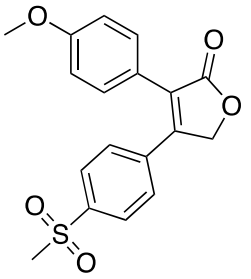

***R*f** 0.08 (hexane/EtOAc, 6:4); **^{1}H NMR** (500 MHz, $CDCl_3$) δ 7.95–7.89 (m, 2H), 7.56–7.51 (m, 2H), 7.38–7.32 (m, 2H), 6.94–6.87 (m, 2H), 5.15 (s, 2H), 3.83 (s, 3H), 3.07 (s, 3H); **^{13}C NMR** (126 MHz, $CDCl_3$) δ 172.9, 160.7, 152.0, 141.9, 136.8, 130.7, 128.7, 128.6, 128.2, 121.4, 114.6, 70.4, 55.5, 44.4; **IR** (ATR) ν_{max} 1024; 1114; 1126; 1178; 1253; 1287; 1310; 1365; 1458; 1541; 1607; 1753; 1922; 2894; 2952; 2958; 3009 cm^{-1}; **LRMS** (APCI$^+$): *m/z* (relative intensity) 345 $[M+H]^+$, 327 (4), 299 (2), 222 (1); **Anal**. Calcd for $C_{18}H_{16}O_5S$: C, 62.78; H, 4.68; found: C, 62.84; H, 4.73

6.1.2.4.5 4-(3,4-Dimethoxyphenyl)-3-(4-methoxyphenyl)-2,5-dihydrofuran-2-one (30e)

The title compound was synthesized using the general method starting from ketoester **40e** (2.50 g, 7.52 mmol) and using sodium hydride 60% dispersion in mineral oil (301 mg, 7.53 mmol, 1.0 equiv.) that was added in two batches. Unlike in the general procedure, the reaction mixture was cooled using an ice bath, and conc. HCl was used for quenching. The yellow crude product was purified by silica gel column chromatography using hexane/EtOAc (7:3) to give **30e** as a yellow solid (1.41 g, 54% yield). *Analytical data are on the next page.*

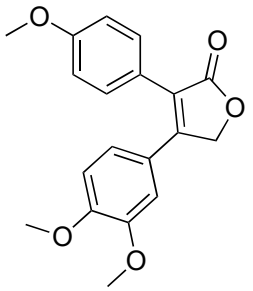

***R*f** 0.25 (hexane/EtOAc, 6:4); **^{1}H NMR** (500 MHz, $CDCl_3$) δ 7.41–7.37 (m, 2H), 6.96–6.91 (m, 3H), 6.87–6.82 (m, 2H), 5.15 (s, 2H), 3.89 (s, 3H), 3.82 (s, 3H), 3.58 (s, 3H); **^{13}C NMR** (126 MHz, $CDCl_3$) δ 174.1, 160.0, 154.7, 151.2, 149.1, 130.9, 124.2, 123.7, 123.0, 120.6, 114.3, 111.2, 110.7, 70.5, 56.1, 55.7, 55.5; **IR** (ATR) ν_{max} 1015, 1151, 1179, 1249, 1263, 1329, 1449, 1464, 1507, 1653, 1792, 1844, 1868, 2838, 2935, 3618, 3629 cm^{-1}; **HRMS** (TOF-ESI+) *m/z* calcd for: $C_{19}H_{19}O_5$ $[M+H]^+$: 327.1227, found: 327.1234; **Anal.** Calcd for $C_{19}H_{18}O_5$: C, 69.93; H, 5.56; found: C, 69.94; H, 5.59

6.1.2.4.6 3-(3,4-Methylenedioxophenyl)-4-(3,4-dimethoxyphenyl)-2,5-dihydrofuran-2-one (30f)

The title compound was synthesized using the general method starting from ketoester **40f** (1.84 g, 5.14 mmol) and using sodium hydride 60% dispersion in mineral oil (226 mg, 5.65 mmol, 1.1 equiv.). Unlike in the general procedure, hydride was added in two batches and the reaction mixture was stirred for 3 hours. The yellow solid product was purified by silica gel column chromatography using hexane/EtOAc (6:4) to give **30f** as a yellow solid (0.96 g, 55% yield).

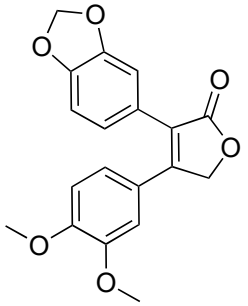

***R*f** 0.26 (hexane/EtOAc, 6:4); **^{1}H NMR** (500 MHz, $CDCl_3$) δ 6.95 (dd, J = 7.9, 1.7 Hz, 2H), 6.92 (d, J = 1.7 Hz, 1H), 6.87 (d, J = 2.1 Hz, 1H), 6.86 – 6.83 (m, 2H), 5.97 (s, 2H), 5.14 (s, 2H), 3.90 (s, 3H), 3.63 (s, 3H); **^{13}C NMR** (126 MHz, $CDCl_3$) δ 173.9, 155.2, 151.3, 149.1, 148.1, 148.0, 124.3, 124.2, 123.6, 123.4, 120.7, 111.3, 110.7, 110.0, 108.8, 101.4, 70.5, 56.1, 55.8; **IR** (ATR) ν_{max} 1018, 1071, 1124, 1163, 1250, 1272, 1335, 1441, 1548, 1640, 1728, 1754, 1778, 1820, 1900, 1950, 2031, 2855, 2927, 3019 cm^{-1}; **HRMS** (TOF-ESI+) *m/z* calcd for: $C_{19}H_{17}O_6$ $[M+H]^+$: 341.1020, found: 341.1024; **Anal.** Calcd for $C_{19}H_{16}O_6$: C, 67.06; H, 4.74; found: C, 67,44; H, 5.75.

6.1.2.4.7 3-(3-(Benzyloxy)-4-methoxyphenyl)-4-(4-methoxy-3-nitrophenyl)-2,5-dihydrofuran-2-one (30g)

The title compound was tried to be synthesized using the general method starting from ketoester **40g** (0.80 g, 1.72 mmol) and using sodium hydride 60% dispersion in mineral oil (76 mg, 1.89 mmol, 1.1 equiv.). Unlike with other combretafuranones, numerous products were detected on TLC (hexane/EtOAc, 3:7). The crude ^{1}H NMR analysis showed a mixture of several products. Two singlets at 5.16 ppm were detected in a very low concentration and indicated the possible presence of combretafuranone or combretafuranones. However, due to numerous tailing and overlapping products and traces of the possible product the purification was not attempted.

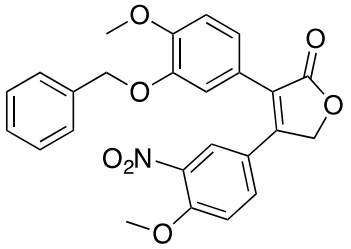

6.1.2.4.8 3-(2,4-Dichlorophenyl)-4-(4-methylphenyl)-2,5-dihydrofuran-2-one (30h)

The title compound was synthesized using the general method starting from ketoester **40h** (3.81 g, 11.3 mmol) and using sodium hydride 60% dispersion in mineral oil (497 mg, 12.4 mmol, 1.1 equiv.). Unlike in the general procedure, hydride was added in two batches and the reaction mixture was stirred for 3 hours. The crude product was purified by silica gel column chromatography using hexane/EtOAc (8:2) to give **30h** as a white solid (3.47 g, 96% yield).

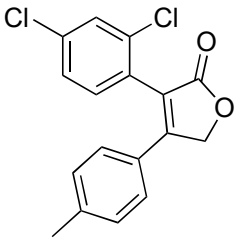

***R*f** 0.64 (hexane/EtOAc, 6:4); **^{1}H NMR** (500 MHz, $CDCl_3$) δ 7.51 (d, J = 2.1 Hz, 1H), 7.34 (dd, J = 8.3, 2.1 Hz, 1H), 7.27–7.23 (m, 1H), 7.17–7.09 (m, 4H), 5.29 (d, J = 17.7 Hz, 2H), 2.35 (s, 3H); **^{13}C NMR** (126 MHz, $CDCl_3$) δ 172.8, 158.5, 142.2, 135.7, 134.9, 132.3, 130.2, 130.0, 129.1, 127.9, 127.5, 127.1, 122.6, 70.8, 21.7; **IR** (ATR) ν_{max} 1044, 1062, 1070, 1163, 1188, 1337, 1368, 1476, 1558, 1610, 1646, 1683, 1746, 1792, 1844, 1868, 1922, 2929, 3674 cm^{-1}; **HRMS** (TOF-ESI+) *m/z* calcd for: $C_{17}H_{13}Cl_2O_2$ $[M+H]^+$: 319.0287, found: 319.0295; **Anal.** Calcd for $C_{17}H_{12}Cl_2O_2$: C, 63.97; H, 3.79; found: C, 64.27; H, 3.77.

6.1.2.4.9 3-(3,4-Dichlorophenyl)-4-(4-methylphenyl)-2,5-dihydrofuran-2-one (30i)

The title compound was synthesized using the general method starting from ketoester **40i** (4.12 g, 12.2 mmol) and using sodium hydride 60% dispersion in mineral oil (0.54 g, 13.42 mmol, 1.1 equiv.). Unlike in the general procedure, the hydride was added in two batches and the reaction mixture was stirred for 2 hours and 30 minutes. The worked-up crude reaction mixture was purified by silica gel column chromatography using hexane/EtOAc (6:4) to give **30i** as a yellow solid (3.72 g, 95% yield).

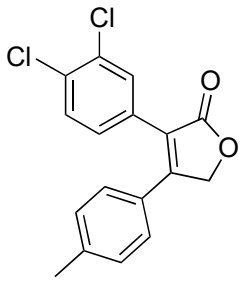

***R*f** 0.65 (hexane/EtOAc, 6:4); **^{1}H NMR** (500 MHz, $CDCl_3$) δ 7.59 (d, J = 2.0 Hz, 1H), 7.43 (d, J = 8.3 Hz, 1H), 7.28–7.24 (m, 1H), 7.22–7.15 (m, 4H), 5.16 (s, 2H), 2.38 (s, 3H). **^{13}C NMR** (126 MHz, $CDCl_3$) δ 173.0, 157.9, 142.0, 133.1, 133.1, 131.3, 130.8, 130.5, 130.1, 128.8, 127.5, 127.4, 123.2, 70.8, 21.7; **IR** (ATR) ν_{max} 1070, 1137, 1166, 1190, 1230, 1321, 1344, 1368, 1437, 1457, 1473, 1489, 1517, 1541, 1558, 1610, 1637, 1652, 1684, 1717, 1737, 1934, 3082 cm^{-1}; **HRMS** (TOF-ESI+) *m/z* calcd for $C_{17}H_{13}Cl_2O_2$ $[M+H]^+$: 319.0287, found: 319.0294; **Anal.** Calcd for $C_{17}H_{12}Cl_2O_2$: C, 63.97; H, 3.79; found: C, 63.64; H, 3.77.

6.1.2.5 Dealkylation – general procedure

Dealkylation of aromatic methoxy groups was performed 4 times similarly as follows:

Furanone **31a–31c** (0.36–3.81 mmol) was dissolved in dry freshly-distilled DCM (10 mL per 1 mmol of starting material), and the solution was cooled to -50 °C under argon atmosphere. Boron tribromide (1 M solution in hexane, 2.8–5 equiv.) was then added dropwise and the mixture turned dark orange to dark brown. After 10-minute stirring at -50 °C, the cold bath was exchanged for ice bath and the mixture was stirred for 1 h. The mixture was then quenched with water (5 mL per 0.5 mmol) and stirred for 30 min at room temperature.

6.1.2.5.1 3-(4-Bromophenyl)-4-(4-hydroxyphenyl)-2,5-dihydrofuran-2-one (31a)

The reaction was performed twice similarly. The purification method varied.

1st try: The title compound was synthesized from **30a** (123 mg, 0.356 mmol) and 2.8 equiv. of BBr_3 were used. Since some lipophilic impurities were seen on TLC (hexane/EtOAc 1:1, R_f 0.63), the compound was extracted as follows: the reaction mixture was diluted with EtOAc (1 × 30 mL) and washed with sat. Na_2CO_3 (20 mL). TLC indicated that the assumed product was present in both water and organic layer so the extraction was repeated similarly. Subsequently, the water layer was acidified to pH 2–3 and re-extracted three times with EtOAc (3 × 50 mL). The combined organic layers were dried over Na_2SO_4, filtered and the solvent was removed *in vacuo*. The crude product was purified by silica gel column chromatography using hexane/EtOAc + 1% CH_3COOH, 6:4 to give **31a** as a yellow solid (94 mg, 79% yield).

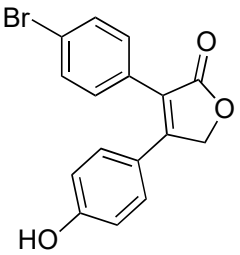

2nd try: The title compound **31a** was synthesized from **30a** (1.32 g, 3.81 mmol) and 2.0 equiv. of BBr_3 were used. Organic and water layer were separated after quenching and the water phase was extracted with EtOAc (1 × 65 mL). The organic layer was then washed with sat. NaCl (30 mL) and the water phase was re-extracted with EtOAc (1 × 65 mL). The combined organic layers were dried over Na_2SO_4, filtered and the solvent was removed *in vacuo*. The crude product was purified by silica gel column chromatography using a gradient elution: hexane/EtOAc + 1% CH_3COOH (8:2 → 7:3). The obtained product was then washed twice with water and extracted with EtOAc in

order to get rid of CH_3COOH. The combined organic layers were dried over Na_2SO_4, filtered and the solvent was removed *in vacuo* to give **31a** as a yellow solid (1.16 g, 92% yield).

***R*f** 0.29 (hexane/EtOAc, 6:4); **^{1}H NMR** (500 MHz, $CDCl_3$) δ 7.61–7.48 (m, 2H), 7.35–7.28 (m, 2H), 7.29–7.22 (m, 2H), 6.84–6.70 (m, 2H), 5.28 (s, 2H); (500 MHz, CD_3OD) δ 7.61–7.57 (m, 2H), 7.36–7.31 (m, 2H), 7.30–7.25 (m, 2H), 6.80–6.74 (m, 2H), 5.29 (s, 2H); **^{13}C NMR** (125 MHz, $CDCl_3$) δ 176.0, 161.6, 160.0, 132.9, 132.4, 131.7, 130.7, 123.6, 122.8, 122.7, 116.9, 72.3; (126 MHz, CD_3OD) δ 176.0, 161.6, 160.0, 133.0, 132.4, 131.7, 130.7, 123.6, 122.9, 122.7, 116.9, 72.3; **IR** (ATR) ν_{max} 1037, 1043, 1064, 1171, 1251, 1344, 1396, 1540, 1608, 1636, 1709, 1792, 1869, 3237 cm^{-1}; **HRMS** (TOF-ESI+) *m/z* calcd for: $C_{16}H_{12}BrO_3$ $[M+H]^+$: 330.9964, found: 330.9961; **Anal**. Calcd for $C_{16}H_{11}BrO_3$: C, 58.03; H, 3.35; found: C, 58.12; H, 3.42.

6.1.2.5.2 4-(3,4-Dihydroxyphenyl)-3-(4-hydroxyphenyl)-2,5-dihydrofuran-2-one (31b)

The title compound **31b** was synthesized from furanone **30e** (201 mg, 0.554 mmol) and 4.0 equiv. of BBr_3 were used. The compound was purified as follows:

The reaction mixture was diluted with EtOAc (1 × 50 mL), washed with sat. NaCl (40 mL) and the water phase was re-extracted with EtOAc (2 × 40 mL). The combined organic layers were dried over Na_2SO_4, filtered and the solvent was removed *in vacuo*. The crude brown solid (193 mg) was purified by gradient silica gel column chromatography: hexane/EtOAc + 2% CH_3COOH (1:1 → 2:8). After some lipophilic impurities were eluted, the amount of CH_3COOH was increased to 5% since the elution was lengthy and the product was hardly detected on TLC (EtOAc, 2:8). The collected fractions were combined and solvents were removed *in vacuo*. Finally, the compound **31b** was obtained as a brown solid (137 mg, 87% yield).

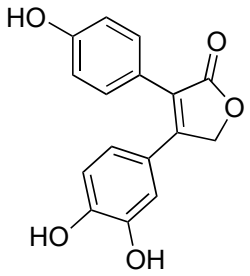

Analytical data are on the next page.

***R*f** 0.28 (hexane/EtOAc, 2:8; tailing yellow spot); **^{1}H NMR** (500 MHz, CD_3OD) δ 7.25–7.20 (m, 2H), 6.86–6.80 (m, 4H), 6.74–6.71 (m, 1H), 5.19 (s, 2H); **^{13}C NMR** (126 MHz, CD_3OD) δ 177.0, 159.0, 158.1, 149.4, 146.6, 131.8, 123.9, 123.8, 123.2, 121.3, 116.5, 116.5, 115.7, 72.2; **IR** (ATR) ν_{max} 1043, 1101, 1127, 1164, 1226, 1263, 1437, 1489, 1559, 1570, 1606, 1653, 1716, 1792, 1868, 2853, 2923, 3314, 3566, 3629 cm^{-1}; **LRMS (APCI$^+$)**: *m/z* (rel. intensity) 285 $[M+H]^+$, 267 (5), 249 (1); **Anal.** Calcd for $C_{16}H_{12}O_5$: C, 67.60; H, 4.26; found: C, 67.62; H, 4.29.

6.1.2.5.3 4-(3,4-Dihydroxyphenyl)-3-(3,4-dihydroxyphenyl)-2,5-dihydrofuran-2-one (31c)

The title compound **31c** was attempted to be synthesized from furanone **30f** (141 mg, 0.414 mmol) and 5.0 equiv. of BBr_3. The mixture was purified as follows:

The reaction mixture was diluted with EtOAc (1 × 50 mL), washed with sat. NaCl (40 mL) and the water phase was re-extracted with EtOAc (4 × 50 mL). The TLC (EtOAc - a white spot on baseline; and $CHCl_3$/MeOH, 1:1) showed possible product in both organic and water layer. The water layer was acidified with 5% HCl to pH = 1 and the extraction with EtOAc was repeated (3 × 50 mL). The combined organic layers were dried over Na_2SO_4, filtered and the solvent was removed *in vacuo*. The combined water layers were concentrated *in vacuo*, the crude product was suspended in acetone and filtered using Celite®. The solvent was then removed *in vacuo*. The crude dry mixtures were left unpurified.

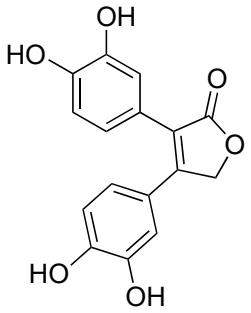

6.1.2.6 γ-Substituted derivatives

6.1.2.6.1 3-(3,4-Dichlorophenyl)-5,5-bis(hydroxymethyl)-4-(4-methoxyphenyl)-2,5-dihydrofuran-2-one (32a)

Furanone **30c** (1.09 g, 3.25 mmol), powdered sodium carbonate (0.69 g, 6.50 mmol, 2.0 equiv.) and paraformaldehyde (195 mg, 6.50 mmol, 2.0 equiv.) were suspended in dry methanol (20 mL). The resultant mixture was stirred at room temperature and a color change to light green was observed after 2 hours of stirring. The total stirring time was 48 hours after which the starting material was still detected in the reaction mixture. The mixture was nevertheless extracted with EtOAc (70 mL) and washed with water (3 × 60 mL). The organic layer was dried over Na_2SO_4, filtered and the solvent was removed *in vacuo*. The crude orange solid was purified by silica gel column chromatography using a gradient: hexane/EtOAc (7:3 → 1:1) to give **32a** as a white solid (321 mg, 25% yield).

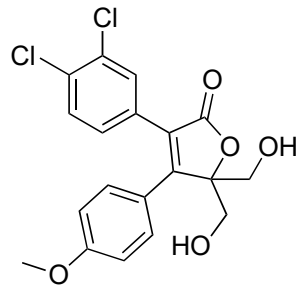

***R*f** 0.10 (hexane/EtOAc, 1:1); **^{1}H NMR** (500 MHz, $CDCl_3$) δ 7.56 (d, J = 2.1 Hz, 1H), 7.26–7.23 (m, 1H), 7.20–7.16 (m, 2H), 7.12 (dd, J = 8.4, 2.0 Hz, 1H), 6.95–6.87 (m, 2H), 3.95 (dd, J = 12.6, 4.4 Hz, 2H), 3.81 (s, 3H), 3.81–3.76 (m, 2H), 3.03 (br t, J = 6.7 Hz, 1H), 1.87 (br s, 1H); **^{13}C NMR** (126 MHz, $CDCl_3$) δ 172.1, 162.2, 160.8, 132.9, 132.6, 131.1, 130.3, 129.8, 129.4, 128.6, 127.4, 123.0, 115.0, 93.0, 62.2, 55.5; **IR** (ATR) ν_{max} 1030, 1053, 1092, 1179, 1252, 1292, 1349, 1473, 1512, 1570, 1607, 1645, 1736, 2840, 2934, 3401 cm^{-1}; **Anal.** Calcd for $C_{19}H_{16}Cl_2O_5$: C, 57.74; H, 4.08; found: C, 57.78; H, 4.13.

6.1.2.6.2 4-(3,4-Dimethoxyphenyl)-5-(hydroxymethyl)-3-(4-methoxyphenyl)-2,5-dihydrofuran-2-one (32b) and 4-(3,4-dimethoxyphenyl)-5,5-bis(hydroxymethyl)-3-(4-methoxyphenyl)-2,5-dihydrofuran-2-one (32c)

Furanone **30e** (0.99 g, 2.74 mmol) was suspended in dry methanol (20 mL). Due to observed solubility issues, THF (5 mL) was added to the mixture, followed by powdered sodium carbonate (294 mg, 2.74 mmol, 1.0 equiv.) and paraformaldehyde (82 mg, 2.74 mmol, 1.0 equiv.). The resultant mixture was stirred at room temperature as a light yellow suspension for 18 hours. The starting material was still detected in the

reaction mixture using TLC (hexane/EtOAc, 1:1). The mixture was therefore heated to 40 °C and remained stirred for an additional day. Then the heating was turned off and the mixture was stirred for additional 3 days. After the said time, the starting material could be still detected by TLC. The mixture was nevertheless extracted with EtOAc (80 mL) and washed with water (3 × 60 mL). The combined water phases were re-extracted with EtOAc (2 ×, together 120 mL). The combined organic layers were dried over Na_2SO_4, filtered and the solvent was removed *in vacuo*. The crude yellow solid was purified by silica gel column chromatography using a gradient elution: hexane/EtOAc (6:4 → 2:8).

The starting material got eluted in 6:4 in high amount (54%).

Monohydroxymethylated derivative **32b**. Eluted with hexane/EtOAc (1:1), a pale yellow solid, 258 mg, 26% yield. ***R*f** 0.07 (hexane/EtOAc, 1:1); 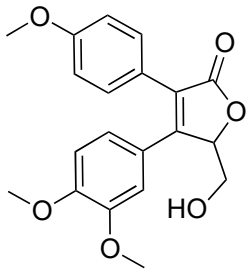

^{1}H NMR (500 MHz, $CDCl_3$) δ 7.41–7.36 (m, 2H), 6.94–6.84 (m, 4H), 6.79 (d, J = 2.0 Hz, 1H), 5.49 (dd, J = 5.2, 2.7 Hz, 1H), 4.07–4.00 (m, 1H), 3.90 (s, 3H), 3.80 (s, 3H), 3.73–3.66 (m, 1H), 3.61 (s, 3H); **^{13}C NMR** (126 MHz, $CDCl_3$) δ 172.9, 160.0, 155.5, 150.9, 149.3, 130.9, 126.2, 123.5, 122.5, 121.2, 114.2, 111.4, 111.3, 82.3, 63.3, 56.1, 55.9, 55.4; **Anal.** Calcd for $C_{20}H_{20}O_6$: C, 67.41; H, 5.66; found: C 68.00; H, 5.67.

Bishydroxymethylated derivative **32c**. Eluted in hexane/EtOAc (2:8), a pale yellow solid, 156 mg, 15% yield. ***R*f** 0.31 (hexane/EtOAc, 2:8); 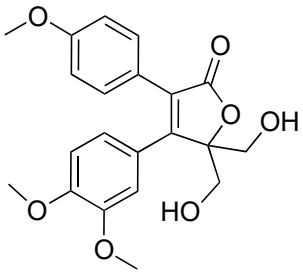

^{1}H NMR (500 MHz, $CDCl_3$) δ 7.41–7.33 (m, 2H), 6.90–6.85 (m, 2H), 6.80–6.69 (m, 3H), 3.95 (t, J = 10.5 Hz, 2H), 3.89 (s, 3H), 3.84–3.79 (m, 2H), 3.76 (s, 3H), 3.73 (s, 3H), 2.60 (br s, 1H), 1.72 (br s, 1H); **^{13}C NMR** (126 MHz, $CDCl_3$) δ 172.6, 159.9, 158.3, 149.9, 149.6, 130.7, 128.9, 124.4, 122.2, 120.8, 113.8, 111.7, 111.3, 92.1, 62.7, 56.1, 56.0, 55.3; **Anal.** Calcd for $C_{21}H_{22}O_7$: C, 65.28; H, 5.74; found: C 65.30; H, 5.75.

6.1.2.6.3 4-(3,4-Dimethoxyphenyl)-5-(aminomethyl)-3-(4-methoxyphenyl)-2,5-dihydrofuran-2-one (32d)

Combretafuranone **32b** (106 mg, 0.297 mmol) was dissolved in dry DMF (1.6 mL) and CCl_4 (0.4 mL) under argon atmosphere. PPh_3 (164 mg, 0.625 mmol, 2.1 equiv.) was added and the mixture was stirred until the phosphine dissolved (2 min). Afterwards, NaN_3 (23.2 mg, 0.357 mmol, 1.2 equiv.) was added and the mixture was gradually heated to 90 °C. Within 5 minutes of stirring, the light yellow color turned into red, then brown. TLC analysis (hexane/EtOAc, 2:8) done after 15 minutes showed several compounds including both UV-active starting materials and triphenylphosphine oxide. The heating continued for next 6 hours during which the reaction mixture was regularly monitored by TLC. However, no major changes in the reaction mixtures were observed afterwards and the reaction mixture remained unchanged even for the next 22 hours of heating. The reaction mixture was therefore quenched by water (3 mL), extracted to Et_2O (20 mL) and washed with water (3 × 30 mL). The organic layer was dried over Na_2SO_4, filtered and the solvent was removed *in vacuo*. No major change was observed on TLC after the aqueous quench and nor after the extraction. The bright yellow crude material was purified by silica gel column chromatography using hexane/EtOAc, 6:4. From the numerous products, the major one (bright yellow spot on TLC (R_f 0.50 in hexane/EtOAc, 1:1)) was able to be isolated, although as a mixture of other products (24 mg). ^{1}H NMR analysis suggested a dehydration product could be present in the mixture [δ 5.28 (d, J = 2.4 Hz, 1H), 4.90 (d, J = 2.5 Hz, 1H) ppm]. Other products could not be purified.

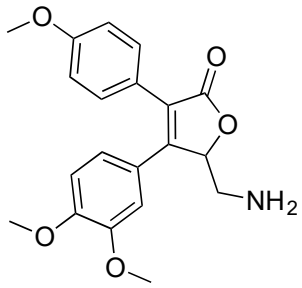

6.1.3 Biological testing

6.1.3.1 Cytotoxicity

The cytotoxicity screening was performed by Mgr. David Sedlák, PhD and RNDr. Petr Bartůněk, CSc. at the CZ-OPENSCREEN: National Infrastructure for Chemical Biology, Institute of Molecular Genetics, Czech Academy of Sciences. The methodology was discussed with Assoc. Prof. Ing. Jan Vacek, PhD of Palacký University.

6.1.3.1.1 Cell lines

Cellular profiling was carried out on a panel of cell lines of diverse tissue origin that cover several major oncological diseases (Table 5).

Table 5 Cell lines used for cytotoxicity testing.

Cell name:	Description:
RPE-1	Human normal immortalized cells
BJ	Human primary fibroblasts
Hep G2	Human hepatocellular carcinoma
K562	Human chronic myelogenous leukemia
HL-60	Human acute myeloid leukemia
PC-3	Human prostate adenocarcinoma
MCF7	Human breast adenocarcinoma

Cell lines were purchased from the American Type Culture Collection (ATCC). The cells were propagated in a monolayer in the cell culture medium supplemented with 10% fetal bovine serum, 2 mM glutamax, 1 mM non-essential amino acids (NEAA) and penicillin/streptomycin (Thermo Fisher Scientific, MA, USA) and incubated in a 5% CO_2 humidified atmosphere at 37 °C. IMDM was used as a culture medium for K562 and HL-60, DMEM for RPE-1, Hep G2 and BJ cells and F-12K for PC3. BJ cells were propagated in the medium supplemented with 10 ng/mL of bFGF.

6.1.3.1.2 Cell viability and apoptosis assay

Cells were propagated in the cell growth medium to the amount needed for the experiment. The cells were harvested, counted and diluted in the growth medium to the final concentration of 0.1×10^6/mL and dispensed with a liquid dispenser Multidrop

(Thermo Fisher Scientific, MA, USA) to the cell culture treated, white solid 1536-well plates (Corning Inc., NY, USA) at 500 cells/well in 5 mL of the total media volume. The test compounds were diluted in DMSO and transferred to the cells using acoustic dispenser Echo 520 (Labcyte) integrated in the fully automated robotic HTS station CellTExplorer (Perkin Elmer). The compounds were tested at 12 different concentration points in the concentration range from 40 mM to 1 nM, in triplicates. Cell viability was assessed after 48 h incubation with the compounds by determining the level of intracellular ATP using the ATPliteTM (Perkin Elmer, USA) luminescent assay. Induction of apoptosis was assessed after 24 h of incubation with the compounds by measuring the activity of caspase-3 and caspase-7 using Caspase-Glo® 3/7 luminescent assay (Promega, USA). In both cases, luciferase signal was measured on the multimode plate reader Envision (Perkin Elmer, USA). The data were collected and processed with an in-house developed LIMS system ScreenX. Here, the data were processed, normalized, and ED_{50} values were calculated using a nonlinear regression function (dose response, variable slope).

6.1.3.2 Antimicrobial activity

The antimicrobial activity screening was performed by RNDr. Klára Konečná, PhD of the Charles University, Hradec Králové, Czech Republic.

6.1.3.2.1 Antibacterial activity

In vitro antibacterial activities of target combretafuranones were evaluated[109] on a panel of three ATCC strains and five clinical isolates from the collection of antibacterial strains deposited at the Department of Biological and Medical Sciences, Faculty of Pharmacy, Charles University, Hradec Kralové, Czech Republic (Table 6).

Table 6 Bacterial strains.

Type:	Strain name:
ATCC strains	• *Staphylococcus aureus* ATCC 6538 • *Escherichia coli* ATCC 8739 • *Pseudomonas aeruginosa* ATCC 9027
Clinical isolates	• *Staphylococcus aureus* MRSA HK5996/08 • *Staphylococcus epidermidis* HK6966/08 • *Enterococcus species* HK14365/08 • *Klebsiella pneumoniae* HK11750/08 • *Klebsiella pneumoniae* ESBL HK14368/08

The ATCC strains also served as the quality control strains. All the isolates were maintained on Mueller-Hinton agar prior to being tested.

DMSO (100%) served as a diluent for all compounds; the final concentration did not exceed 2%. Mueller-Hinton agar (MH, HiMedia, Cadersky-Envitek, Czech Republic) buffered to pH 7.4 (±0.2) was used as the test medium. The wells of the microdilution tray contained 200 L of the Mueller-Hinton medium with 2-fold serial dilutions of the compounds (2000–0.488 mmol/L) and 10 L of inoculum suspension. Inoculum in MH medium was prepared to give a final concentration of 0.5 McFarland scale (1.5×10^8 cfu mL^{-1}). The trays were incubated at 37 °C and MICs were read visually after 24 h and 48 h. The MICs were defined as 95% inhibition of the growth of control. MICs were determined twice, and in duplicate. The deviations from the usually obtained values were no higher than the nearest concentration value up and down the dilution scale.

6.1.3.2.2 Antifungal activity

Antifungal activities of the target combretafuranones were evaluated on a panel of four ATCC strains and eight clinical isolates of yeasts and filamentous fungi from the collection of fungal strains deposited at the Department of Biological and Medical Sciences, Faculty of Pharmacy, Charles University, Hradec Králové, Czech Republic (Table 7). Three ATCC strains were used as the quality control strains. All the isolates were maintained on Sabouraud dextrose agar prior to being tested.

Table 7 Fungal strains.

Type:	Strain name:
ATCC strains	• *Candida albicans* ATCC 44859 • *Candida albicans* ATCC 90028 • *Candida parapsilosis* ATCC 22019 • *Candida krusei* ATCC 6258
Clinically isolated yeast	• *Candida krusei* E28 • *Candida tropicalis* 156 • *Candida glabrata* 20/I • *Candida lusitaniae* 2446/I • *Trichosporon asahii* 1188
Clinically isolated filamentous fungi	• *Aspergillus fumigatus* 231 • *Absidia corymbifera* 272 • *Trichophyton mentagrophytes* 445

Minimum inhibitory concentrations (MICs) were determined by modified CLSI standard of microdilution format of the M27-A3 and M38-A2 documents.[107,108] DMSO (100%) served as a diluent for all compounds; the final concentration did not exceed 2%. RPMI 1640 (Sevapharma, Prague) medium supplemented with *L*-glutamine and buffered with 0.165 M morpholinepropanesulfonic acid (Serva) to pH 7.0 by 10 M NaOH was used as the test medium. The wells of the microdilution tray contained 200 mL of the RPMI 1640 medium with 2-fold serial dilutions of the compounds (2000–0.488 mmol/L for the new compounds) and 10 mL of inoculum suspension. Fungal inoculum in RPMI 1640 was prepared to give a final concentration of $5 \times 10 \pm 0.2$ cfu mL^{-1}. The trays were incubated at 35 °C and MICs were read visually after 24 h and 48 h. The MIC values for the dermatophytic strain (*T. mentagrophytes*) were determined after 72 h and 120 h. The MICs were defined as 80% inhibition (IC_{80}) of the growth of control for yeasts and as 50% inhibition (IC_{50}) of the growth of control for filamentous fungi. MICs were determined twice and in duplicate. The deviations from the usually obtained values were no higher than the nearest concentration value up and down the dilution scale.

6.2 Purpurealidin analogues

6.2.1 Reagents and devices

All reactions were carried out using commercially available starting materials unless otherwise stated. The melting points were measured with Stuart SMP40 automated melting point apparatus and are uncorrected. ^{1}H NMR (300 MHz) and ^{13}C NMR (75 MHz) spectra in $CDCl_3$, d_6-DMSO, or CD_3OD at ambient temperature were recorded on a Varian Mercury *Plus* 300 spectrometer. Chemical shifts (δ) are given in parts per million (ppm) relative to the NMR reference solvent signals ($CDCl_3$: 7.26 ppm and 77.16 ppm; CD_3OD: 3.31 ppm and 49.0 ppm; d_6-DMSO: 2.50 ppm and 39.52 ppm). Multiplicities are indicated by s (singlet), br s (broad singlet), d (doublet), dd (doublet of doublet), ddd (doublet of doublet of doublets), t (triplet), dt (doublet of triplets), q (quartet), quin (quintet) and m (multiplet). The coupling constants *J* are quoted in Hertz (Hz). LC-MS and HRMS-spectra were recorded using Waters Acquity UPLC®-system (with Acquity UPLC® BEH C18 column (1.7 µm, 50 × 2.1 mm, Waters)) with Waters Synapt G2 HDMS with the ESI (+), high resolution mode. The mobile phase consisted of H_2O (A) and acetonitrile (B) both containing 0.1% HCOOH. Microwave syntheses were performed in sealed tubes using Biotage Initiator+ instrument equipped with an external IR sensor. The column chromatography was carried out using Merck Silica gel 60 (0.040–0.063 mm). The flash chromatography was performed with Biotage SP1 flash chromatography purification system with 254 nm UV-detector using SNAP KP-Sil 10 or 25 g cartridges. The TLC-plates were provided by Merck (Silica gel 60-F_{254}) and CAMAG dual wavelenght (254/366) was used for TLC detection (Muttenz, Switzerland). Visualization of some compounds was done using ninhydrin staining (1.5 g ninhydrin in 100 mL of ethanol) and plate heating.

6.2.2 Synthesis of purpurealidin analogues

6.2.2.1 Synthesis of purpurealidin E

6.2.2.1.1 2-(3,5-Dibromo-4-hydroxyphenyl)ethan-1-amine hydrobromide (46)

Tyramine **45** (1.00 g, 7.29 mmol) was dissolved in AcOH (15 mL). Then, bromine (1.31 mL, 25.5 mmol, 3.5 equiv.) was added dropwise over a period of 10 minutes and the reaction mixture was stirred for 26 hours at room temperature. The mixture was then diluted with Et_2O (15 mL), the solid was filtered off and washed with Et_2O (40 mL) to give **46** as a white solid (2.67 g, 97% yield).

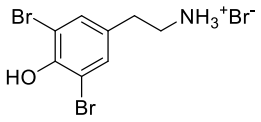

^{1}H NMR (300 MHz, DMSO-d_6) δ 9.79 (s, 1H), 7.78 (br s, 3H), 7.46 (s, 2H), 3.12–2.94 (m, 2H), 2.79 (t, J = 7.4 Hz, 2H); **^{13}C NMR** (75 MHz, DMSO-d_6) δ 149.5, 132.5, 131.6, 112.0, 39.6, 31.2; **HRMS** (TOF-ESI+): *m/z* calcd for $C_8H_{10}Br_2NO$ $[M\text{-}Br]^+$: 293.9129, found: 293.9128.

6.2.2.1.2 *tert*-Butyl (3,5-dibromo-4-hydroxyphenethyl)carbamate (47)

Hydrobromide **46** (2.62 g, 6.97 mmol) and Boc_2O (1.82 g, 8.36 mmol, 1.2 equiv.) were dissolved in anhydrous MeOH (50 mL). TEA (2.91 mL, 20.9 mmol, 3.0 equiv.) was added dropwise over a period of 4 minutes. The reaction mixture was then stirred at room temperature. TLC (hexane/EtOAc, 1:1) indicated the reaction was completed in 4 hours. The solvent was removed *in vacuo* and the crude product was extracted with EtOAc (40 mL) and washed with 0.5 M HCl (40 mL). The water phase was re-extracted with EtOAc (2 × 25 mL). The combined organic phases were washed with water three times (2 × 20 mL, 1 × 40 mL), dried over Na_2SO_4, filtered and the solvent was removed *in vacuo* to give **47** as a white solid (2.71 g, 98% yield).

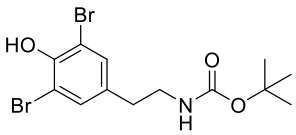

***R*f** 0.77 (hexane/EtOAc, 1:1); **^{1}H NMR** (300 MHz, $CDCl_3$) δ 7.28 (s, 2H), 5.84 (s, 1H), 4.54 (br s, 1H), 3.37–3.26 (m, 2H), 2.69 (t, J = 7.0 Hz, 2H), 1.44 (s, 9H); **^{13}C NMR** (75 MHz, $CDCl_3$) δ 155.9, 148.1, 133.8, 132.4, 110.0, 77.0, 41.8, 34.9, 28.5.

6.2.2.1.3 *tert*-Butyl (3,5-dibromo-4-(3-(dimethylamino)propoxy)phenethyl)carbamate (49a)

Carbamate **47** (1.02 g, 2.83 mmol), 3-Chloro-*N*,*N*-dimethylpropylamine hydrochloride **48a**•HCl (0.54 g, 3.39 mmol, 1.2 equiv.) and anhydrous K_2CO_3 (0.98 g, 7.07 mmol, 2.5 equiv.) were suspended in anhydrous acetone (40 mL) under argon atmosphere. The mixture was heated to reflux (85 °C) and stirred for 26 hours. Then the solvent was removed *in vacuo*. The crude product was washed with 0.1 M NaOH (20 mL) and extracted with $CHCl_3$ (20 mL). The water phase was re-extracted 2x with $CHCl_3$ (together 50 mL). Combined organic layers were washed with water (2 × 20 mL) and each of the water layers was then re-extracted with $CHCl_3$ (1 × 20 mL). The organic phase was then dried with Na_2SO_4, filtered and the solvent was removed *in vacuo* to give a white solid. The solid was recrystallized from hexane using the following procedure. The crude product was just dissolved in boiling hexane. A brown solid appeared in the flask. The remaining solution without the brown solid was transferred into another flask by pipetting, heated to reflux and left to cool down. Resultant solid was filtered, carefully washed with hexane (< 5 mL, freezer-cold) to give **49a** as a white crystalline solid (1.15 g, 85% yield).

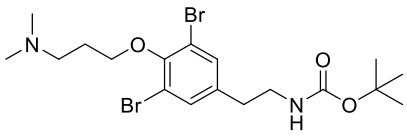

Melting point: 84.6–85.6 °C; **^{1}H NMR** (300 MHz, $CDCl_3$) δ 7.31 (s, 2H), 4.58 (br s, 1H), 4.03 (t, J = 6.5 Hz, 2H), 3.36–3.26 (m, 2H), 2.70 (t, J = 7.0 Hz, 2H), 2.59–2.37 (m, 2H), 2.26 (s, 6H), 2.09–1.92 (m, 2H), 1.43 (s, 9H); **^{13}C NMR** (75 MHz, $CDCl_3$) δ 155.9, 152.0, 137.7, 133.0, 118.4, 79.7, 72.1, 56.5, 45.7, 41.6, 35.2, 28.5, 28.5; **HRMS** (TOF-ESI+): *m/z* calcd for $C_{18}H_{29}Br_2N_2O_3$ $[M+H]^+$: 479.0545, found: 479.0545.

6.2.2.1.4 3-(4-(2-Aminoethyl)-2,6-dibromophenoxy)-*N,N*-dimethylpropan-1-amine (26)

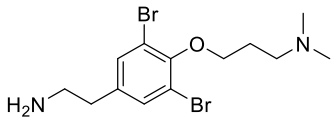

Carbamate **49a** (1.09 g, 2.27 mmol) was dissolved in anhydrous DCM (16 mL) under argon atmosphere. TFA (8 mL, excess amount) was added dropwise over a period of 12 min. The mixture was stirred under argon atmosphere at room temperature for 20 h. The reaction mixture was then concentrated using pressurized air. The remaining solvent and TFA were removed *in vacuo*. The crude mixture was then washed with 2 M NaOH (24 mL) and extracted to EtOAc (20 mL). The water phase was re-extracted with EtOAc (2 × 20 mL). Combined organic layers were washed with water (40 mL). The water phase was re-extracted with EtOAc (1 × 15, 1 × 20 mL). The combined organic layers were dried over Na_2SO_4, filtered and the solvent was removed *in vacuo* to give purpurealidin E **26** as clear light yellow oil (0.86 g, 99% yield).

***R*f** 0.37 (DCM/MeOH, 4:1); **^{1}H NMR** (300 MHz, $CDCl_3$) δ 7.33 (s, 2H), 4.03 (t, J = 6.5 Hz, 2H), 2.93 (t, J = 6.8 Hz, 2H), 2.64 (t, J = 6.7 Hz, 2H), 2.59–2.50 (m, 2H), 2.27 (s, 6H), 2.11–1.96 (m, 2H), 1.31 (br s, 2H); **^{13}C NMR** (75 MHz, $CDCl_3$) δ 151.8, 138.7, 133.0, 118.3, 72.1, 56.5, 45.7, 43.3, 38.9, 28.5; **HRMS** (TOF-ESI+): *m/z* calcd for $C_{13}H_{21}Br_2N_2O$ $[M+H]^+$: 379.0024, found: 379.0021.

6.2.2.2 Synthesis of purpurealidin E analogues

6.2.2.2.1 *tert*-Butyl (3,5-dibromo-4-((4-methylpentyl)oxy)phenethyl)carbamate (49b)

Carbamate **47** (0.50 g, 1.27 mmol) and anhydrous K_2CO_3 (0.437 g, 3.16 mmol, 2.5 equiv.) were suspended in anhydrous acetone (3 mL) under argon atmosphere. 1-bromo-4-methylpentane **48b** (0.230 mL, 1.58 mmol, 1.25 equiv.) was added via the condenser. The condenser was then washed with anhydrous acetone (6 mL), the mixture was heated to reflux (77 °C) and stirred under argon atmosphere. After 6 hours, TLC (hexane/EtOAc 4:1) showed a consumption of the starting material. The mixture was left stirred overnight at room temperature. The total reaction time was 23 hours. The solvent was then removed *in vacuo*. The crude product was washed with H_2O (20 mL) and extracted with EtOAc (1 × 15 mL, 1 × 20 mL) and hexane (1 × 15 mL). Due to observed problems with solubility, the remaining solid in the flask was dissolved in DCM and washed with water (15 mL). The combined water layers were re-extracted with DCM 2x (40 mL together). Combined organic layers were dried with Na_2SO_4, filtered and the solvent was removed *in vacuo*. A white solid appeared upon evaporation from DCM. The crude product was recrystallized from hexane to give **49b** as a white crystalline solid (0.54 g, 89% yield).

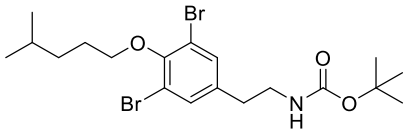

***R*f** 0.41 (hexane/EtOAc, 8:2); **Melting point**: 108.3–109.9 °C; **^{1}H NMR** (300 MHz, $CDCl_3$) δ 7.32 (s, 2H), 4.53 (br s, 1H), 3.97 (t, J = 6.7 Hz, 2H), 3.37–3.27 (m, 2H), 2.71 (t, J = 7.0 Hz, 2H), 1.95–1.72 (m, 2H), 1.72–1.55 (m, 1H), 1.44 (s, 9H), 1.43–1.36 (m, 2H), 0.93 (d, J = 6.6 Hz, 6H); **^{13}C NMR** (75 MHz, $CDCl_3$) δ 155.9, 152.2, 137.6, 133.0, 118.5, 74.0, 41.6, 35.1, 28.6, 28.1, 28.1, 22.7; **HRMS** (TOF-ESI+): *m/z* calcd for $C_{19}H_{29}Br_2NO_3Na$ $[M+Na]^+$: 500.0412, found: 500.0416.

Notes: Overlapping peaks in ^{13}C NMR.

6.2.2.2.2 2-(3,5-Dibromo-4-((4-methylpentyl)oxy)phenyl)ethan-1-amine (33a)

Carbamate **49b** (0.50 g, 1.04 mmol) was dissolved in anhydrous DCM (10 mL) under argon atmosphere. TFA (5 mL, excess amount) was added dropwise over a period of 10 min. The mixture was then stirred under argon atmosphere at room temperature for 20 h. The reaction mixture was then concentrated using pressurized air. The remaining solvent and TFA were removed *in vacuo*. The crude mixture was then washed with 2 M NaOH (10 mL) and extracted to EtOAc (1 × 20 mL, 1 × 15 mL). Combined organic layers were washed with water (20 mL). The water phase was re-extracted with EtOAc (2 × 10 mL). The combined organic layers were dried over Na_2SO_4, filtered and the solvent was removed *in vacuo* to give **33a** as clear yellow oil (385 mg, 97% yield).

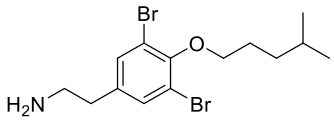

***R*f** 0.42 (hexane/EtOAc, 3:2); **^{1}H NMR** (300 MHz, $CDCl_3$) δ 7.33 (s, 2H), 3.96 (t, J = 6.7 Hz, 2H), 2.94 (t, J = 6.8 Hz, 2H), 2.70–2.59 (m, 2H), 1.94–1.78 (m, 2H), 1.74–1.54 (m, 1H), 1.48–1.36 (m, 2H), 1.32 (br s, 2H), 0.93 (d, J = 6.6 Hz, 6H); **^{13}C NMR** (75 MHz, $CDCl_3$) δ 152.0, 138.5, 133.0, 118.4, 74.0, 43.2, 38.8, 35.1, 28.1, 28.0, 22.7.

6.2.2.2.3 *tert*-Butyl (3,5-dibromo-4-(2-morpholinoethoxy)phenethyl)carbamate (49c)

Carbamate **47** (1.00 g, 2.53 mmol), 4-(2-chloroethyl)morpholin-4-ium chloride **48c**•HCl (0.59 g, 3.16 mmol, 1.25 equiv.) and anhydrous K_2CO_3 (0.88 g, 6.33 mmol, 2.5 equiv.) were suspended in anhydrous acetone (40 mL) under argon atmosphere. The mixture was heated to reflux (80 °C) and stirred for 29 hours. TLC (hexane/EtOAc, 1:1) showed traces of the starting material. The reaction was left stirred over the weekend at room temperature after which no more starting material was detected. The solvent was then removed *in vacuo*. The crude product was extracted to DCM (25 mL) and washed with H_2O (35 mL). The water phase was re-extracted with DCM (1 × 20 mL, 1 × 15 mL). Combined organic layers were dried over Na_2SO_4, filtered and the solvent was removed *in vacuo*. The crude yellow oil (1.49 g) was purified by Biotage chromatography: Biotage SNAP Cartridge KP-Sil 25 g; eluent: hexane/EtOAc; gradient: 4:1 → 3:2, 10CV; 3:2, 30CV to give a white solid (1.23 g). The solid was re-crystallized from boiling hexane/DCM (approximately 20:1 ratio) to give **49c** as a white crystalline solid (1.13 g, 88% yield).

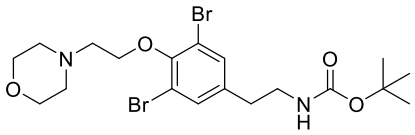

***R*f** 0.36 (hexane/EtOAc, 1:1); **Melting point:** 85.8–87.2 °C; **^{1}H NMR** (300 MHz, $CDCl_3$) δ 7.32 (s, 2H), 4.55 (br s, 1H), 4.12 (t, J = 5.7 Hz, 2H), 3.79–3.65 (m, 4H), 3.37–3.24 (m, 1H), 2.88 (t, J = 5.7 Hz, 2H), 2.71 (t, J = 7.0 Hz, 2H), 2.65–2.56 (m, 4H), 1.43 (s, 9H); **^{13}C NMR** (75 MHz, $CDCl_3$) δ 155.9, 151.9, 137.9, 133.1, 118.3, 70.3, 67.1, 58.4, 54.1, 41.7, 35.2, 28.5.

Notes: A missing peak for the carbamate moiety in ^{13}C NMR even though the measurement had been run repeatedly - the signal is most likely hidden under $CDCl_3$ peak.

6.2.2.2.4 2-(3,5-Dibromo-4-(2-morpholinoethoxy)phenyl)ethan-1-amine (33b)

Carbamate **49c** (1.05 g, 2.07 mmol) was dissolved in anhydrous DCM (10 mL) under argon atmosphere. TFA (356 µL, 4.65 mmol, 2.25 equiv.) was added dropwise over a period of 1 min. The mixture was stirred under argon atmosphere at room temperature for 4 h 30 min. A mini work-up with a small amount of the reaction mixture was performed in a vial after the stated time (2 M NaOH/EtOAc) and TLC (hexane/EtOAc, 3:7) showed no product in the reaction mixture. To the mixture was therefore added an extra amount of TFA (5 mL) to follow the previously used ratio DCM/TFA, 2:1 and the reaction mixture was left stirred overnight. The starting material was no longer present in the mixture after 21 hours of stirring at room temperature. The reaction mixture was then concentrated using pressurized air. The remaining solvent and TFA were removed *in vacuo*. The crude mixture was then extracted to EtOAc (1 × 20 mL) and washed with 2 M NaOH (20 mL). The water phase was re-extracted with EtOAc (2 × 20 mL). The combined organic layers were washed with water (2 × 25 mL). The combined water layers were re-extracted with EtOAc (2 × 25 mL). The combined organic layers were dried over Na_2SO_4, filtered and the solvent was removed *in vacuo* to give **33b** as light yellow clear oil (0.85 g, 100% yield).

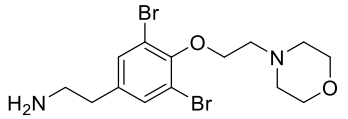

^{1}H NMR (300 MHz, $CDCl_3$) δ 7.34 (s, 2H), 4.12 (t, J = 5.7 Hz, 2H), 3.80–3.64 (m, 4H), 3.01–2.82 (m, 4H), 2.71–2.54 (m, 6H); **^{13}C NMR** (75 MHz, $CDCl_3$) δ 151.7, 138.7, 133.0, 118.2, 70.3, 67.1, 58.4, 54.1, 43.2, 38.7.

6.2.2.3 Syntheses of amides

6.2.2.3.1 *N*-(3,5-Dibromo-4-(3-(dimethylamino)propoxy)phenethyl)-3,5-bis(trifluoromethyl) benzamide (34a)

The compound **34a** was successfully synthesized using the general procedure, see Chapter 6.2.2.4.

Purpurealidin E **26** used from Master's student Mäki-Lohiluoma, E.[104] (100 mg, 0.263 mmol; orange gum) and 3,5-bis(trifluoromethyl)benzoic acid **50a** (67.9 mg, 0.263 mmol, 1.0 equiv.) were suspended in anhydrous DCM (5 mL) under argon atmosphere. TEA (73 µL, 0.526 mmol, 2.0 equiv.) was added dropwise to the mixture. Afterwards, EDC•HCl (63.0 mg, 0.329 mmol, 1.25 equiv.) was added under positive argon pressure, followed by an additional amount of DCM (1 mL). The reaction mixture was then stirred at room temperature under argon atmosphere for 1 day. TLC (DCM/MeOH, 4:1) indicated that the starting materials were still present in the mixture. DMAP (32.1 mg, 0.263 mmol, 1.0 equiv.) and EDC•HCl (25.2 mg, 0.132 mmol, 0.5 equiv.) were therefore added to the mixture. After 5 days, the reaction was diluted with DCM (10 mL) and washed with 25% NH_3/brine 1:1 (15 mL). The water and organic layer did not separate. Extra DCM (5 mL), H_2O (5 mL) and MeOH (a few drops) were added to the mixture and the layers separated. The organic layer was washed again with 25% NH_3/brine 1:1 (10 mL), H_2O (10 mL) and MeOH (<0.5 mL). The combined water layers were re-extracted with DCM (1 × 20, 1 × 10 mL). The combined organic layers were washed with H_2O (25 mL), dried over Na_2SO_4, filtered and the solvent was removed *in vacuo*. The crude product – brown solid (200 mg) was purified by Biotage chromatography: Biotage SNAP Cartridge KP-Sil 25 g; eluent: DCM/MeOH; gradient: 95:5 → 3:2, 60CV. Two fractions were collected separately and solvents were then removed *in vacuo*. The fraction that contained the assumed product was impure according to ^{1}H NMR. The product was attempted to be crystallized from several solvents (hexane, DCM, MeOH, acetone, EtOAc) by making a saturated solution while boiling. All recrystallizations were unsuccessful.

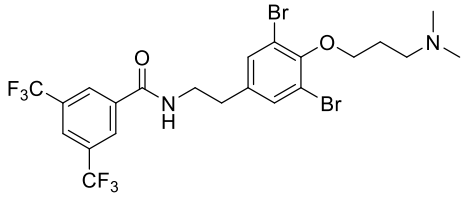

6.2.2.3.2 2-Bromo-*N*-(3,5-dibromo-4-(3-(dimethylamino)propoxy)phenethyl)benzamide (34b)

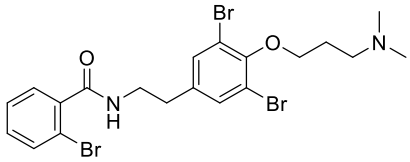

Purpurealidin E **26** (132 mg, 0.347 mmol), 2-bromobenzoic acid **50b** (69.8 mg, 0.347 mmol, 1.0 equiv.), EDC•HCl (79.9 mg, 0.417 mmol, 1.2 equiv.) and HOBt (63.8 mg, 0.417 mmol, 1.2 equiv.) were dissolved in anhydrous DCM (7 mL) under argon atmosphere. DIPEA (145 µL, 0.833 mmol, 2.4 equiv.) was added dropwise after 3 min and the reaction was then stirred at room temperature under argon atmosphere for 3 days and 18 hours. The reaction mixture was quenched with H_2O (4 mL). The mixture was washed with 1 M NaOH (4 mL) and extracted to DCM (5 mL). The water phase was re-extracted with DCM twice (1 × 7 mL, 1 × 8 mL). The combined organic layers were washed with H_2O (20 mL). The water phase was re-extracted with DCM twice (together 35 mL). The combined organic layers were dried over Na_2SO_4, filtered and the solvent was removed *in vacuo*. The crude white oily product (182 mg) was purified by silica gel column chromatography eluting with hexane/acetone + 3% TEA; gradient: 9:1 → 7:3. ^{1}H-NMR showed an aliphatic impurity (possibly amine residues from TEA) in the oily product (140 mg). A part of the product (95.0 mg) was purified by Biotage chromatography: Biotage SNAP Cartridge KP-Sil 10 g; eluent: DCM/MeOH; gradient: 1:0, 8CV; 1:0 → 2:3, 10 CV to give **34b** as light yellow sticky oil (91.0 mg, 46% yield).

***R*f** 0.36 (hexane/acetone, 1:1 + 3% TEA); **^{1}H NMR** (300 MHz, $CDCl_3$) δ 7.56 (dd, J = 7.9 Hz, J = 1.3 Hz, 1H), 7.48 (dd, J = 7.6 Hz, J = 1.8 Hz, 1H), 7.41 (s, 2H), 7.34 (ddd, J = 7.6 Hz, J = 7.5, J = 1.3 Hz, Hz, 1H), 7.25 (ddd, J = 7.9 Hz, J = 7.5 Hz, J = 1.8 Hz, 1H), 6.09 (br t, J = 5.3 Hz, 1H), 4.03 (t, J = 6.5 Hz, 2H), 3.72–3.63 (m, 2H), 2.88 (t, J = 6.9 Hz, 2H), 2.54 (t, J = 7.4, 2H), 2.26 (s, 6H), 2.10–1.96 (m, 2H); **^{13}C NMR** (75 MHz, $CDCl_3$) δ 167.8, 152.2, 137.8, 137.4, 133.5, 133.2, 131.5, 129.7, 127.7, 119.3, 118.5, 72.2, 56.5, 45.7, 41.1, 34.3, 28.5; **HRMS** (TOF-ESI+): *m/z* calcd for $C_{20}H_{24}Br_3N_2O_2$ $[M+H]^+$: 560.9388, found: 560.9388.

6.2.2.3.3 *N*-(3,5-Dibromo-4-(3-(dimethylamino)propoxy)phenethyl)-3,5-difluorobenzamide (34c)

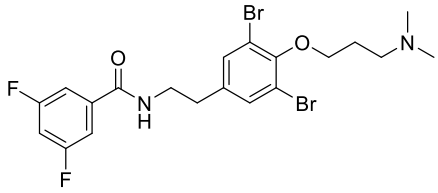

Purpurealidin E **26** (102 mg, 0.268 mmol), 3,5-difluorobenzoic acid **50c** (45.0 mg, 0.282 mmol, 1.05 equiv.) and HOBt (49.3 mg, 0.322 mmol, 1.2 equiv.) were dissolved in anhydrous DCM (7 mL) under argon atmosphere. The mixture was stirred for 5 minutes. DIC (40.6 mg, 0.322 mmol, 1.2 equiv.) was added dropwise to a clear mixture. DIPEA (112 µL, 0.644 mmol, 2.4 equiv.) was added dropwise after 3 hours 50 min and the reaction was then stirred at room temperature under argon atmosphere for 42 hours. The reaction mixture was quenched with H_2O (4 mL). The mixture was washed with 1M NaOH (4 mL) and extracted to DCM (10 mL). The water phase was re-extracted with DCM twice (together 22 mL). The combined organic layers were washed with H_2O (25 mL). The water phase was re-extracted with DCM twice (together 30 mL). The combined organic layers were dried over Na_2SO_4, filtered and the solvent was removed *in vacuo*. The crude white and yellow solid product (167 mg) was purified by silica gel column chromatography: eluent: hexane/acetone + 3%TEA; gradient: 8:2 → 7:3. Two fractions containing the product were collected (1: 38.0 mg, white solid and 2: 70.0 mg, light yellow solid). ^{1}H-NMR showed an aliphatic impurity in both of the fractions. The fraction 1 (38.0 mg) was purified by Biotage chromatography: Biotage SNAP Cartridge KP-Sil 10 g; eluent: DCM/MeOH; gradient: 1:0 → 52:48 to give **34c** as a white solid (30.0 mg, 21% yield).

***R*f** 0.33 (hexane/acetone, 3:2 + 3% TEA); **^{1}H NMR** (300 MHz, $CDCl_3$) δ 7.35 (s, 2H), 7.28–7.14 (m, 2H), 6.98–6.88 (m, 1H), 6.27 (br t, J = 5.5 Hz, 1H), 4.04 (t, J = 6.5 Hz, 2H), 3.63 (dt, J = 6.7 Hz, J = 6.7 Hz, 2H), 2.84 (t, J = 7.0 Hz, 2H), 2.55 (t, J = 7.4 Hz, 2H), 2.27 (s, 6H), 2.10–1.98 (m, 2H); **^{13}C NMR** (75 MHz, $CDCl_3$) δ 165.4 (t, $^4J_{C,F}$ = 2.9 Hz), 163.1 (dd, $^3J_{C,F}$ = 12.1 Hz, $^1J_{C,F}$ = 251.0 Hz), 152.3, 137.9 (t, $^3J_{C,F}$ = 8.3 Hz), 137.3, 133.0, 118.6, 110.3 (m_c), 107.1 (t, $^2J_{C,F}$ = 25.3 Hz), 72.2, 56.5, 45.6, 41.3, 34.5, 28.4; **HRMS** (TOF-ESI+): *m/z* calcd for $C_{20}H_{23}Br_2F_2N_2O_2$ $[M+H]^+$: 519.0094, found: 519.0090.

6.2.2.3.4 *N*-(3,5-Dibromo-4-(3-(dimethylamino)propoxy)phenethyl)-2-fluorobenzamide (34d)

Purpurealidin E **26** (103 mg, 0.271 mmol), 2-fluorobenzoic acid **50d** (41.8 mg, 0.298 mmol, 1.1 equiv.), EDC•HCl (62.3 mg, 0.325 mmol, 1.2 equiv.) and HOBt (49.8 mg, 0.325 mmol, 1.2 equiv.) were dissolved in anhydrous DCM (8 mL) under argon atmosphere. DIPEA (113 µL, 0.650 mmol, 2.4 equiv.) was added dropwise after 5 min and the reaction was then stirred at room temperature under argon atmosphere for 42 hours. The reaction mixture was quenched with H_2O (4 mL). The mixture was washed with 1 M NaOH (5 mL) and extracted to DCM (15 mL). The water phase was re-extracted with DCM twice (together 20 mL). The combined organic layers were washed with H_2O twice (1 × 25, 1 × 15 mL). The water phase was re-extracted with DCM twice (2 × 15 mL). The combined organic layers were dried over Na_2SO_4, filtered and the solvent was removed *in vacuo*. The crude yellow sticky oil (129 mg) was purified by silica gel column chromatography: eluent: hexane/acetone + 3%TEA; gradient: 4:1 → 75:25 to give ivory solid (101 mg). ^{1}H-NMR showed an aliphatic impurity (possibly amine residues from TEA). The product was therefore purified by Biotage chromatography: Biotage SNAP Cartridge KP-Sil 10 g; eluent: DCM/MeOH; gradient: 1:0, 6CV; 1:0 → 2:3, 12CV to give **34d** as a white solid (83.7 mg, 62% yield).

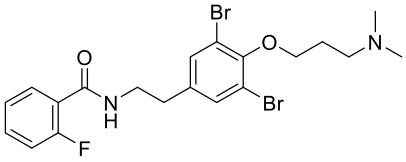

***R*f** 0.58 (DCM/MeOH, 4:1). **^{1}H NMR** (300 MHz, $CDCl_3$) δ 8.08 (ddd, J = 7.9, 7.8, 1.8 Hz, 1H), 7.46 (dddd, J = 8.3, 7.3, 5.3, 1.9 Hz, 1H), 7.38 (s, 2H), 7.26 (ddd, J = 7.8, 7.6, 1.1 Hz, 1H), 7.10 (ddd, J = 12.2, 8.3, 1.1 Hz, 1H), 6.83–6.69 (m, 1H), 4.05 (t, J = 6.5 Hz, 2H), 3.72–3.64 (m, 2H), 2.85 (t, J = 7.1 Hz, 2H), 2.55 (t, J = 7.4 Hz, 2H), 2.28 (s, 6H), 2.10–1.99 (m, 2H); **^{13}C NMR** (75 MHz, $CDCl_3$) δ 163.5 (d, $^3J_{C,F}$ = 3.3 Hz), 160.8 (d, $^1J_{C,F}$ = 247.5 Hz), 152.2, 137.6, 133.5 (d, $^3J_{C,F}$ = 9.2 Hz), 133.0, 132.1 (d, $^4J_{C,F}$ = 2.2 Hz), 125.0 (d, $^3J_{C,F}$ = 3.4 Hz), 121.0 (d, $^2J_{C,F}$ = 11.6 Hz), 118.5, 116.2 (d, $^2J_{C,F}$ = 24.9 Hz), 72.1, 56.5, 45.6, 41.2, 34.6, 28.4.; **HRMS** (TOF-ESI+): *m/z* calcd for $C_{20}H_{24}Br_2FN_2O_2$ $[M+H]^+$: 501.0189, found: 501.0193.

6.2.2.4 General procedure: Synthesis of amides

The following products were synthesized and worked-up using the following general procedure:

Purpurealidin E **26** or its carbon analogue **33a** (0.256–0.295 mmol), carboxylic acid **50** (1.0 equiv.), EDC•HCl (1.2 equiv.), HOBt (1.2 equiv.) were dissolved in anhydrous DCM (7 mL) under argon atmosphere. DIPEA (3.0 equiv.) was added dropwise to the mixture and the reaction was then stirred at room temperature under argon atmosphere for 2–4 days. The reaction mixture was then quenched with H_2O (4 mL), washed with 1 M NaOH (10 mL) and extracted to DCM (10 mL). The water phase was re-extracted with DCM (2 × 10 mL). The combined organic layers were washed with H_2O (30 mL). The water phase was re-extracted with DCM (2 × 20 mL). The combined organic layers were dried over Na_2SO_4, filtered and the solvent was removed *in vacuo.*

6.2.2.4.1 *N*-(3,5-Dibromo-4-(3-(dimethylamino)propoxy)phenethyl)-3,5-bis(trifluoromethyl) benzamide (34a)

The compound was synthesized using the general method, starting from purpurealidin E **26** (113 mg, 0.297 mmol) and acid **50a** (77.0 mg, 0.297 mmol, 1.0 equiv.).

The crude product (189 mg) was purified by Biotage chromatography: Biotage SNAP Cartridge KP-Sil 25 g; eluent: DCM/MeOH; gradient: 1:0 → 8:2 to give a yellow solid (143 mg). ^{1}H-NMR and ^{13}C-NMR showed an impurity – grease. The grease was removed by silica gel column chromatography (3 × 3 cm) by eluting the sample with: hexane (120 mL), EtOAc (50 mL) and acetone (70 mL). ^{1}H-NMR showed a successful removal of the grease but new aliphatic impurities appeared due to which an extraction was performed as follows: The product was dissolved in 10 DCM (10 mL) and washed with H_2O twice (1 × 10 mL, 1 × 15 mL). The combined water layers were re-extracted with DCM twice (together 40 mL). The combined organic layers were dried over Na_2SO_4, filtered and the solvent was removed *in vacuo* to give a light yellow solid (115 mg). ^{1}H-NMR showed a successful removal of aliphatic impurities but the grease impurity appeared again. Another removal of the grease impurity was performed similarly as before to give **34a** as a light yellow solid (56.0 mg, 30% yield). *Analytical data are on the next page.*

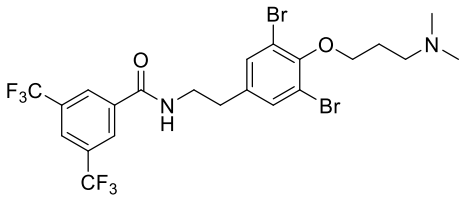

***R*f** 0.49 (hexane/acetone, 3:2 + 3% TEA); **^{1}H NMR** (300 MHz, $CDCl_3$) δ 8.16 (s, 2H), 8.01 (s, 1H), 7.38 (s, 2H), 6.36 (br t, J = 5.6 Hz, 1H), 4.04 (t, J = 6.4 Hz, 2H), 3.74–3.63 (m, 1H), 2.88 (t, J = 7.0 Hz, 2H), 2.55 (t, J = 7.4 Hz, 2H), 2.28 (s, 6H), 2.12–1.96 (m, 2H); **^{13}C NMR** (75 MHz, $CDCl_3$) δ 164.9, 152.4, 137.1, 136.6, 133.0, 132.5 (q, $^2J_{C,F}$ = 34.0 Hz), 127.4 (q, $^3J_{C,F}$ = 3.3 Hz), 125.3 (quin, $^3J_{C,F}$ = 3.6 Hz), 123.0 (q, $^1J_{C,F}$ = 273.1 Hz), 118.7, 72.2, 56.5, 45.7, 41.5, 34.4, 28.5; **HRMS** (TOF-ESI+): *m/z* calcd for $C_{22}H_{23}Br_2F_6N_2O_2$ $[M+H]^+$: 619.0030, found: 6190.0032.

6.2.2.4.2 3-Chloro-*N*-(3,5-dibromo-4-(3-(dimethylamino)propoxy)phenethyl)benzamide (34e)

The compound was synthesized using the general method, starting from purpurealidin E **26** (111 mg, 0.292 mmol) and 3-chlorobenzoic acid **50e** (45.7 mg, 0.292 mmol, 1.0 equiv.).

The crude oily product (154 mg) was purified by Biotage chromatography: Biotage SNAP Cartridge KP-Sil 25 g; eluent: DCM/MeOH; gradient: 1:0 → 82:18, 60 CV to give gummy oil (115 mg). ^{1}H-NMR and ^{13}C-NMR showed an impurity – grease. The grease was removed by silica gel column chromatography (2 × 3 cm) by eluting the sample with: hexane (70 mL), EtOAc (70 mL) and acetone (120 mL), respectively. ^{1}H-NMR showed a successful removal of the grease but new aliphatic impurities appeared. Because the NMR tube was washed with grease-contaminated DCM again, an extraction was not performed as with **34a**. The product (101.6 mg) was purified by Biotage chromatography: Biotage SNAP Cartridge KP-Sil 10 g; eluent: hexane/EtOAc; gradient: 1:0, 6 CV; 1:0 → 0:1, 3 CV; 1:0, 5.6 CV; then the strong solvent was exchanged for acetone which was used to elute the product. ^{1}H-NMR of the clear light yellow oil (88.0 mg, 58%) nevertheless showed some aliphatic impurities (9.6%).

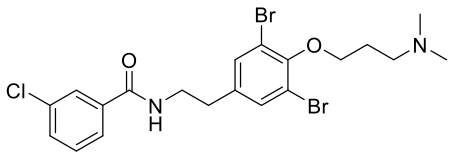

***R*f** 0.36 (hexane/acetone, 3:2 + 3% TEA); **^{1}H NMR** (300 MHz, $CDCl_3$) δ 7.72–7.69 (m, 1H), 7.56 (ddd, J = 7.6, 1.7, 1.2 Hz, 1H), 7.47 (ddd, J = 8.0, 2.1, 1.2 Hz, 1H), 7.39–7.33 (m, 3H), 6.20 (s, 1H), 4.04 (t, J = 6.5 Hz, 2H), 3.69–3.60 (m, 2H), 2.84 (t, J = 7.0 Hz, 2H), 2.54 (t, J = 7.0 Hz, 2H), 2.27 (s, 6H), 2.12–1.96 (m, 2H).

6.2.2.4.3 4-Bromo-*N*-(3,5-dibromo-4-(3-(dimethylamino)propoxy)phenethyl)benzamide (34f)

The compound was synthesized using the general method, starting from purpurealidin E **26** (112 mg, 0.295 mmol) and 4-bromobenzoic acid **50f** (59.2 mg, 0.295 mmol, 1.0 equiv.). This time 1.5 equivalents of EDC•HCl (84.7 mg, 0.442 mmol, 1.5 equiv.) and HOBt (67.7 mg, 0.442 mmol, 1.5 equiv.) were used.

The crude oily product (162 mg) was purified by Biotage chromatography: Biotage SNAP Cartridge KP-Sil 25 g; eluent: DCM/MeOH; gradient: 1:0 → 82:18, 65 CV to give gummy oil (113 mg). ^{1}H NMR and ^{13}C NMR showed impurity – grease. The grease was removed by silica gel column chromatography (1 × 3 cm) by eluting the sample with: hexane (80 mL), EtOAc (80 mL) and acetone (350 mL). The product was then transferred from a flask into a vial using DCM contaminated with grease. Therefore another grease removal was performed similarly as before without a previous NMR characterization. The purification gave **34f** as a white solid (98.0 mg, 59% yield).

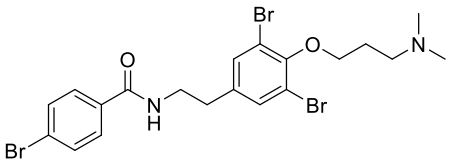

***R*f** 0.31 (hexane/acetone, 3:2 + 3% TEA); **^{1}H NMR** (300 MHz, $CDCl_3$) δ 7.63–7.52 (m, 4H), 7.36 (s, 2H), 6.28 (br t, J = 5.9 Hz, 1H), 4.05 (t, J = 6.2 Hz, 2H), 3.68–3.58 (m, 2H), 2.88–2.74 (m, 4H) 2.43 (s, 6H), 2.22–2.07 (m, 2H); **^{13}C NMR** (75 MHz, $CDCl_3$) δ 166.6, 151.7, 137.6, 133.2, 132.9, 131.8, 128.5, 126.3, 118.3, 71.3, 56.2, 44.8, 41.0, 34.4, 27.4; **HRMS** (TOF-ESI+): *m/z* calcd for $C_{20}H_{24}Br_3N_2O_2$ $[M+H]^+$: 560.9388, found: 560.9387.

6.2.2.4.4 3,5-Dichloro-*N*-(3,5-dibromo-4-((4-methylpentyl)oxy)phenethyl)benzamide (35a)

The compound was synthesized using the general method, starting from amine **33a** (97.0 mg, 0.256 mmol), and 2,4-dichlorobenzoic acid **50i** (48.9 mg, 0.256 mmol, 1.0 equiv.).

The crude brownish product (149 mg) was purified by Biotage chromatography: Biotage SNAP Cartridge KP-Sil 25 g; eluent: hexane/EtOAc; gradient: 9:1, 7 CV; 9:1 → 83:17, 6 CV; 83:17, 8 CV to give **35a** as a white solid (89.0 mg, 63% yield).

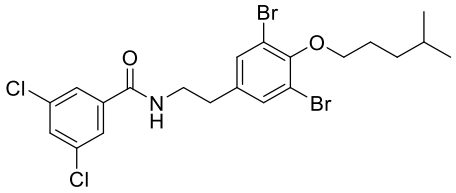

***R*f** 0.63 (hexane/acetone, 3:2 + 3% TEA); **^{1}H NMR** (300 MHz, $CDCl_3$) δ 7.56 (d, J = 1.9 Hz, 2H), 7.48 (t, J = 1.9 Hz, 1H), 7.36 (s, 2H), 6.16 (br t, J = 3.9 Hz, 1H), 3.98 (t, J = 6.7 Hz, 2H), 3.68–3.59 (m, 2H), 2.84 (t, J = 7.0 Hz, 2H), 1.95–1.77 (m, 2H), 1.71–1.54 (m, 1H), 1.50–1.32 (m, 2H), 0.93 (d, J = 6.6 Hz, 6H); **^{13}C NMR** (75 MHz, $CDCl_3$) δ 165.3, 152.5, 137.5, 137.1, 135.7, 133.0, 131.6, 125.7, 118.7, 74.1, 41.3, 35.1, 34.5, 28.1, 28.0, 22.7; **HRMS** (TOF-ESI+): *m/z* calcd for $C_{21}H_{24}Br_2Cl_2NO_2$ $[M+H]^+$: 549.9551, found: 549.9554.

6.2.2.4.5 5-Bromo-*N*-(3,5-dibromo-4-(3-(dimethylamino)propoxy)phenethyl)nicotinamide (34g)

The compound was synthesized using the general method, starting from purpurealidin E **26** (0.100 mg, 0.263 mmol) and 5-bromonicotinic acid **50g** (53.1 mg, 0.263 mmol, 1.0 equiv.).

The crude brown product – partially solidified oil, (133 mg) was purified by Biotage chromatography: Biotage SNAP Cartridge KP-Sil 25 g; eluent: DCM/MeOH; gradient: 1:0 → 79:21, 48 CV to give **34g** as a white solid (84.0 mg, 57% yield).

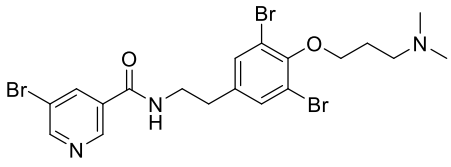

Analytical data are on the next page.

***R*f** 0.29 (hexane/acetone, 3:2 + 3% TEA); **^{1}H NMR** (300 MHz, $CDCl_3$) δ 8.80 (d, J = 1.9 Hz, 1H), 8.77 (d, J = 2.3 Hz, 1H), 8.21 (t, J = 2.1 Hz, 1H), 7.36 (s, 2H), 6.43 (br t, J = 5.5 Hz, 1H), 4.04 (t, J = 6.4 Hz, 2H), 3.71–3.62 (m, 2H), 2.86 (t, J = 7.0 Hz, 2H), 2.60 (t, J = 7.4 Hz, 2H), 2.31 (s, 6H), 2.13–1.97 (m, 2H); **^{13}C NMR** (75 MHz, $CDCl_3$) δ 164.5, 153.6, 152.2, 145.9, 137.9, 137.3, 133.0, 131.6, 121.2, 118.6, 72.0, 56.5, 45.5, 41.3, 34.5, 28.2; **HRMS** (TOF-ESI+): *m/z* calcd for $C_{19}H_{23}Br_3N_3O_2$ $[M+H]^+$: 561.9340, found: 561.9339.

6.2.2.4.6 *N*-(3,5-Dibromo-4-(3-(dimethylamino)propoxy)phenethyl)-5-methylisoxazole-3-carboxamide (34h)

The compound was synthesized using the general method, starting from purpurealidin E **26** (0.101 mg, 0.266 mmol), and 5-methylisoxazole-3-carboxylic acid **50h** (33.7 mg, 0.266 mmol, 1.0 equiv.).

The crude product, white and yellow solids (123 mg), was purified by crystallization as follows. The crude material was dissolved in warm hexane. The yellow solids stayed undissolved. The remaining solution was transferred into another flask, brought to reflux and left to cool to room temperature. A white solid appeared. The mixture was left in a freezer and then filtrated to give **34h** as a white solid (16.8 mg, 13% yield).

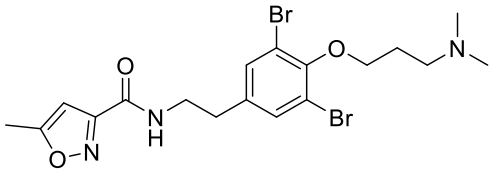

^{1}H NMR (300 MHz, $CDCl_3$) δ 7.36 (s, 2H), 6.86 (br t, J = 5.4 Hz, 1H), 6.43 (q, J = 0.8 Hz, 1H), 4.04 (t, J = 6.5 Hz, 2H), 3.68–3.52 (m, 2H), 2.82 (t, J = 7.3 Hz, 2H), 2.57–2.50 (m, 2H), 2.47 (d, J = 0.9 Hz, 3H), 2.27 (s, 6H), 2.09–1.97 (m, 2H); **^{13}C NMR** (75 MHz, $CDCl_3$) δ 171.4, 159.4, 158.7, 152.2, 137.1, 133.0, 118.6, 101.5, 72.1, 56.5, 45.7, 40.5, 34.6, 28.5, 12.5; **HRMS** (TOF-ESI+): *m/z* calcd for $C_{18}H_{24}Br_2N_3O_3$ $[M+H]^+$: 488.0184, found: 488.0184.

6.2.2.4.7 3,5-Dibromo-N-(3,5-dibromo-4-((4-methylpentyl)oxy)phenethyl)benzamide (35b)

The compound was synthesized using the general method, starting from amine **33a** (100 mg, 0.264 mmol), and 2,4-dibromobenzoic acid **50j** (73.8 mg, 0.264 mmol, 1.0 equiv.).

The crude yellow solid (162 mg) was purified by recrystallization from hexane/DCM (25:1). Some impurities were seen in ^{1}H NMR spectrum. The afforded white solid (109 mg) was therefore purified by Biotage chromatography: Biotage SNAP Cartridge KP-Sil 25 g; eluent: hexane/EtOAc; gradient: 1:0 → 9:1, 10 CV; 9:1, 20 CV to give **35b** as a white solid (100.2 mg, 59% yield).

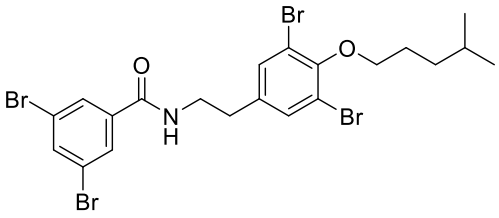

***R*f** 0.78 (hexane/EtOAc, 1:1); **^{1}H NMR** (300 MHz, $CDCl_3$) δ 7.79–7.77 (m, 1H), 7.76–7.74 (m, 2H), 7.36 (s, 2H), 6.16 (br t, J = 5.9 Hz, 1H), 3.98 (t, J = 6.7 Hz, 2H), 3.69–3.53 (m, 2H), 2.84 (t, J = 7.0 Hz, 2H), 1.97–1.79 (m, 2H), 1.72–1.51 (m, 1H), 1.48–1.31 (m, 2H), 0.93 (d, J = 6.6 Hz, 6H); **^{13}C NMR** (75 MHz, $CDCl_3$) δ 165.0, 152.5, 137.9, 137.1, 133.0, 129.0, 123.5, 118.7, 74.1, 41.3, 35.1, 34.5, 28.1, 28.0, 22.72; **HRMS** (TOF-ESI+): *m/z* calcd for $C_{21}H_{24}Br_4NO_2$ $[M+H]^+$: 637.8541, found: 637.8537.

Notes: Missing peak in ^{13}C NMR probably due to overlapping.

6.2.2.5 Amide coupling using microwave irradiation

6.2.2.5.1 *N*-(3,5-Dibromo-4-(3-(dimethylamino)propoxy)phenethyl)-4-methoxybenzamide (34i)

Purpurealidin E **26** (100 mg, 0.263 mmol), 4-methoxybenzoic acid **50k** (40.0 mg, 0.263 mmol, 1.0 equiv.), EDC•HCl (60.5 mg, 0.316 mmol, 1.2 equiv.), HOBt (48.3 mg, 0.316 mmol, 1.2 equiv.) were dissolved in anhydrous DCM (7 mL). DIPEA (137 µL, 0.789 mmol, 3.0 equiv.) was then added dropwise to the mixture. The mixture was irradiated in a microwave reactor for 1 hour at 50 °C (average 25 W) after which TLC (hexane/acetone, 3:2 + 3% TEA) indicated the presence of starting materials. The mixture (yellow) was therefore irradiated further under the same reaction conditions for

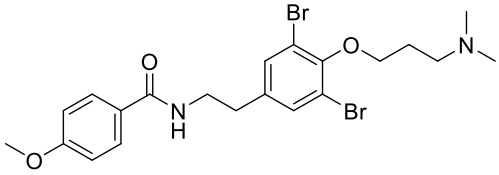

an additional 1 hour. The starting amine was then no longer detected. The reaction mixture was quenched with H_2O (4 mL), washed with 2 M NaOH (10 mL). The water phase was re-extracted with DCM (2 × 10 mL). The combined organic layers were washed with H_2O (40 mL). The water phase was re-extracted with DCM (2 × 20 mL). The combined organic layers were dried over Na_2SO_4, filtered and the solvent was removed *in vacuo*. The crude yellow oil, partially solidified (153.3 mg) was purified by Biotage chromatography: Biotage SNAP Cartridge KP-Sil 25 g; eluent: DCM/MeOH; gradient: 1:0, 18CV; 1:0 → 9:1, 10CV, 9:1 → 84:16, 17CV; 84:16, 15CV to give **34i** as a white solid (100.0 mg, 74% yield).

***R*f** 0.25 (hexane/acetone, 3:2 + 3% TEA); **^{1}H NMR** (300 MHz, $CDCl_3$) δ 7.71–7.65 (m, 2H), 7.37 (s, 2H), 6.94–6.88 (m, 2H), 6.15 (br t, J = 5.8 Hz, 1H), 4.05 (t, J = 6.3 Hz, 2H), 3.84 (s, 3H), 3.69–3.53 (m, 2H), 2.84 (t, J = 7.0 Hz, 2H), 2.73 (t, J = 7.5 Hz, 2H), 2.40 (s, 6H), 2.18–2.07 (m, 2H); **^{13}C NMR** (75 MHz, $CDCl_3$) δ 167.3, 162.4, 151.9, 138.0, 133.1, 128.8, 126.8, 118.4, 114.0, 71.6, 56.4, 55.6, 45.2, 41.0, 34.8, 27.8.

6.2.2.6 Synthesis of non-brominated analogue 36a

6.2.2.6.1 3,5-Dichloro-*N*-(4-hydroxyphenethyl)benzamide (51)

Tyramine (130 mg, 0.948 mmol), 3,5-dichlorobenzoic acid **50i** (181 mg, 0.948 mmol, 1.0 equiv.) and HBTU (431 mg, 1.14 mmol, 1.2 equiv.) were suspended in anhydrous DCM (8 mL) under argon atmosphere. After 10 minutes, the mixture became very dense and was not stirred properly. An extra amount of anhydrous DCM (2 mL) was added. The reaction was stirred at room temperature for 74 hours after which the starting materials appeared to be still present in the mixture (TLC DCM/MeOH, 9:1). The mixture was then diluted with DCM (10 mL) and washed with sat. NH_4Cl (15 mL). The water phase was re-extracted twice with DCM (1x 15 mL, 1 × 20 mL). The combined organic phases were dried with Na_2SO_4, filtered and the solvent was removed *in vacuo*. When preparing a samplet for a column chromatography, the crude product (331 mg, brown solid) could not be dissolved in a large amount of DCM. Therefore another work-up was performed. The crude product was washed with H_2O (2 × 20 mL) and extracted to DCM (20 mL). Each water layer was then re-extracted with DCM (1 × 20 mL each). The combined organic layers were dried with Na_2SO_4, filtered and the solvent was removed *in vacuo*. The crude product was then purified by Biotage chromatography: Biotage SNAP Cartridge KP-Sil 25 g; eluent: hexane/EtOAc; gradient: 8:2 → 6:4, 10CV; 6:4, 20CV to give a white powder (121 mg). ^{13}C NMR showed an impurity – the starting acid. The product was recrystallized from DCM/MeOH (40:1 ratio, approximately 20.5 mL) to give **51** as a white crystalline solid (87.3 mg, 30% yield).

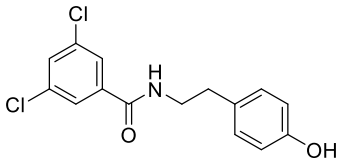

***R*f** 0.34 (hexane/EtOAc, 6:4); **Melting point:** 165.1–169.3 °C; **^{1}H NMR** (300 MHz, DMSO-d_6) δ 9.16 (s, 1H), 8.73 (t, J = 5.6 Hz, 1H), 7.83 (d, J = 1.9 Hz, 2H), 7.78 (t, J = 1.9 Hz, 1H), 7.11–6.87 (m, 2H), 6.76–6.56 (m, 2H), 3.47–3.35 (m, 2H), 2.72 (t, J = 7.8 Hz, 2H). ^{13}C NMR (75 MHz, DMSO-d_6) δ 163.3, 155.7, 137.8, 134.2, 130.5, 129.5, 129.3, 126.0, 115.1, 41.4, 34.0; **HRMS** (TOF-ESI+): *m/z* calcd for $C_{15}H_{14}Cl_2NO_2$ $[M+H]^+$: 310.0402, found: 310.0401.

6.2.2.6.2 3-5-Dichloro-*N*-(4-3-(dimethylamino)propoxy)phenethyl)benzamide (36a)

Phenol **51** (50.0 mg, 0.161 mmol), 3-Chloro-*N*,*N*-dimethylpropylamine hydrochloride **48a**•HCl (30.7 mg, 0.193 mmol, 1.2 equiv.) and anhydrous K_2CO_3 (55.7 mg, 0.403 mmol, 2.5 equiv.) were suspended in anhydrous acetone (2.5 mL) under argon atmosphere. The mixture was heated to reflux (85 °C) and stirred for 24 hours. After that, the reaction mixture was brought to room temperature and stirred over the weekend. TLC (hexane/EtOAc, 1:1) indicated that the starting material was still present in the mixture, now a dense suspension. An additional amount of anhydrous acetone was added (2 mL) and the mixture was refluxed for 9 hours until the starting material was not detected by TLC. The total reaction time was 4 days 18 hours. The total time of reflux was 2 days 2 hours. The solvent was then removed *in vacuo*. The crude product was extracted to DCM (10 mL) and washed with H_2O (8 mL). The water phase was re-extracted with DCM (2 × 8 mL). Combined organic layers were dried over Na_2SO_4, filtered and the solvent was removed *in vacuo* to give the crude product as a light yellow solid (73.0 mg). The solid was purified by Biotage chromatography: Biotage SNAP Cartridge KP-Sil 10 g; eluent: DCM/MeOH; gradient: 1:0 → 94:6, 7CV; 94:6 → 9:1, 5CV; 9:1 → 87:13, 9CV; 87:13, 3CV; 87:13 → 4:1, 9CV to give **36a** as a white solid (43.0 mg, 68% yield).

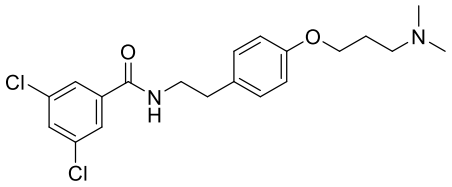

***R*f** 0.23 (hexane/acetone, 3:2 + 3% TEA); **^{1}H NMR** (300 MHz, $CDCl_3$) δ 7.54 (d, J = 1.9 Hz, 2H), 7.47–7.44 (m, 1H), 7.15–7.08 (m, 2H), 6.90–6.83 (m, 2H), 6.14 (br s, 1H), 4.00 (t, J = 6.4 Hz, 2H), 3.70–3.60 (m, 2H), 2.86 (t, J = 6.9 Hz, 2H), 2.52 (t, J = 7.3 Hz, 2H), 2.30 (s, 6H), 2.04–1.92 (m, 2H); **^{13}C NMR** (75 MHz, $CDCl_3$) δ 165.0, 158.0, 137.8, 135.6, 131.4, 130.6, 129.8, 125.7, 115.0, 66.3, 56.5, 45.5, 41.7, 34.8, 27.8; **HRMS** (TOF-ESI+): *m/z* calcd for $C_{20}H_{25}Cl_2N_2O_2$ $[M+H]^+$: 395.1293, found: 395.1292.

6.2.3 Biological testing

6.2.3.1 K_V10.1 inhibition

The screening for K_V10.1 inhibition was done by Lien Moreels, PhD and Hannah Goovaerts of University of Leuven (KU Leuven), Leuven, Belgium. The conceptualization, methodology and/or resourcing was done by Prof. Jan Tytgat, PhD and Steve Peigneur, PhD of KU Leuven and Farrah Zahed, PhD and professor Luis Pardo, PhD of the Max-Planck-Institute of Experimental Medicine, Göttingen, Germany.

6.2.3.1.1 Expression of voltage-gated ion channels in *Xenopus laevis* oocytes

For the expression of human K_V10.1a (GeneBank accession number: NM_002238.3) in *Xenopus* oocytes, the human K_V10.1a-pSGEM plasmid was linearized with SfiI (ThermoFisher Scientific, Waltham, Massachusetts, USA) and transcribed using the T7 mMESSAGE-mMACHINE transcription kit (Ambion®, Carlsbad, California, USA).

Isolation of stage V-VI *Xenopus laevis* (African clawed frog) oocytes was done by partial ovariectomy. Mature female animals were purchased from Nasco (Fort Atkinson, Wisconsin, USA) and were housed in the Aquatic Facility (KU Leuven) in concordance with the regulations of the European Union (EU) concerning the welfare of laboratory animals as declared in Directive 2010/63/EU. The Animal Ethics Committee of the KU Leuven approved the use of *Xenopus laevis* (Project No. P038/2017). Prior to harvesting the oocytes, the animals were anesthetized by a 15-min submersion in 0.1% tricaine methanesulfonate (pH 7.0). Isolated oocytes were defolliculated with 1.5 mg/mL collagenase.

Defolliculated oocytes were injected with 4 nL of cRNA at a concentration of 1 ng/nL using a micro-injector (Drummond Scientific®, Broomall, Pennsylvania, USA). The oocytes were incubated in a solution containing (in mM): NaCl, 96; KCl, 2; $CaCl_2$, 1.8; $MgCl_2$, 2 and HEPES, 5 (pH 7.4), supplemented with 50 mg/L gentamycin sulfate.

6.2.3.1.2 Electrophysiological recordings

Two-electrode voltage-clamp recordings were performed at room temperature (18–22 °C) using a Geneclamp 500 amplifier (Molecular Devices, USA) controlled by

a pClamp data acquisition system (Axon Instruments®, Union City, California, USA). Whole cell currents from oocytes were recorded 1–4 days after injection. Bath solution composition was (in mM): NaCl, 96; KCl, 2; $CaCl_2$, 1.8; $MgCl_2$, 2 and HEPES, 5 (pH 7.5). Voltage and current electrodes were filled with a 3 M solution of KCl in H_2O. Resistances of both electrodes were kept between 0.5 and 1.5 MΩ. The elicited K_V10.1 currents were filtered at 1 kHz and sampled at 2 kHz using a four-pole low-pass Bessel filter. Leak subtraction was performed using a -P/4 protocol. K_V10.1 currents were evoked by 2-s depolarizing pulses to 0 mV from a holding potential of -90 mV unless otherwise indicated.

6.2.3.1.3 Data analysis

All electrophysiological data are presented as means ± S.E.M of $n \geq 3$ independent experiments unless otherwise indicated. All data was analyzed using pClamp Clampfit 10.4 (Molecular Devices®, Downingtown, Pennsylvania, USA) and OriginPro 8 (Originlab®, Northampton, Massachusetts, USA) or GraphPad Prism 5 software (GraphPad Software, Inc., San Diego, California, USA).

6.2.3.2 Cytotoxicity

The cytotoxicity testing was performed by Katja-Emilia Lillsunde of the University of Helsinki, Helsinki, Finland.

6.2.3.2.1 Growth and assay media used

Growth medium: Glutamax DMEM with high glucose (222.5 mL), FBS (heat-inactivated) 10% (25 mL), Pen-Strep (100 x) (2.5 mL).

Assay medium (5% FBS): Glutamax DMEM with high glucose (117.5 mL), FBS (heat-inactivated) 10% (6.25 mL), Pen-Strep (100 x) (1.25 mL).

6.2.3.2.2 Protocol

A375 cells were seeded into a 96-well Perkin Elmer View Plate at a density of 10,000 cells/well and Hs27 cells were planted at a density of 7500 cells/well. 100 µL of the cell suspension was dispensed per well and the cells were incubated for 20–24 hours at 37 °C, 5% CO_2 and 95% humidity. Prior to starting the assay, the cells were observed

under microscope and checked if they were properly attached, evenly growing in all wells and forming an almost confluent monolayer.

The samples were dissolved in DMSO, diluted with assay medium (3.5 µL stock ad 700 µL assay medium) and the samples were transferred, 200 µL per well, to the 96-well plate, in triplicates. As a positive control, 1 µM camptothecin and 0.5% DMSO were used.

After 48 hours of incubation at 37 °C, 5% CO_2, 95% humidity, cell viability was first checked by microscope and then determined by CellTiter-Glo® Luminescence Cell Assay Kit. The cells were washed with 100 µL of PBS, followed by 50 µL of the assay media and 50 µL of the prepared CellTiter-Glo® reagent (per well). The contents of cells were mixed for 2 minutes on a plate shaker and then incubated for 10 min at room temperature to stabilize the luminescent signal before measurement. The measurement of luminescence was performed using VarioSkan Microplate Reader (Thermo Fisher Scientific, Finland).

Initially, preliminary screening was performed against malignant melanoma A375 cells at 50 µM concentration. If the cytotoxicity observed in preliminary testing was at least 80%, IC_{50} values were determined. Compounds with IC_{50} of less than 20 µM were then tested against normal foreskin fibroblast cells Hs27 to evaluate selectivity. All dose-response assays were performed in a concentration range of 1.56 to 50 µM in a 2-fold dilution set at least twice to make the results repetitive.

7 REFERENCES

1. World Health Organization (WHO). Cancer: Fact sheet. February 2017. [Internet]. 2017 [cited 18 Nov 2017]. Available online: who.int/mediacentre/factsheets/fs297/en/
2. Amin, A.R.; Kucuk, O.; Khuri, F.R.; Shin, D.M. Perspectives for cancer prevention with natural compounds. *J. Clin. Oncol.* **2009**, *27*, 2712–2725.
3. Pettit, G.R.; Singh, S.B.; Niven, M.L.; Hamel, E.; Schmidt, J.M. Isolation, structure, and synthesis of combretastatins A-1 and B-1, potent new inhibitors of microtubule assembly, derived from *Combretum caffrum*. *J. Nat. Prod.* **1987**, *50*, 119–131.
4. Tilvi, S.; D'Souza, L. Identifying the related compounds using electrospray ionization tandem mass spectrometry: Bromotyrosine alkaloids from marine sponge *Psammaplysilla purpurea*. *Eur. J. Mass Spectrom.* **2012**, *18*, 333–343.
5. Rajak, H.; Dewangan, P.K.; Patel, V.; Jain, D.K.; Singh, A.; Veerasamy, R.; Sharma P.C.; Dixit, A. Design of combretastatin A-4 analogues as tubulin targeted vascular disrupting agent with special emphasis on their *cis*-restricted isomers. *Curr. Pharm. Des.* **2013***, 19,* 1923–1955.
6. Cragg, G.M.; Kingston, D.G.I.; Newman, D.J. Anticancer agents from natural products; CRC Press, Taylor & Francis Group; Boca Raton, USA, **2005**, Ch. 3, 23-47, ISBN: 0-8493-1863-7.
7. Lin, C.M.; Singh, S.B.; Chu, P.S.; Dempcy, R.O.; Schmidt. J.M.; Pettit, G.R.; Hamel, E. Interactions of tubulin with potent natural and synthetic analogues of the antimitotic agent combretastatin: a structure-activity study. *Mol. Pharm*. **1988**, *34,* 200–208.
8. Pettit, G.R.; Singh, S.B.; Boyd, M.R.; Hamel, E.; Pettit, R.K.; Schmidt, J.M.; Hogan, F. Antineoplastic Agents. 291. Isolation and Synthesis of Combretastatins A-4, A-5, and A-6. *J. Med. Chem.* **1995**, *38*, 1666–1672.
9. Sherbet, G.V. Suppression of angiogenesis and tumour progression by combretastatin and derivatives. *Cancer Lett.* **2017**, *403*, 289–295.
10. Mikstacka, R.; Stefanski, T.; Rozanski, J. Tubulin-interactive stilbene derivatives as cancer agents. *Cell. Mol. Biol. Lett.* **2013**, *18*, 368–397.
11. Nagaiah, G.; Remick, S.C. Combretastatin A4 phosphate: a novel vascular disrupting agent. *Future Oncol*. **2010**, *6*, 1219–1228.
12. Siemann, D.W. Vascular targeting agents: an introduction. *Int. J. Radiat. Oncol. Biol. Phys.* **2002**, *54*, 1472.
13. Chaplin, D.J.; Hill, S.A. The development of combretastatin A4 phosphate as a vascular targeting agent. *Int. J. Radiat. Oncol. Biol. Phys.* **2002**, *54*, 1491–1496.
14. Eatock, M.M.; Schätzlein, A.; Kaye, S.B. Tumour vasculature as a target for anticancer therapy. *Cancer Treat. Rev.* **2000**, *26*, 191–204.

15. Kanthou, C.; Tozer, G.M. The tumor vascular targeting agent combretastatin A-4-phosphate induces reorganization of the actin cytoskeleton and early membrane blebbing in human endothelial cells. *Blood* **2002**, *99*, 2060–2069.

16. Tozer, G.M. Kanthou, C.; Parkins C.S.; Hill, S.A.The biology of the combretastatins as tumour vascular targeting agents. *Int. J. Exp. Path.* **2002**, *83*, 21–38.

17. Gaspari, R.; Prota, A.E.; Bargsten, K.; Cavalli, A.; Steinmets, M.O. Structural basis of *cis*- and *trans*-combretastatin binding to tubulin. *Chem* **2017**, *2*, 102–113.

18. Krishnaiah, Y.S.R. Pharmaceutical technologies for enhancing oral bioavailability of poorly soluble drugs. *J. Bioequiv. Bioavailab.* **2010**, *2*, 28–36.

19. Williams, H.D.; Trevaskis, N.L.; Charman, S.A.; Shanker, R.M.; Charman, W.N.; Pouton, C.W.; Porter, C.J. Strategies to address low drug solubility in discovery and development. *Pharmacol. Rev.* **2013**, *65*, 315–499.

20. Pettit, G.R.; Temple, Jr. C.; Narayanan, V.L.; Varma, R.; Simpson, M.J.; Boyd, M.R. Antineoplastic agents 322. Synthesis of combretastatin A-4 prodrug. *Anti-Cancer Drug Des*. **1995**, *10*, 299–309.

21. Tozer, G.M.; Prise, V.E.; Wilson, J.; Locke, R.J.; Vojnovic, B.; Stratford, M.R.L.; Dennis, M.F.; Chaplin, D.J. Combretastatin A-4 phosphate as a tumor vascular-targeting agent: early effects in tumors and normal tissues. *Cancer Res.* **1999**, *59*, 1626–1634.

22. European Medicines Agency. European Medicines Agency – Human medicines – EU/3/11/853 [Internet]. 1995–2018 [cited 3 Feb 2018]. Available online: http://www.ema.europa.eu/ema/index.jsp?curl=pages/medicines/human/orphans/2011/04/human_orphan_000912.jsp&mid=WC0b01ac058001d12b&murl=menus/medicines/medicines.jsp&jsenabled=true

23. Jaroch, K.; Karolak, M.; Górski, P.; Jaroch, A.; Krajewski, A.; Ilnicka, A.; Sloderbach, A.; Stefanski, T.; Sobiak, S. Combretastatins: *in vitro* structure-activity relationship, mode of action and current clinical status. *Pharmacol. Rep.* **2016**, 68, 1266–1275.

24. ClinicalTrials.gov. National Library of Medicine (US). Search of: CA4P. [Internet]. 2000–2018 [cited 28 Jan 2018]. Available online: https://clinicaltrials.gov/ct2/results?term=CA4P&Search=Search

25. Liu, P.; Qin, Y.; Wu, L.; Yang, S.; Li, N.; Wang, H.; Xu, H.; Sun, K.; Zhang, S.; Han, X.; Sun, Y.; Shi, Y. A phase I clinical trial assessing the safety and tolerability of combretastatin A4 phosphate injections. *Anticancer Drugs* **2014,** *25*, 462–471.

26. Siemann, D.W.; Chaplin, D.J.; Walicke, P.A. A review and update of the current status of the vasculature-disabling agent combretastatin-A4 phosphate (CA4P). *Expert Opin. Invest. Drugs* **2009**, *18*, 189–97.

27. Görner, H; Kuhn, H.J. *Cis-trans* photoisomerization of stilbenes and stilbene-like molecules. *Adv. Photochem.* **1995**, *19*, 1–117.

28. Sun, L.; Vasilevich, N.I.; Fuselier, J.A.; Hocart, S.J.; Coy. D.H. Examination of the 1,4-disubstituted azetidinone ring system as a template for combretastatin A-4 conformationally restricted analog design. *Bioorg. Med. Chem. Lett.* **2004**, *14*, 2041–2046.

29. O'Boyle, N.M.; Carr, M.; Greene, L.M.; Bergin, O.; Nathwani, S.M.; McCabe, T.; Llyod, D.G.; Zisterer D.M.; Meegan, M.J. Synthesis and evaluation of azetidinone analogues of combretastatin A-4 as tubulin targeting agents. *J. Med. Chem.* **2010**, *53*, 8569–8584.

30. Banwell, M.G.; Hamel. E.; Hockless, D.C.R.; Verdier-Pinard, P.; Willisa, A.C.; Wong, D.J. 4,5-Diaryl-1*H*-pyrrole-2-carboxylates as combretastatin A-4/lamellarin T hybrids: Synthesis and evaluation as antimitotic and cytotoxic agents. *Bioorg. Med. Chem*. **2006**, *14*, 4627–4638.

31. Ohsumi, K.; Hatanaka, T.; Fujita, K.; Nakagawa, R.; Fukuda, Y.; Nihei, Y.; Suga, Y.; Morinaga, Y.; Akiyama, Y.; Tsuji, T. Synthesis and antitumor activity *cis*-restricted combretastatins: 5-membered heterocyclic analog. *Bioorg. Med. Chem. Lett.* **1998**, *8*, 3153–3158.

32. Burja, B.; Cimbora-Zovko, T.; Tomic, S.; Jelusic, T.; Kocevar, M.; Polanc, S.; Osmak, M. Pyrazolone-fused combretastatins and their precursors: synthesis, cytotoxicity, antitubulin activity and molecular modeling studies. *Bioorg. Med. Chem.* **2010**, 18, 2375–2387.

33. Wang, L.; Woods, K.W.; Li, Q.; Barr, K.J.; McCroskey, R.W.; Hannick, S.M.; Gherke, L.; Credo, R.B.; Hui, Y.H.; Marsh, K.; Warner, R.; Lee, J.Y.; Zielinski-Mozng, N.; Frost, D.; Rosenberg, S.H.; Sham, H.L. Potent, orally active heterocycle-based combretastatin A-4 analogues: synthesis structure-activity relationship, pharmacokinetics and *in vivo* antitumor activity evaluation. *J. Med. Chem.* **2002**, *45*, 1697–1711.

34. Bellina, F.; Cauteruccio, S.; Montib, S.; Rossia, R. Novel imidazole-based combretastatin A-4 analogues: evaluation of their *in vitro* anti-tumor activity and molecular modeling study of their binding to the colchicine site of tubulin. *Bioorg. Med. Chem. Lett.* **2006**, *16*, 5757–5762.

35. Romagnoli, R.; Baraldi, P.G.; Salvador, M.K.; Preti, D.; Aghazadeh, T.M.; Brancale, A.; Fu, X.H.; Li, J.; Zhang, S.Z.; Hamel, E.; Bortolozzi, R.; Basso, G.; Viola, G. Synthesis and evaluation of 1,5-disubstituted tetrazoles as rigid analogues of combretastatin A-4 with potent antiproliferative and antitumor activity. *J. Med. Chem.* **2012**, *55*, 475–488.

36. Lu, Y.; Li, C.M.; Wang, Z.; Chen, J.; Mohler, M.L.; Li, W.; Dalton, J.T.; Miller D.D. Design, synthesis and SAR studies of 4-substituted methoxybenzoyl-aryl-thiazoles analogs as potent and orally bioavailable anticancer agents. *J. Med. Chem.* **2011**, *54*, 4678–4693.

37. Maya, A.B.S.; Perez-Melero, C.; Salvador, N.; Pelaez, R.; Caballero, E.; Medarde, M.; New naphthyl combretastatins: modifications on the ethylene bridge. *Bioorg. Med. Chem.* **2005**, *13*, 2097–2107.

38. Kim, Y.; Nam, N.H.; You, Y.J.; Ahn, B.Z.; Synthesis and cytotoxicity of 3,4-diaryl 2(5*H*)-furanones. *Bioorg. Med. Chem. Lett.* **2002**, *12*, 719–722.

39. Pirali, T.; Busacca, S.; Beltrami, L.; Imovilli, D.; Pagliai, F.; Miglio, G.; Massarotti, A.; Verotta, L.; Tron, G.C.; Sorba, G.; Genezzani, A.A. Synthesis and cytotoxic evaluation of combretafurans, potential scaffolds for dual-action antitumoral agents. *J. Med. Chem.* **2006**, *49*, 5372–5376.

40. Romagnoli, R.; Baraldi, P.G.; Remusat, V.; Carrion, M.D.; Cara, C.L.; Preti, D.;Fruttarolo, F.; Pavani, M.G.; Tabrizi, M.A.; Tolomeo, M.; Grimaudo, S.; Balzarini, J.; Jordan, M.A.; Hamel, E. Synthesis and biological evaluation of 2-(3'4'5'-trimethoxybenzoyl)-3-amino-5-aryl thiophenes as a new class of tubulin inhibitors. *J. Med. Chem.* **2006**, *49*, 6425–6428.

41. Flynn, B.L.; Flynn, G.P.; Hamel, E.; Jung, M.K. The synthesis and tubulin binding activity of thiophene-based analogues of combretastatin A-4. *Bioorg. Med. Chem. Lett*. **2001**, *11*, 2341–2343.

42. Guan, Q.; Yang, F.; Guo, D.; Xu, J.; Jiang, M.; Liu, C.; Bao, K.; Wu, Y.; Zhang, W. Synthesis and biological evaluation of novel 3,4-diaryl-1,2,5-selenadiazol analogues of combretastatin A-4. *Eur. J. Med. Chem.* **2014***, 87*, 1–9.

43. Tron, G.C.; Pirali, T.; Sorba, G.; Pagliai, F.; Busacca, S.; Genazzani, A.A. Medicinal chemistry of combretastatin A4: present and future directions, *J. Med. Chem.* **2006,** *49*, 3033–3044.

44. Cushman, M.; Nagarathnam, D.; Gopal, D.; He, H.M.; Lin, C.M.; Hamel, E. Synthesis and evaluation of analogues of (*Z*)-1-(4-methoxyphenyl)-2-(3,4,5-trimethoxyphenyl)ethene as potential cytotoxic and antimitotic agents. *J. Med. Chem.* **1992**, *35*, 2293–2306.

45. Ana, B.; Sánchez Maya, A.B.; Pérez-Melero, C.; Salvador, N.; Peláez, R.; Caballero, E.; Medarde, M. New naphthylcombretastatins. Modifications on the ethylene bridge. *Bioorg. Med. Chem.* **2005**, *13*, 2097–2107.

46. ClinicalTrials.gov. National Library of Medicine (US). Search of: combretastatin or CA4 or CA4 analogues or CA4P. [Internet]. 2000–2018. [Cited 1 May 2018]. Available online: https://clinicaltrials.gov/ct2/home.

47. Banerjee, R.; Kumar, H.K.S.; Banerjee, M. Medicinal significance of furan derivatives: a review. *Int. J. Rev. Life. Sci.* **2012**, *2*, 7–16.

48. Sibbald, B. Rofecoxib (Vioxx) voluntarily withdrawn from market. *Can. Med. Assoc. J.* **2004,** *171*, 1027–1028.

49. Pour, M.; Spulak, M.; Buchta, V.; Kubanova, P.; Voprsalova, M.; Wsol, V.; Fakova, H.; Koudelka, P.; Pourova, H.; Schiller, R. 3-Phenyl-5-acyloxymethyl-2*H*,5*H*-furan-2-ones: synthesis and biological activity of a novel group of potential antifungal drugs. *J. Med. Chem.* **2001**, *44*, 2701–2706.

50. Šenel, P. Structure-Antifungal Activity Relationships in Substituted Butenolides. Dissertation thesis. Charles University, Faculty of Pharmacy in Hradec Králové, Czech Republic, **2009**.

51. Peng, J.; Li, J.; Hamann, M.T. The marine bromotyrosine derivatives. *Alkaloids Chem. Biol.* **2005**; *61*, 59–262.

52. Kiuru, P.; D'Auria, M.V.; Muller, C.D.; Tammela, P.; Vuorela, H.; Yli-Kauhaluoma, J. Exploring marine resources for bioactive compounds. *Planta Med.* **2014**, *80*, 1234–1246.

53. Zidar, N.; Žula, A.; Tomašič, T.; Rogers, M.; Kirby R.W.; Tytgat, J.; Peigneur, S.; Kikelj, D.; Ilaš, J.; Mašič, L.P. Clathrodin, hymenidin and oroidin, and their synthetic analogues as inhibitors of the voltage-gated potassium channels. *Eur. J. Med. Chem.* **2017***, 139*, 232-241.

54. Kottakota, S.K.; Evangelopoulos, D.; Alnimr, A.; Bhakta, S.; McHugh, T.D.; Gray, M.; Groundwater, P.W.; Marrs, E.C.L.; Perry, J.D.; Spilling, C.D. Harburn, J.J. Synthesis and biological evaluation of purpurealidin E-derived marine sponge metabolites: aplysamine-2, aplyzanzine A, and suberedamines A and B. *J. Nat. Prod.* **2012**, *75*, 1090–1101.

55. Bergquist, P.R. Dictryoceratida, dendroceratida and Verongida from the new caledonia lagoon (Porifera: Demonspongiae). *Mem. Queensl. Mus*. **1995**, *38*, 1–51.

56. Tsukamoto, S; Kato, H.; Hirota, H.; Fusetani, N. Ceratinamine: an unprecedented antifouling cyanoformamide from the marine sponge *Pseudoceratina purpurea*. *J. Org. Chem*. **1996**, *61*, 2936–2937.

57. Kobayashi, J.; Honma, K.; Sasaki, T.; Tsuda, M. Purealidins J-R, new bromotyrosine alkaloids from the okinawan marine sponge *Psammaplysilla purea*. *Chem. Pharm. Bull.* **1995**, *43*, 403–407.

58. Tilvi, S.; Rodrigues, C.; Naik, C.G.; Parameswaran P.S.; Wahidhulla, S. New bromotyrosine alkaloids from the marine sponge *Psammaplysilla purpurea*. *Tetrahedron* **2004**, *60*, 10207–10215.

59. Jurek, J.; Yoshida, W.Y.; Scheuer, P.J.; Kelly-Borges, M. Three new bromotyrosine-derived metabolites of the sponge *Psammaplysilla purpurea*. *J. Nat. Prod.* **1993**, *56*, 1609–1612.

60. Carney, J.R.; Scheuer, P.J.; Kelly-Borges, M. A new bastadin from the sponge *Psammaplysilla purpurea*. *J. Nat. Prod.* **1993**, *56*, 153–157.

61. European Commission: CORDIS : Home. Final Report Summary - MAREX (Exploring Marine Resources for Bioactive Compounds: From Discovery to Sustainable Production and Industrial Applications). April 2015 [Internet] [cited 30 Apr 2018]. Available online: https://cordis.europa.eu/result/rcn/159271_en.html

62. Ouadid-Ahidouch, H.; Ahidouch, A.; Pardo, A.L. K(+) channel: from physiology to cancer. *Pflugers Arch.* **2016**, *468*, 75–762.

63. Ordoñez, C.V.; Pardo, L.A.; Kv10.1 potassium channel: from the brain to the tumors. *Biochem. Cell Biol.* **2017,** *95*, 531–536.

64. Pardo, L.A.; del Camino, D.; Sanchez, A.; Alves, F.; Brüggemann, A.; Beckh, S.; Stühmer, W. Oncogenic potential of EAG K^+ channels. *EMBO J.* **1999**, *18*, 5540–5547.

65. Patt, S.; Preussat, K.; Beetz, C.; Kraft, R.; Schrey, M.; Kalff, R.; Schönherr, K.; Heinemann, S.H. Expression of ether à go-go potassium channels in human gliomas. *Neurosci. Lett*. **2014**, *368*, 249–253.

66. Napp, J.; Pardo, L.A.; Hartung, F.; Tietze, L.F.; Stühmer, W.; Alves, F. *In vivo* imaging of tumour xenografts with an antibody targeting the potassium channel K_V10.1. *Eur. Biophys. J.* **2016**, *45*, 721–733.

67. Hemmerlein, B.; Weseloh, R.M.; Queiroz, F.; Knötgen, H.; Sanchéz, A.; Rubio, M.; Martin, S.; Schliephacke, T.; Radzun, H.; Stümer, W.; Pardo, L.A. Overexpression of Eag1 potassium channels in clinical tumours. *Mol. Cancer.* ***2006***, *5*.

68. Agarwal, J.; Griesinger, F.; Stuhmer, W.; Pardo, L.A. The potassium channel ether à go-go is a novel prognostic factor with functional relevance in acute myeloid leukemia. *Mol. Cancer.* **2010***, 27*, 9–18.

69. Martínez, R.; Stühmer, W.; Martin, S.; Schell, J.; Reichmann, A.; Rohde, V.; Pardo, L.A. Analysis of the expression of K_V10.1 potassium channel in patients with brain metastases and glioblastoma multiforme: impact on survival. *BMC Cancer*. **2015**, *15*, 1–9.

70. Ousingsawat, J.; Spitzner, M.; Puntheeranurak, S.; Terracciano, L.; Tornillo, L.; Bubendorf, L.; Kunzelmann, K.; Schreiber, R. Expression of voltage-gated potassium channels in human and mouse colonic carcinoma. *Clin. Cancer Res*. **2007**, *13*, 824–831.

71. Queiroz, F.; Suarez-Kurtz, G.; Stühmer, W.; Pardo, L.A. Ether à go-go potassium channel expression in soft tissue sarcoma patients. *Mol. Cancer*. **2006**. *5*, 42.

72. Ortiz, C.S.; Montante-Montes, D.; Saqui-Salces, M.; Hinojosa, L.M.; Gamboa-Dominguez, A.; Hernández-Gallegos, E.; Martínez-Benítez, B.; Solís-Pancoatl, M.R.; Garcia-Villa, E.; Ramírez. A.; Aguilar-Guadarrama, R.; Gariglio, P.; Pardo, L.A.; Stühmer. W; Camacho, J. Eag1 potassium channels as markers of cervical dysplasia. *Oncol. Rep*. **2011**, *26*, 1377–1383.

73. Menéndez, S.T.; Villaronga, M.A.; Rodrigo, J.P.; Alvarez-Teijeiro, S., García-Carracedo, D.; Urdinguio, R.G.; Fraga, M.F.; Pardo, L.A.; Viloria, C.G.; Suárez, C.; García-Pedrero, J.M. Frequent aberrant expression of the human ether à go-go (hEAG1) potassium channel in head and neck cancer: pathobiological mechanisms and clinical implications. *J. Mol. Med.* **2012**, *90*, 1173–1184.

74. Wu, W.; Dong, M.Q.; Wu, X.G.; Sun, H.Y.; Tse, H.F.; Lau, C.P.; Li, G.R. Human ether-à-go-go gene potassium channels are regulated by EGFR tyrosine kinase. *Biochim. Biophys. Acta.* **2012**, *1823*, 282–289.

75. Lin, H.; Li, Z.; Chen, C.; Luo, X.; Xiao, J.; Dong, D.; Lu, Y.; Yang, B.; Wang, Z. Transcriptional and post-transcriptional mechanisms for oncogenic overexpression of ether à go-go K^+ channel. *PLoS One* **2011**, *6*, e20362.

76. Zhu, L.; Lu. Z.; Zhao, H. Antitumor mechanisms when pRb and p53 are genetically inactivated. *Oncogene* **2015**, *34*, 4547–4557.

77. Weber, C.; Mello de Queiroz, F.; Downie, B.R.; Suckow, A.; Stühmer, W.; Pardo, L.A. Silencing the activity and proliferative properties of the human EagI Potassium Channel by RNA Interference. *J. Biol. Chem*. **2006**, *281*, 13030–13037.

78. Gomez-Varela, D.; Zwick-Wallasch, E.; Knotgen, H.; Sanchez, A.; Hettmann, T.; Ossipov, D.; Weseloh, R.; Contreras-Jurado, C.; Rothe, M.; Stuhmer, W.; Pardo, L.A. Monoclonal antibody blockade of the human Eag1 potassium channel function exerts antitumor activity. *Cancer Res.* **2007**, *67*, 7343–7349.

79. Moreels, L.; Peigneur, S.; Yamaguchi, Y.; Vriens, K.; Waelkens, E.; Zhu, S.; Thevissen, K.; Cammue, B.P.A.; Sato, K.; Tytgat, J. Expanding the pharmacological profile of κ-hefutoxin 1 and analogues: A focus on the inhibitory effect on the oncogenic channel K_V10.1. *Peptides* **2017**, *98*, 43–50.

80. Moreels, L.; Peigneur, S.; Galan, D.T.; De Pauw, E.; Béress, L.; Waelkens, E.; Pardo, L.A.; Quinton, L.; Tytgat, J. APETx4, A novel sea anemone toxin and a modulator of the cancer-relevant potassium channel K_V10.1. *Mar. Drugs* **2017**, *15*.

81. Garcia-Quiroz, J.; Garcia-Becerra, R.; Barrera, D.; Santos, N.; Avila, E.; Ordaz-Rosado, D.; Rivas-Suarez, M.; Halhali, A.; Rodriguez, P.; Gamboa-Dominguez, A.; Medina-Franco, H.; Camacho, J.; Larrea, F.; Diaz, L. Astemizole synergizes calcitriol antiproliferative activity by inhibiting CYP24A1 and upregulating VDR: a novel approach for breast cancer therapy. *Plos One* **2012**, *7*, e45063.

82. Gavrilova-Ruch, O.; Schönherr, K.; Gessner, G.; Schönherr, R.; Klapperstuck, T.; Wohlrab, W.; Heinemann, S.H. Effects of imipramine on ion channels and proliferation of IGR1 melanoma cells. *J. Membr. Biol*. **2002**, *188*, 137–149.

83. Bernal-Ramos, G.; Hernández-Gallegos, E.; Vera, E.; Chávez-López, M.G.; Zúñiga-García, V.; Sánchez-Pérez, Y.; Garrido, E.; Camacho, J. Astemizole inhibits cell proliferation in human prostate tumorigenic cells expressing ether à-go-go-1 potassium channels. *Cell. Mol. Biol. (Noisy-le-grand)* **2017**, *63*, 11–13.

84. García-Ferreiro, R.E.; Kerschensteiner, D.; Major, F.; Monje, F.; Stühmer W.; Pardo L.A. Mechanism of block of hEag1 K+ channels by imipramine and astemizole. *J. Gen. Physiol.* **2004**, *124*, 301–317.

85. De Guadalupe Chávez-López, M.; Pérez-Carreón, J.I.; Zuñiga-García, V.; Díaz-Chávez, J.; Herrera, L.A.; Caro-Sánchez, C.H.; Acuña-Macías, I.; Gariglio, P.; Hernández-Gallegos, E.; Chiliquinga, A.J.; Camacho, J. Astemizole-based anticancer therapy for hepatocellular carcinoma (HCC), and Eag1 channels as potential early-stage markers of HCC. *Tumour Biol.* **2015**, *36*, 6149–6158.

86. De Gaudalupe Chávez-López, M.; Zúñiga-García, V.; Hernández-Gallegos, E.; Vera, E.; Chasiquiza-Anchatuña, C.A.; Viteri-Yánez, M.; Sanchez-Ramos, J.; Garrido, E.; Camacho, J. The combination astemizole-gefitinib as a potential therapy for human lung cancer. *OncoTargets Ther.* **2017** *10*, 5795–5803.

87. De Gaudalupe Chávez-López, M.; Hernández-Gallegos, E.; Vázquez-Sánchez, A.Y.; Gariglio, P.; Camacho, J. Antiproliferative and proapoptotic effects of astemizole on cervical cancer cells. *Int. J. Gynecol. Cancer* **2014**, *24*, 824–828.

88. García-Quiroz, J.; García-Becerra, R.; Santos-Martínez, N.; Barrera, D.; Ordaz-Rosado, D.; Avila, E.; Halhali, A.; Villanueva, O.; Ibarra-Sánchez, M.J.; Esparza-López, J.; Gamboa-Domínguez, A.; Camacho, J.; Larrea, F.; Díaz, L. *In vivo* dual targeting of the oncogenic Ether-à-go-go-1 potassium channel by calcitriol and astemizole results in enhanced antineoplastic effects in breast tumors. *BMC Cancer* **2014**, *14.*

89. García-Quiroz, J.; García-Becerra, R.; Barrera, D.; Santos, N.; Avila, E.; Ordaz-Rosado, D.; Rivas-Suárez, M.; Halhali, A.; Rodríguez, P.; Gamboa-Domínguez, A.; Medina-Franco, H.; Camacho, J.; Larrea, F, Díaz, L. Astemizole synergizes calcitriol antiproliferative activity by inhibiting CYP24A1 and upregulating VDR: a novel approach for breast cancer therapy. *PLoS One* **2012**, *7*, e45063.

90. García-Quiroz, J., Camacho, J. Astemizole: an old anti-histamine as a new promising anti-cancer drug. *Anticancer Agents Med. Chem.* **2011**, *11*, 307–314.

91. Zhou, Z.; Vorperian, V.R.; Gong, Q.; Zhang, S.; January, C.T. Block of HERG potassium channels by the antihistamine astemizole and its metabolites desmethylastemizole and norastemizole. *J. Cardiovasc. Electrophysiol.* **1999**, *10*, 836–843.

92. McMurry, J. Organická chemie; VUTIUM, Brno, CZ; Překlady vysokoškolských učebnic, **2007**, ISBN: 978-80-214-3291-8.

93. Theppawong, A.; Ploypradith, P.; Chuawong, P.; Ruchirawat, S.; Chittchang, M. Facile and divergent synthesis of lamellarins and lactam-containing derivatives with improved drug likeness and biological activities. *Chem. Asian J.* **2015**, *10*, 2631–2650.

94. Meyers, R.A. Encyclopedia of analytical chemistry; John Wiley & Sons Ltd; Chichester, UK, **2000**, 10815–10837, ISBN: 9780471976707.

95. Harmon, P.A., Biffar, S.; Pitzenberger, S.M.; Reed, R.A. Mechanism of the solution oxidation of rofecoxib under alkaline conditions. *Pharm. Res.* **2005**, *22*, 1716–1726.

96. Peterson, T.V.; Streamland, T.U.B.; Awad, A.M. A tractable and efficient one-pot synthesis of 5'-azido-5'-deoxyribonucleosides. *Molecules* **2014**, *19*, 2434–2444.

97. Reddy, V.S.; Rao, G.V., Subramanyam, R. V. K.; Iyengar, D. S. A new novel and practical one pot methodology for conversion of alcohols to amines. *Synth. Comm*. **2000**, *30*, 2233–2237.

98. Horký, P.; Voráčová, M.; Konečná, K.; Sedlák, D.; Bartůněk, P.; Vacek, J.; Kuneš, J.; Pour, M. Nontoxic combretafuranone analogues with high *in vitro* antibacterial activity. *Eur. J. Med. Chem*. **2018**, *143*, 843–853.

99. Yet unpublished data.

100. Wada, Y.; Harayama, Y.; Kamimura, D.; Yoshida, M.; Shibata, T.; Fujiwara, K.; Morimoto, K.; Fujioka, H.; Kita, Y. The synthetic and biological studies of discorhabdins and related compounds. *Org. Biomol. Chem.* **2011**, *9*, 4959–4976.

101. García-Egido, E.; Jairo, P.; Iglesiasa, B.; Muñoz, L. Synthesis of cyanoformamides from primary amines and carbon dioxide under mild conditions. Synthesis of ceratinamine. *Org. Biomol. Chem*. **2009**, *7*, 3991–3999.

102. Rablen, P.R.; McLarney, B.D.; Karlow, B.J.; Schneider, J.E. How alkyl halide structure affects E2 and SN2 reaction barriers: E2 reactions are as sensitive as SN2 reactions. *J. Org. Chem.* **2014**, *79*, 867–879.

103. Yoshida, M.; Yamaguchi, K. Total synthesis of dispyrin, purpurealidin E, and aplysamine-1. *Chem. Pharm. Bull.* **2008***, 56*, 1362–1363.

104. Mäki-Lohiluoma, E. Synthesis of purpurealidin E derivatives. Master's thesis. University of Helsinki, Finland, **2015**.

105. Wang, S.S.; Tam, J.P.; Wang, B.S.; Merrifield, R.B. Enhancement of peptide coupling reactions by 4-dimethylaminopyridine. *Int. J. Pept. Protein Res*. **1981**, *18*, 459–467.

106. Moreels, L.; Bhat, C.; Voráčová, M.; Peigneur, S.; Goovaerts, H.; Mäki-Lohiluoma, E; Zahed, F.; Pardo, L.A.; Yli-Kauhaluoma, J.; Kiuru, P.; Tytgat, J. Synthesis of novel purpurealidin analogues and evaluation of their effect on the cancer-relevant potassium channel $K_V10.1$. *PLoS One*, **2017**, *12*, e0188811.

107. Approved standard. Document M27-A3, Reference method for broth dilution antifungal susceptibility testing of yeasts, Clinical Laboratory Standard Institute, Wayne, PA, **2008**.

108. Approved standard. Document M38-A2, Reference method for broth dilution antifungal susceptibility testing of filamentous fungi, Clinical Laboratory Standard Institute, Wayne, PA, **2008**.

109. Approved Standard - Seventh Edition. Document M07-A7, Methods for dilution antimicrobial susceptibility tests for bacteria that grow aerobically, Clinical Laboratory Standard Institute, Wayne, PA, **2006**.

8 APPENDICES

8.1 Appendix A: Solubility and bioavailability data

Calculated LogP, solubility and prediction of bioavailability for all biologically tested combretafuranones are displayed in the table below. Calculator Plugins were used for structure property prediction and calculation, Marvin 15.10.26, 2015, ChemAxon (http://www.chemaxon.com).

Compound:	LogP:	Solubility [mM]:	Bioavailability:
30a	4.33	0.0105	+
30b	4.77	0.0041	+
30d	2.40	0.1932	+
30e	3.25	0.1171	+
30f	2.87	0.0345	+
30h	5.44	0.0013	+
30i	5.44	0.0013	+
31a	4.19	0.0271	+
31b	2.81	2.0857	+
32a	3.37	0.0098	+
32b	2.62	0.2097	+
32c	1.85	0.2755	+

Table A 1 Solubility and bioavailability data for tested combretafuranones.

8.2 Appendix B: Tested combretafuranone analogues

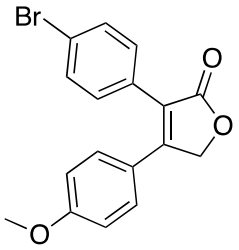

30a

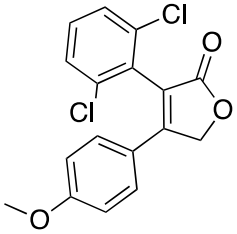

30b

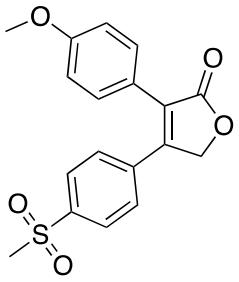

30d

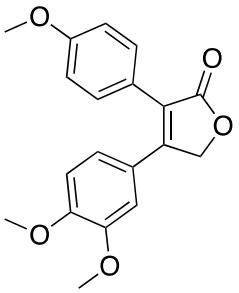

30e

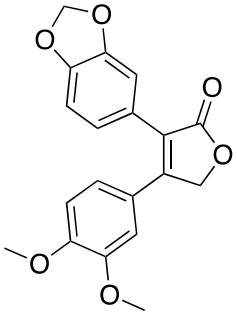

30f

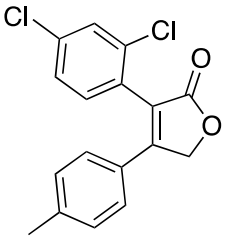

30h

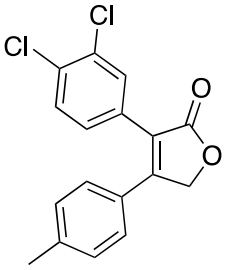

30i

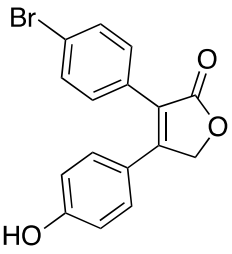

31a

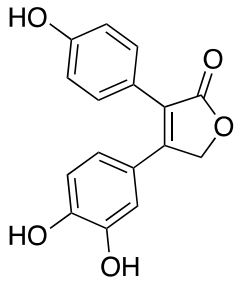

31b

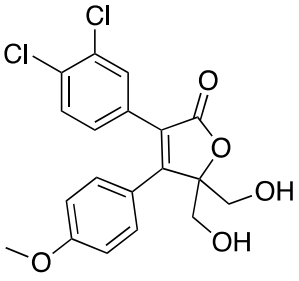

32a

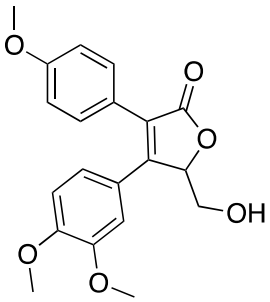

32b

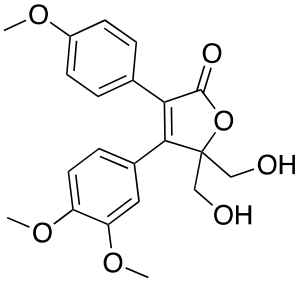

32c

8.3 Appendix C: Tested purpurealidin analogues

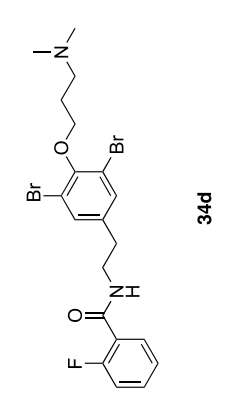

34d

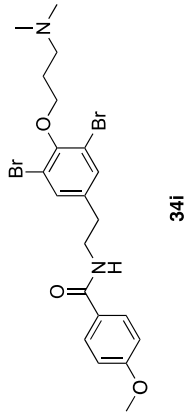

34i

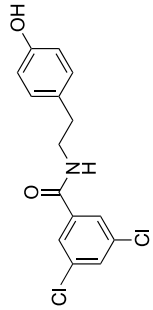

51

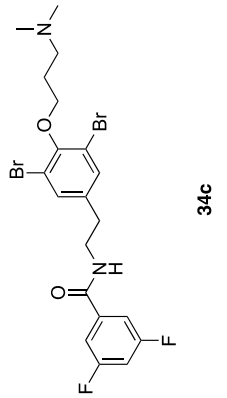

34c

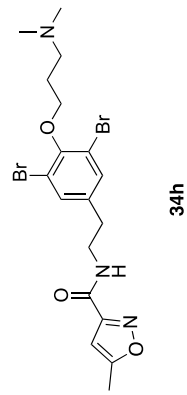

34h

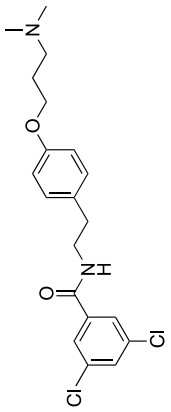

36a

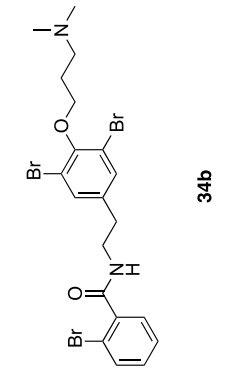

34b

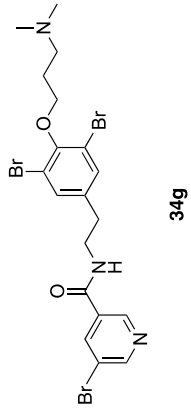

34g

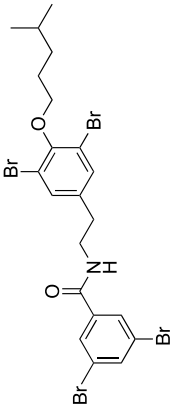

35b

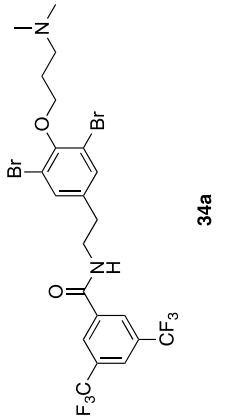

34a

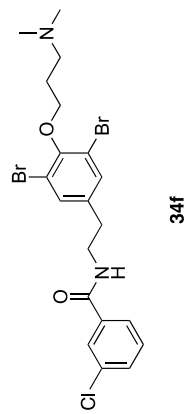

34f

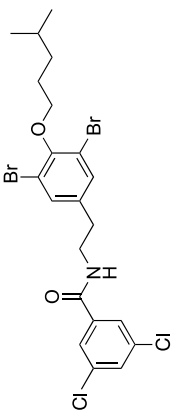

35a